BORYLATION OF PETROLEUM CRACKING OLEFIN PRODUCTS

A Thesis Submitted to the
Graduate School of Engineering and Sciences of
İzmir Institute of Technology
in Partial Fulfillment of the Requirements for the Degree of

MASTER OF SCIENCE

in Chemistry

by
Mehmet Anıl ARAPOĞLU

December 2022
İZMİR

ACKNOWLEDGEMENTS

At the beginning of everything, I would like to thank my advisor Prof. Dr. Levent ARTOK. This thesis could not have been written without him who not only served as my supervisor but also pushed and challenged me throughout my academic program. It was an honor to study with him.

Special thanks to Dr. Onur BÜYÜKÇAKIR and Prof. Dr. Süleyman GÜLCEMAL participating as committee member.

I would thank Prof. Dr. Canan VARLIKLI for letting me use the Glovebox equipment and also Prof. Dr. Durmuş ÖZDEMİR for having permission to use GC instrument. Also, I would like to thank Prof. Dr. Süleyman Gülcemal again for providing us some of the chemicals synthesized in his laboratory.

Additionally, I would like to acknowledge all my colleagues in İYTE, Chemistry Department for their friendship over three years period of my academic life and special thanks to Artok research group. I would like to thank to my family for their, continuous support. Specifically, I would like to thank Nedim Buğra GÖDE for his work in this project and Ece YAZICI for helping me get through the hard times and being with me all the time.

At last, I would like to thank SOCAR Turkey Research & Development and Innovation Inc. for financial support. Also, I would like to thank to Dr. Ayhan EZDEŞİR and Dr. Sıla KARACA for supporting this thesis.

ABSTRACT

BORYLATION OF PETROLEUM CRACKING OLEFIN PRODUCTS

Cracking is a process that long-chain hydrocarbons are broken down into more valuable fragments called naphtha cracking products. The olefins formed as a result of this process have various functions such as forming the smallest building blocks of fine and speciality chemicals. It has been foreseen that borylation processes can be applied as a conversion method of these products into valuable intermediate structures. In this context, this thesis describes first time the transition-metal-catalyzed borylation of a number of petroleum cracking olefin products. Borylation reactions have been extensively investigated in the literature and have become one of the popular methods for synthesizing organoboron reagents, which can also be used in the synthesis of functional materials, pharmaceuticals, and agricultural chemicals.

In the context of this thesis, petroleum cracking olefinic products were converted into high-value-added organoboron derivatives by metal-catalysed hydroboration and dehydrogenative borylation methods. For this purpose, the experimental conditions were optimized using propene and isobutene reagents.

It has been shown in this study that iridium complexes with N-Heterocarbene (NHC) ligands are highly effective catalysts and therefore anti-Markovnikov hydroboration products can be produced in excellent yields even at very low catalyst loadings. On the other hand, alkenyl boron products could be obtained with high yields, which could be performed in the absence of dehydrogenative borylation reactions, ligand, base, and any other additives.

The applicability of these methods in internal and terminal alkenes such as cyclohexene, ethene, decene and styrene has been also demonstrated. Finally, these products were converted into a number of intermediates by Suzuki-Miyaura cross-coupling reactions. Thus, in the conversion of alkenes to valuable intermediates, practical and sustainable applications would be possible by using simple, abundant, and cheap reagents instead of expensive and dangerous chemicals.

ÖZET

PETROL KRAKİNG OLEFİN ÜRÜNLERİNİN BORİLASYONU

Kraking, uzun zincirli hidrokarbonların nafta parçalama ürünleri adı verilen daha değerli parçalara ayrıldığı süreçtir. Bu işlem sonucu oluşan olefinlerin nitelikli ve özel kimyasalların en küçük yapı taşlarını oluşturmak gibi çeşitli fonksiyonları mevcuttur. Bu ürünlerin nitelikli ara yapılara dönüşüm yöntemi olarak borilasyon işlemleri uygulanabileceği ön görülmüştür. Bu amaçla bu tez kapsamında ilk defa petrolyum olefin parçalanma ürünlerinin borilasyon işlemleri gösterilmiştir. Olefinlerin borilasyon yöntemleri literatürde kapsamlı bir şekilde araştırılmış ve fonksiyonel materyallerin, farmasötiklerin ve tarım kimyasallarının sentezinde de kullanılabilen organoboron reaktiflerinin sentezlenmesi için popüler yöntemlerden biri haline gelmiştir.

Bu bağlamda, petrol olefin parçalanma ürünleri, metal katalizli hidroborasyon ve dehidrojenatif borilasyon yöntemleri ile katma değeri yüksek organoboron türevlerine dönüştürülmüştür. Yöntemlerin geliştirilmesi üzerine, propen ve izobüten kullanılarak çeşitli koşullar optimize edilmiştir.

N-Heterokarben (NHC) ligandlı iridyum komplekslerinin oldukça etkili katalizör olduğu ve bu nedenle çok düşük katalizör yüklemelerinde dahi mükemmel verimde anti-Markovnikov hidroborasyon ürünlerinin edilebilebildiği bu çalışmada gösterilmiştir. Öte yandan, dehidrojenatif borilasyon reaksiyonları, ligand, baz ve diğer herhangi bir katkı maddesinin yokluğunda gerçekleştirilebilmiş yüksek verimle alkenil bor ürünleri elde edilebilmiştir.

Bu yöntemlerin siklohekzen, eten, deken ve stiren gibi iç ve uç alkenlere uygulanabilirliği de gösterilmiştir. Son olarak bu ürünler Suzuki-Miyaura çapraz bağlama yöntemi ile çeşitli ara ürünlere dönüştürülerek kullanılabilirlikleri de gösterilmiştir. Bu şekilde alkenlerin nitelikli ara yapılara dönüşümünde pahalı ve tehlikeli kimyasallar yerine basit, bol ve ucuz reaktifler kullanılarak pratik ve sürdürülebilir uygulamalar mümkün olacaktır.

TABLE OF CONTENTS

LIST OF FIGURES

Figure **Page**

Figure **Page**

LIST OF TABLES

Figure **Page**

LIST OF ABBREVIATIONS

$AsPh_3$	Triphenylarsine	IPA	Isopropyl alcohol
B_2pin_2	Bis(pinacolato) diboron	iPr	Isopropyl
BBE	Bis(boronate ester)	KO^tBu	Potassium tert-butoxide
Bu	Butyl	Me	Methyl
COD	Cyclooctadiene	MeCN	Acetonitrile
Cp	Cyclopentadienyl	MeOH	Methanol
CPME	Cyclopentyl methyl ether	min	minute
equiv	equivalent	MHz	megahertz
EtMgBr	Ethylmagnesium bromide	mL	mililiter
dba	Dibenzylideneacetone	m	meter
DBU	1,8-Diazabicyclo[5.4.0]undec-7-ene	mg	miligram
DCE	Dichloroethane	mm	milimeter
DCM	Dichloromethane	μm	micrometer
DHB	dehydrogenative borylation	mmol	millimole
DMF	Dimethyl formamide	MS	Mass Spectrometry
DMSO	Dimethyl sulfoxide	MTBE	Methyl tert-butyl ether
DPPB	1,4-Bis(diphenylphosphino)butane	NHC	N-hetero carbene
DPPE	1,4-Bis(diphenylphosphino)ethane	NMP	N-methyl pyrrolidone
dppm	1,4-Bis(diphenylphosphino)methane	NMR	Nuclear Magnetic Resonance
dtbpy	Di-tert-butyl-2,2 -dipyridyl	OMe	Methoxy
EtOAc	Ethyl acetate	OTf	Trifluoromethanesulfonate
GC	Gas Chromatography	Ph	Phenyl
h	hour	PPh_3	Triphenylphosphine
HBcat	Catecholborane	ppm	parts per million
HBpin	Pinacolborane	PMe_3	Trimethylphospine

PTFE	Polytetrafluoroethylene
pyrr	Pyrrolidine
RF	response factor
rt	room temperature
T	temperature
t	time
terpy	Terpyridine
THF	Tetrahydrofuran
TLC	Thin Layer Chromatography
TMP	3,4,7,8-Tetramethyl-1,10-phenanthroline
VBE	vinyl boronate ester
Xantphos	(9,9-Dimethyl-9H-xanthene-4,5-diyl)bis(diphenylphosphane)
TFA	Trifluoroacetic acid

CHAPTER 1

INTRODUCTION

Crude oil is one of the most important natural resources found on Earth. However, unrefined crude oil has a limited use and thus cracking process is widely used process to obtain valuable products. In this process, long-chain hydrocarbons are broken down into light hydrocarbons (Figure 1.1). While some of the naphtha-cracking products have found various uses, such as building blocks of the most fine and specialty chemicals, and monomers, $\geq C_3$ olefinic hydrocarbons have found limited uses.[1, 2]

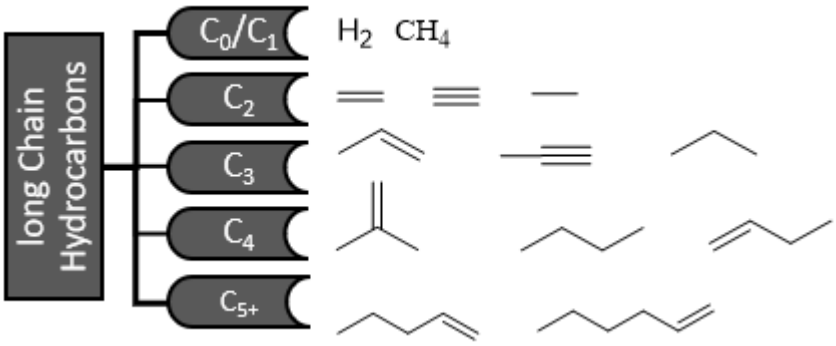

Figure 1.1. The main hydrocarbon cracking fractions.

The most practical and sustainable applications of synthetic processes are possible with the use of simple, abundant, and cheap reagents instead of using costly, insufficient, and dangerous chemicals. In recent years, some organic syntheses have been developed using natural gas and petrochemical products such as methane[3], ethane[4], butadiene[5], ethylene, 2-butene, and other olefins.[6, 7]

Molecules that have at least one carbon-boron bond are classified as organoborons. These organoboron reagents, such as boronic acids and boronic esters, are generally used to form carbon-carbon and carbon-heteroatom bonds.[8-10] Organoborons can easily be functionalized and used as a building block to obtain pharmaceuticals or agricultural chemicals (Figure 1.2).[11, 12]

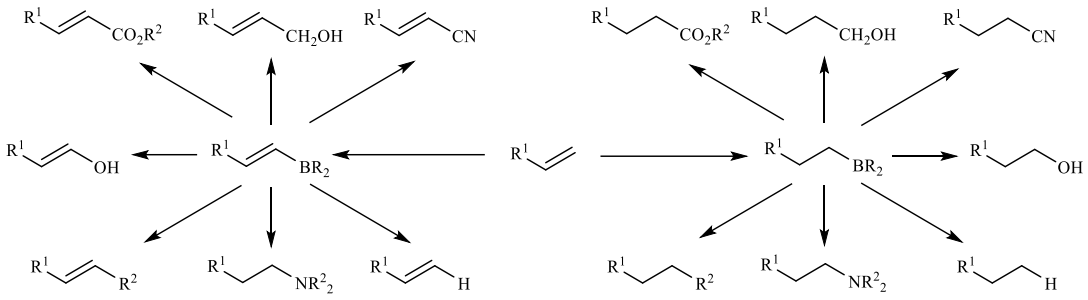

Figure 1.2. Derivatizations of olefins to organoborons via dehydrogenative borylation and hydroboration reactions.

The transition-metal-catalysed borylation reactions are one of the most important methods for synthesizing organoboron compounds in organic synthesis. Transition metals have the ability that ensure products to form with high regio-, chemo-, and stereoselectivities. Intermediates of various biologically active molecules, drugs and natural compounds can be synthesized via these reactions.[7, 13-16]

Transition metal-catalysed borylation of petroleum cracking olefin products is not a subject that have been studied yet. This thesis is the first study that have focused on this subject.

CHAPTER 2

LITERATURE WORKS

2.1. Hydroboration Reactions

The hydroboration of alkenes is a practical method for the preparation of alkylboronates, which are widely used in synthetic chemistry, as C-B bonds can be easily converted into various functional groups.

In the transition-metal-catalysed hydroboration of terminal alkenes, the control of regioselectivity is crucial. According to the literature studies, these reactions are overwhelmingly carried out with *anti*-Markovnikov regioselectivity to obtain primary organoboron compounds (Figure 2.1). However, limited studies reported on the hydroboration of alkyl substituted terminal alkenes with Markovnikov regioselectivity. This section presents literature studies on the hydroboration of alkenes with various metal catalysts and two types of Markovnikov additions. Catecholborane (HBcat) and pinacolborane (HBpin) are the most commonly used reagents in both catalysed and uncatalyzed hydroboration reactions.

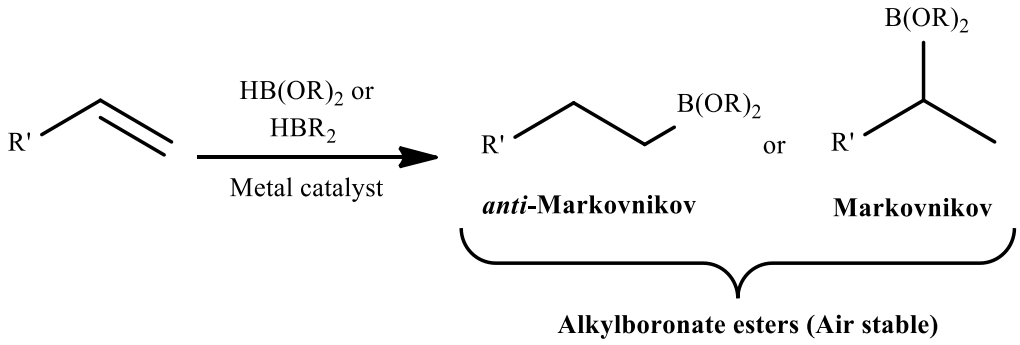

Figure 2.1. Transition-metal-catalyzed hydroboration of terminal alkenes.

The hydroboration of alkenes was first developed in 1956 by Brown et al. A number of trialkylboranes was synthesized with the regioselective addition of diboranes

to alkenes at the least hindered carbon atom, in the presence of sodium borohydride and aluminium chloride.[17]

In 1985, Nöth et al. reported that hydroboration of 5-hexen-2-one with HBcat using low loadings of Wilkinson's catalyst [$Rh(PPh_3)_3Cl$] at room temperature could significantly affect the reactivity and chemoselectivity of the reactions. The catalyst-free hydroboration reaction offered complementary chemoselectivity. In the catalysed-reaction, the hydroboration took place by anti-Markovnikov addition (Figure 2.2)[18]

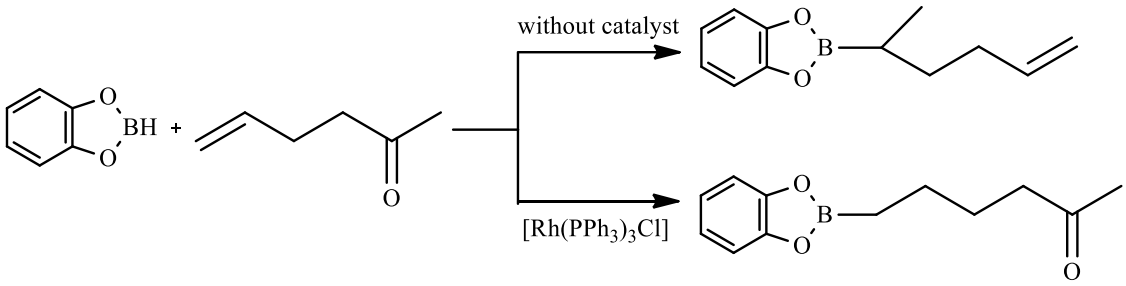

Figure 2.2. The reaction of 5-hexen-2-one and HBcat.

Marder et al. disclosed the first catalytic hydroboration of α-methylstyrene with HBcat and Wilkinson's catalyst at room temperature, and they proposed a reasonable catalytic cycle (Figure 2.3).[19] These reaction pathways comprise hydroboration, dehydrogenative borylation, and hydrogenation steps and led to the formation of corresponding products in the yields of 17, 80, and 3 percentages, respectively.

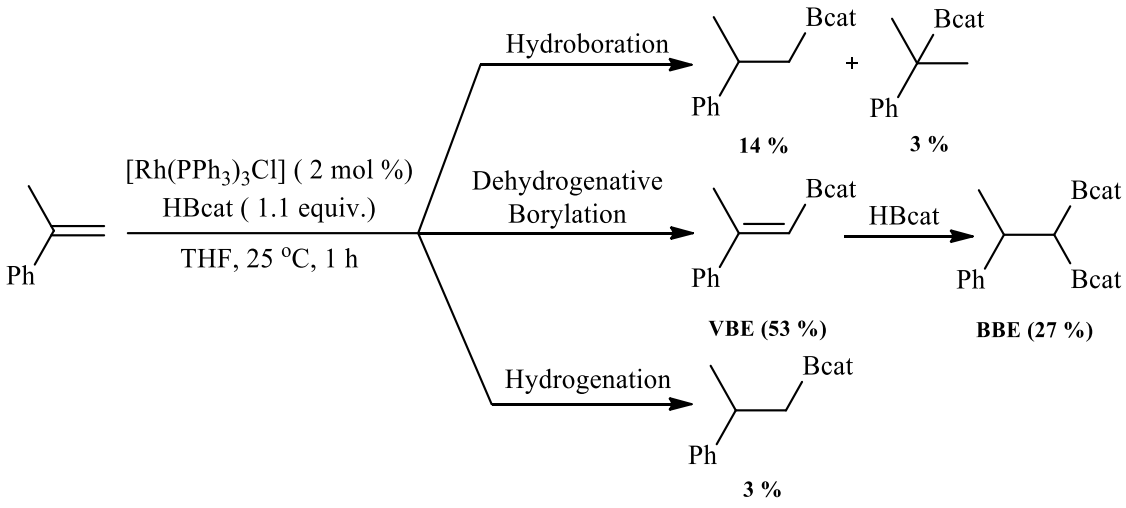

Figure 2.3. The first hydroboration of α-methylstyrene.

Similarly, Srebnik et al. reported that the internally symmetrical alkenes undergoe a highly regioselective hydroboration reactions with HBpin over Wilkinson's catalyst and (Figure 2.4).[20]

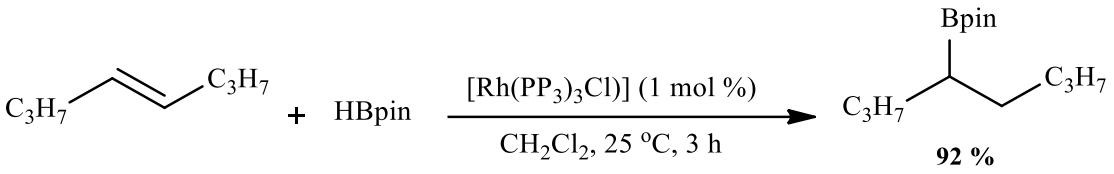

Figure 2. 4.

Figure 2.4. Rhodium-catalysed hydroboration of an internal symmetric alkene.

Numerous iron catalysts have been developed that can be used in alkene hydroboration with HBpin Greenhalgh and Thomas reported that iron-catalysed hydroboration reactions of 4-phenylbutene in the presence of Grignard reagents gave highly selective anti-Markovnikov-product (Figure 2.5).[21]

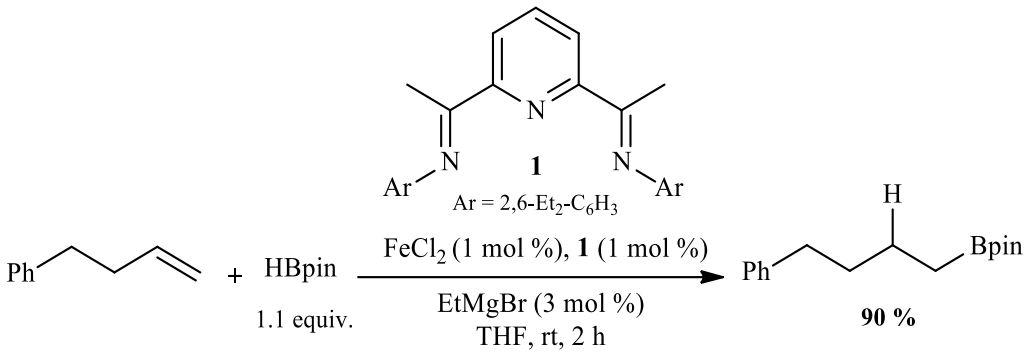

Figure 2.5. Iron-catalysed hydroboration of 4-phenylbutene.

In alkene hydroboration, the control of regioselectivities has been considered to be main problem. In 2020, Liu and Su reported the iron-catalysed regiodivergent hydroboration of terminal alkenes without ligands. These reactions yielded both Markovnikov and anti-Markovnikov products with high regioselectivities. Base, solvents, and ate form of iron−boron alkoxide intermediates are crucial factors in selectivity (Figure 2.6).[22]

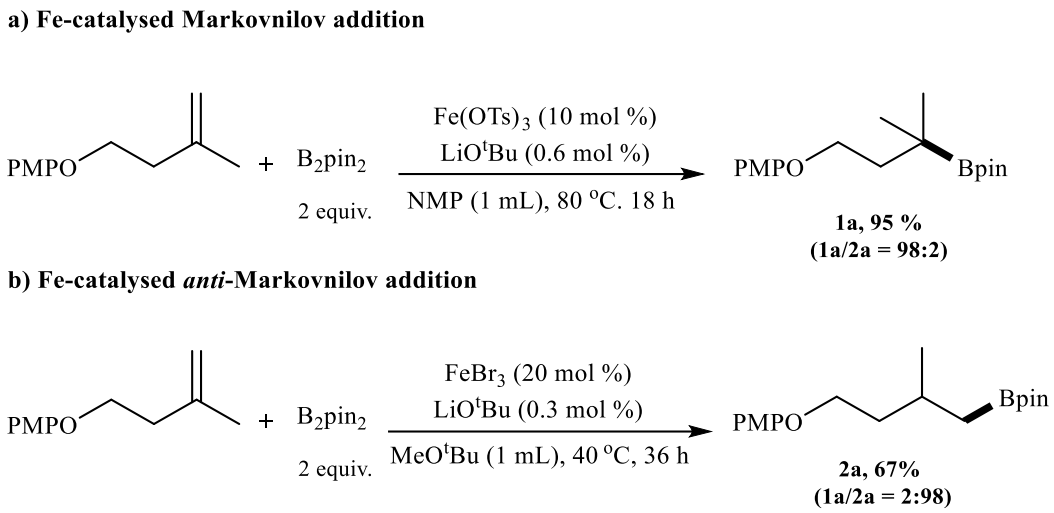

Figure 2.6. The ligand-free Iron-catalysed hydroboration of alkenes.

An amide-based tridentate ligated iron compound catalysed hydroboration of styrene in the form of Markovnikov addition[23] (Figure 2.7a), whereas an N-heterocarbene (NHC) ligated iron compound led to proceed the hydroboration in *anti*-Markovnikov manner (Figure 2.7b).[24]

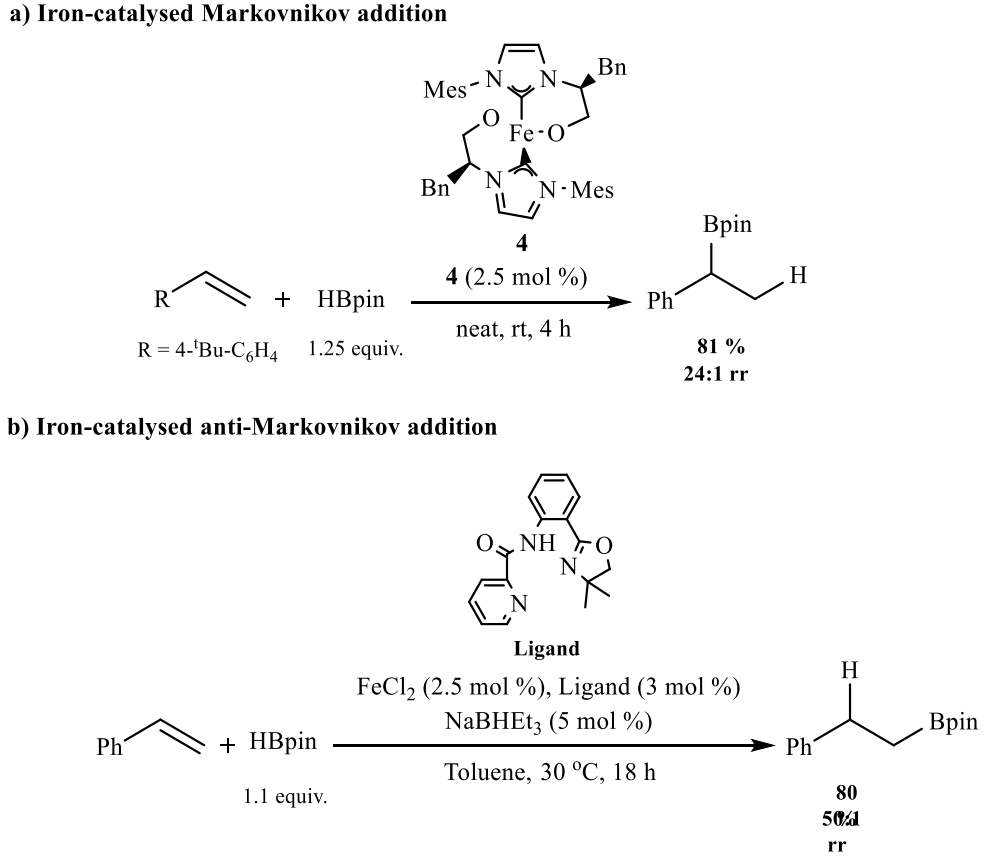

Figure 2.7. Iron-catalysed hydroboration of alkenes in the presence of NHC ligands.

The regioselective Markovnikov hydroboration has also been examined with different catalysts. For example, the hydroboration of styrene with an NHC-ligated nickel precatalyst has been successfully performed by the Schomaker group (Figure 2.8).[25]

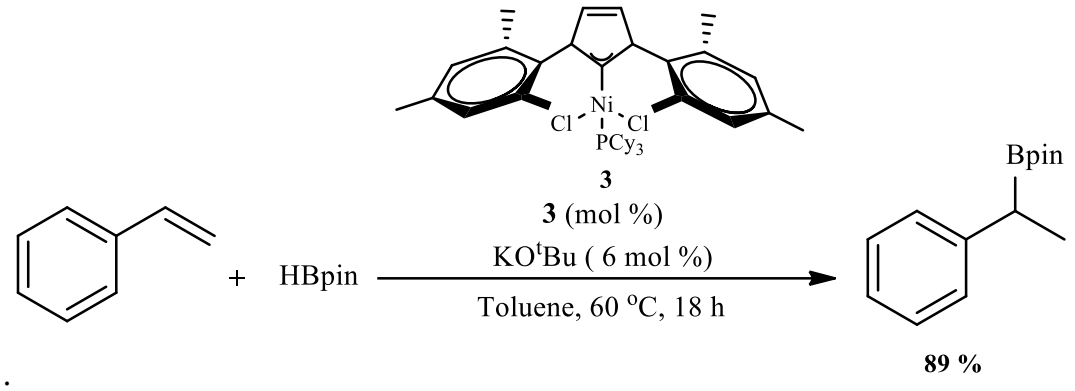

Figure 2.8. Nickel-catalysed hydroboration of styrene with Markovnikov type addition.

Another example of a nickel-catalysed reaction was described by Ye and Wang as follows: hydroboration of terminal aryl and aliphatic alkenes with B_2Pin_2 on the base selectively yielded *anti*-Markovnikov products (Figure 2.9).[26]

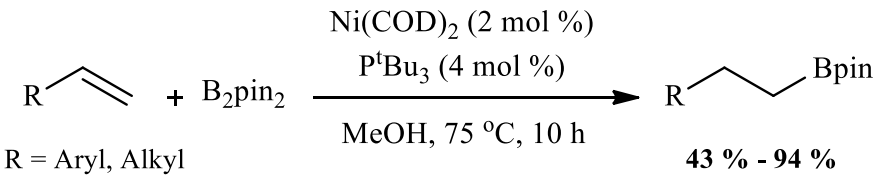

Figure 2.9. Nickel-catalysed hydroboration of alkenes.

Hydroboration of unactivated alkenes has also been enabled through Cu-B-mediated processes. Ito and colleagues investigated the Markovnikov type process using a bulky bisphosphine ligand[27] (Figure 2.10a) and the *anti*-Markovnikov type process using Xantphos as the ligand (Figure 2.10b).[28]

a) Copper-catalysed Markovnikov addition

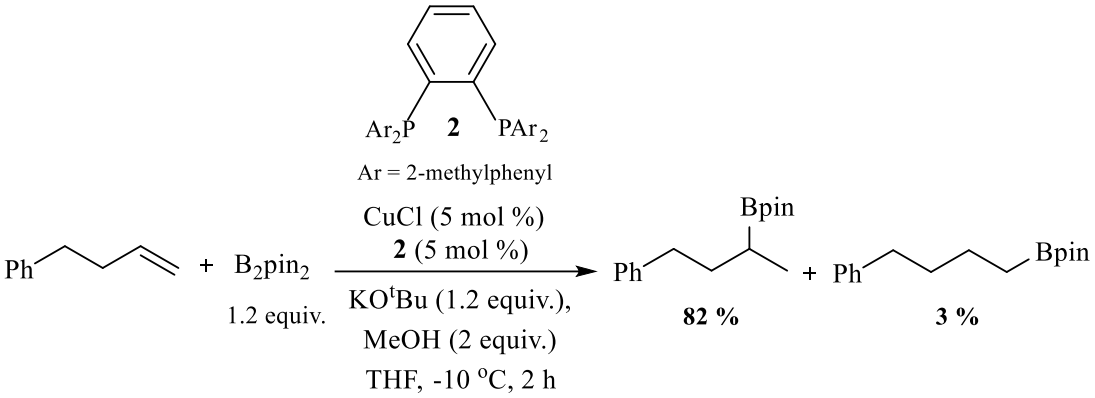

a) Copper-catalysed *anti*-Markovnikov addition

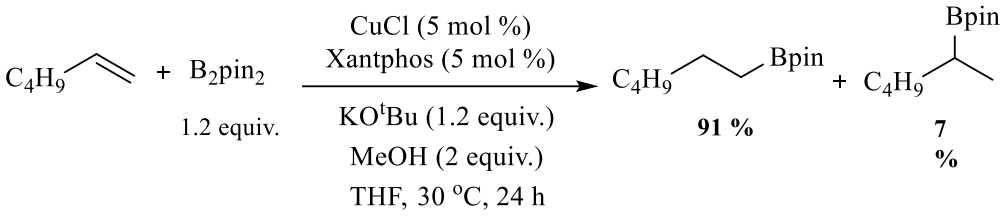

Figure 2.10. Copper-catalysed hydroboration with Markovnikov type addition.

In addition, cobalt-catalysed borylation of alkenes with HBpin has been studied by Chiriket et al. Internal alkenes performed highly regioselective hydroboration by Markovnikov addition over [(terpy)$CoCH_2SiMe_3$][29] (Figure 2.11a) and anti-Markovnikov type addition with [(4-pyrr-^{Mes}PDI)$CoCH_3$] catalyst (Figure 2.11b).[30]

a) Cobalt-catatalysed Markovnikov addition

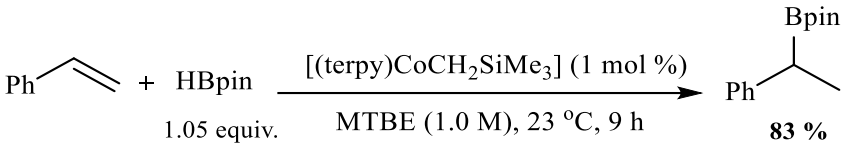

b) Cobaltcatatalysed *anti*-Markovnikov addition

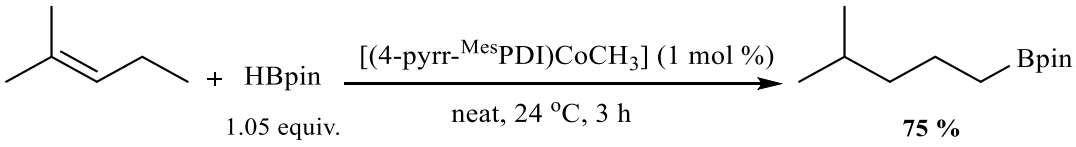

Figure 2.11. Cobalt-catalysed hydroboration with Markovnikov type addition.

In 2004, the Yamamoto group presented the iridium-catalysed hydroboration of 1-octene. They noticed that terminal hydroboration products are formed by the *anti*-Markovnikov addition of HBpin, preferentially from the less hindered side of the alkene (Figure 2.12).[31]

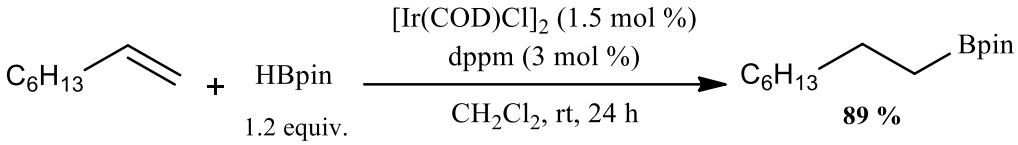

Figure 2.12. Iridium-catalysed hydroboration of 1-octene.

2.2. Dehydrogenative C-H Borylation

Vinyl boronate esters (VBEs) have an important role as intermediates in various transformations or syntheses of targeted alkenes. There has been an increasing interest in to create effective and facile methods for dehydrogenative borylation (DHB) of alkenes. The direct borylation of terminal alkenes has been investigated using complexes of various catalysts with a boron source (Fig 2.13).

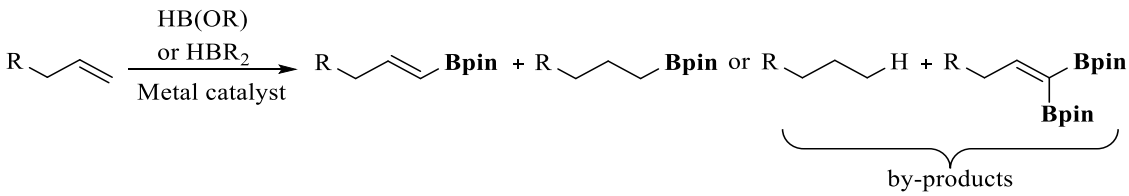

Figure 2.13. Transition-metal-catalysed dehydrogenative borylation of alkenes.

Although valuable practical works were done for their preparation, only a limited number of atomic and economic strategies were available.[32-40] There is great interest in synthesizing VBEs directly from alkenes, because alkenes are inexpensive, and readily available from the petroleum industry or renewable sources.[41] This section presents literature studies on the dehydrogenative borylations of alkenes with various metal catalysts.

2.2.1. Catalytic Dehydrogenative Borylation (DHB) of Alkenes with Boranes

According to the literature studies, for a satifactory chemo- and regioselectivity of the catalytic borylation of alkenes required the use of sensitive boron reagents at low temperatures. Therefore, boranes such as dioxaborolane, catecholborane (HBcat) and pinacolborane (HBpin) have attracted enormous interests.

Brown and Lloyd-Jones were the first reported the dehydrogenative borylation of vinylalkenes with an oxazaborolidene in presence of $[Rh(\mu\text{-}Cl)(\eta^2\text{-}CH_2CHAr)_2]_2$ as the catalyst precursor.[42] As a result of this research, an equal mixture of vinyl boronic ester (VBE) and hydrogenation products was obtained, and no hydroboration product was formed (Fig 2.14a). In the dehydrogenative borylations reactions, due to the strong reducing reactivity of boranes, it is required to consume half of the substrate as an H_2 acceptor or to add a second alkene as an alkene hydroboration using Wilkinson's catalyst with HBcat and found that VBE's could be produced using an unsaturated H_2 acceptor.

Marder and Baker's group investigated dehydrogenative borylation of olefins using Bcat in 1992 (Fig 2.14b). This method involved the addition of a competitive insertion of alkene to the Rh-B bond instead of the Rh-H bond.[43] When α-substituted vinyl alkenes are used as reactants, the reaction favoured the dehydrogenative borylation rather than hydroboration. VBEs were obtained with 76%, and with 15% yields of the hydroboration and 1,1-diborylalkane products, respectively.[19]

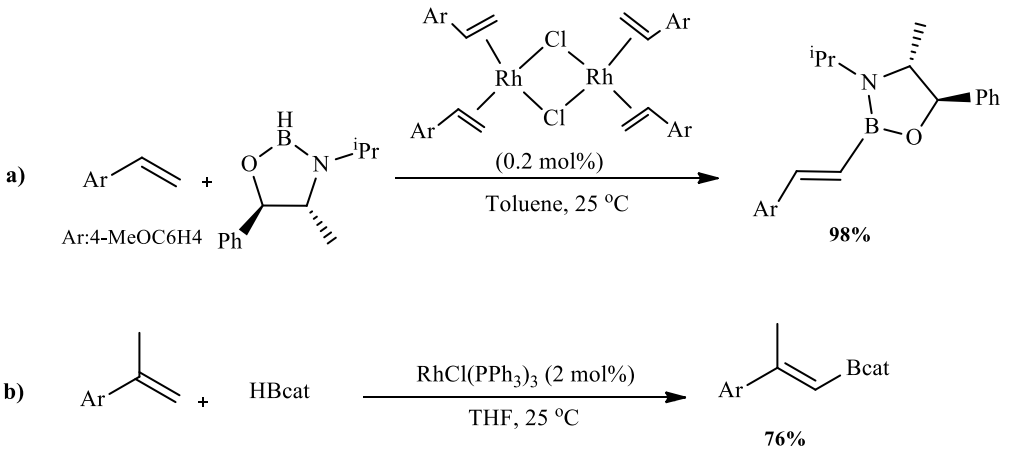

Figure 2.14. The first rhodium-catalysed dehydrogenative borylation of vinylalkenes.

Dehydrogenative borylation of styrene with HBpin was also performed in the presence of $[Rh(COD)Cl]_2$, VBEs were obtained with 94% and alkylboronate ester with 6% yields by Masuda and colleagues (Fig 2.15a).[44] Liu and colleagues reported that in the use of 1,2-azaborinanes as a boron source in the rhodium-catalysed DHB of various arylalkenes, the reaction yield was up to 87% (Fig 2.15b).[45]

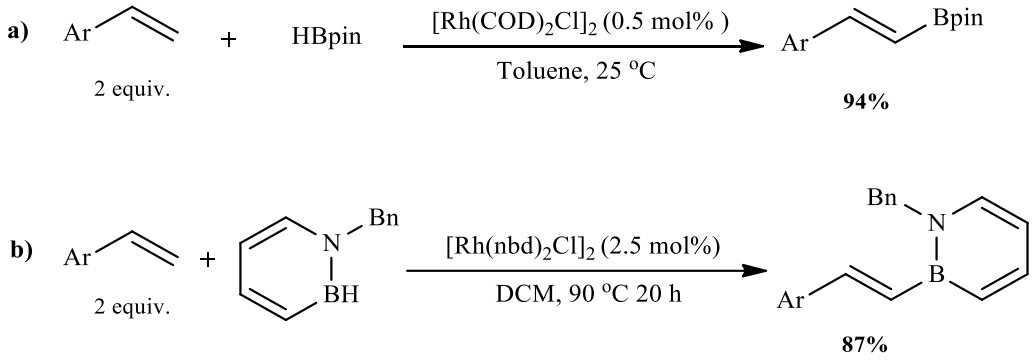

Figure 2.15. Rhodium-catalysed dehydrogenative borylation of styrene.

In 2006, Sabo-Etienne et al. observed that the $[RuH_2(H_2)_2(PCy_3)_2]$ complex selectively catalysed DHB or hydroboration of the cyclic alkenes, depending on the size of the ring (Fig 2.16).[46]

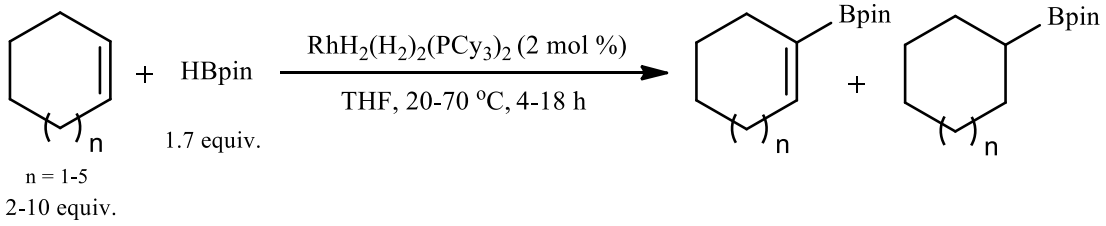

Figure 2.16. Rhodium-catalysed dehydrogenative borylation of cyclic alkenes.

Miura and Murakami reported the first general DHB of aryl and aliphatic alkenes with wide functional group tolerance. When norbornene was used a hydrogen receptor and $[Rh(COD)_2]BF_4$/^{i}Pr-Foxap] as a catalyst, VBE was obtained with 71% yield (Fig 2.17).[47]

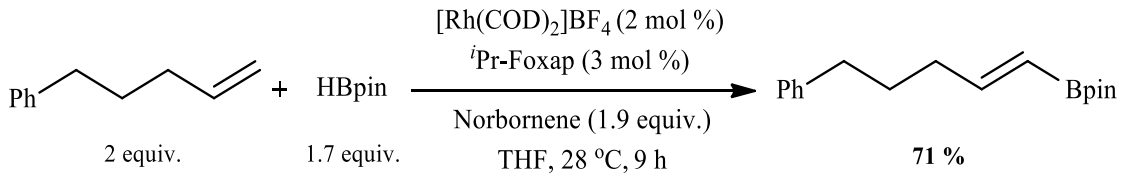

Figure 2.17. The first rhodium-catalysed dehydrogenative borylation of aryl and aliphatic alkenes.

Hartwig and colleagues identified that the first DHB reactions of alkenes yielded products upto 87% yield by irradiation in the presence of $CpFe(CO)_2(Bcat)$ complex in benzene (Fig 2.18).[48]

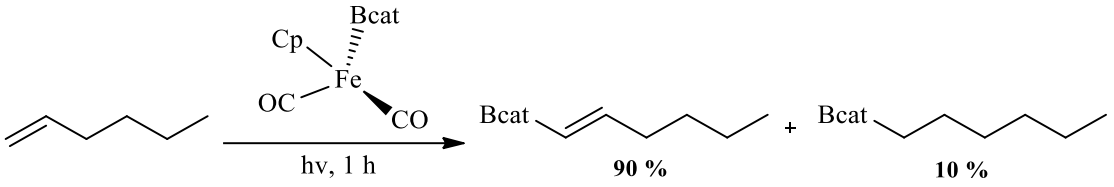

Figure 2.18. The first iron-catalysed dehydrogenative borylation of alkenes.

The Ge's group reported DHB of arylalkenes using HBpin and $Fe(PMe_3)_4$. Various monosubstituted and disubstituted vinylarenes were converted to VBEs in an average of 80% yield in the presence of two equivalents of norbornene. No alkylboronate ester formation was detected in their studies (Fig 2.19).[49]

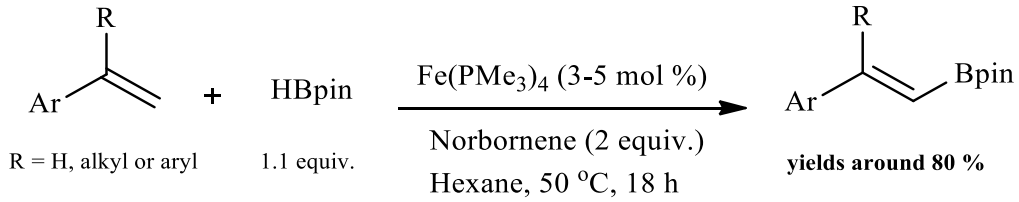

Figure 2.19. Iron-catalysed dehydrogenative borylation of vinylarenes.

2.2.2. Catalytic Dehydrogenative Borylation of Alkenes with Diboranes

In DHB reactions, the requirements of hydrogen acceptors can be eliminated with the use of B_2pin_2 as the boron source.[50] According to Marder and colleagues, it has been observed that *trans*-$[RhCl(CO)(PPh_3)_2]$ catalysed DHB reactions of alkenes with B_2pin_2

requires higher temperatures than reactions with HBpin. The notable point of this reaction is the use of acetonitrile as the co-solvent, so the acetonitrile-coordinated boryl alkyl rhodium structure is formed (Fig 2.20a).[51] In 2010, rhodium-catalysed DHB of cyclic alkenes could be performed in the presence of a bidentate phosphine, leading to VBEs in 54-75% yields (Fig 2.20b).[52]

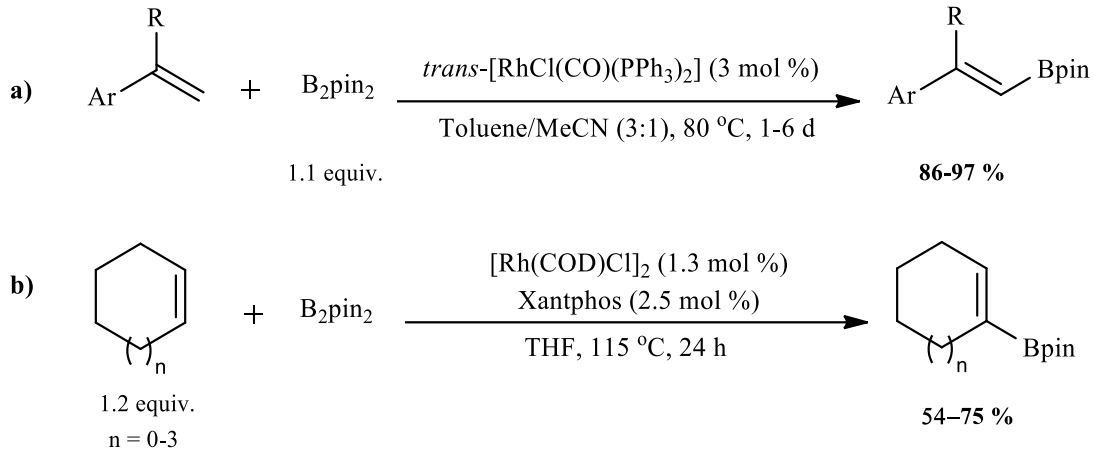

Figure 2.20. Rhodium-catalysed dehydrogenative borylation of vinylarenes and cyclic alkenes.

Palladium NCN-pincer catalysed dehydrogenative borylation of olefin has first been reported by Szabo and co-workers. The reagent [bis(trifluoroacetoxy)iodo]benzene was the oxidant of this reaction. This reaction yields the desired product and an allyl isomer mixture. The ratio of isomers depends on the size of the cycloalkene ring (Fig 2.21).[53]

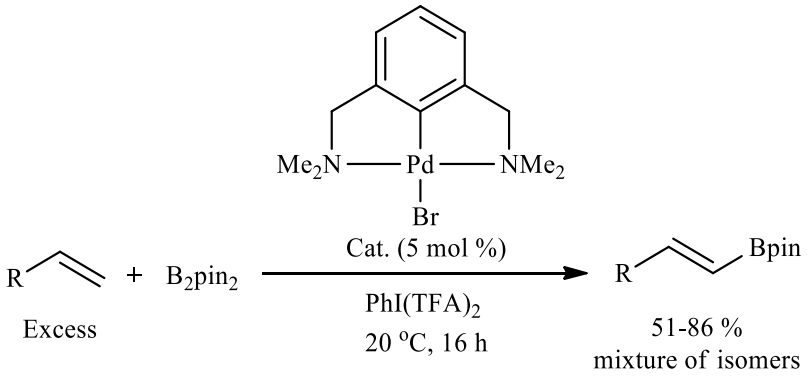

Figure 2.21. The first palladium-catalysed dehydrogenative borylation of alkenes.

Iwasawa reported the synthesis of VBEs or diborylalkenes from alkenes by using anionic PSiP pincer palladium complexes. The selectivity of the borylation is depend on

the ratio of B_2pin_2 to the alkene substrate. In this system, side reactions, such as hydroboration or hydrogenation, are inhibited (Fig 2.22).[54]

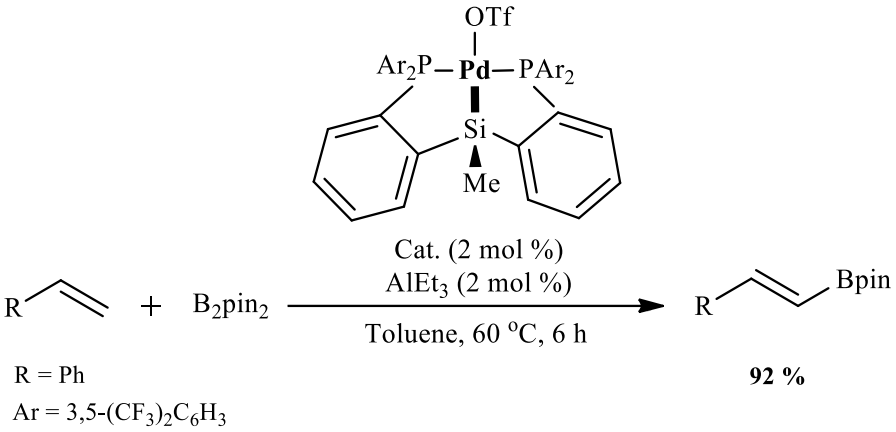

Figure 2.22. Palladium-catalysed dehydrogenative borylation of alkenes.

Olsson and Szabó found that the borylation of cyclic alkenes with B_2pin_2 in the presence of $[Ir(COD)Cl]_2$ is an effective method of producing high added value VBEs. (Fig 2.23).[55]

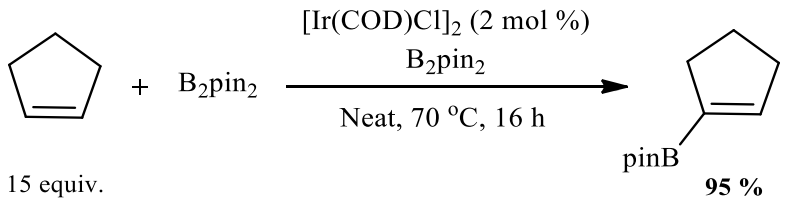

Figure 2.23. Iridium catalysed dehydrogenative borylation of cyclic alkenes.

The mechanism of olefin borylation could not be supported by conclusive evidence in the literature. Subsequent studies suggest that the mechanism involves olefin insertion into the M−B bond followed by product formation through β−H elimination. The mechanism of iridium catalysed borylation was proposed by Szabo on the basis of results obtained from kinetic studies (Fig 2.24).[55]

In the proposed mechanism, the iridium complex initially reacts with excess B_2pin_2 to assure an active triboronate catalyst **1.** The migratory insertion of cycloalkene into the iridium-boron bond produces **2**. This complex then undergoes *syn-β*-H elimination to give the iridium-coordinated allyl boronate **3**. After that, the allylic product left, and the iridium−hydride complex **4** reacts with the diboronate. So active catalyst is regenerated and the alkenyl pinacolborane is produced. As a result of the stereochemistry

of β-H-elimination of hydrogen, an allyl derivative is formed instead of the expected vinyl boronate.

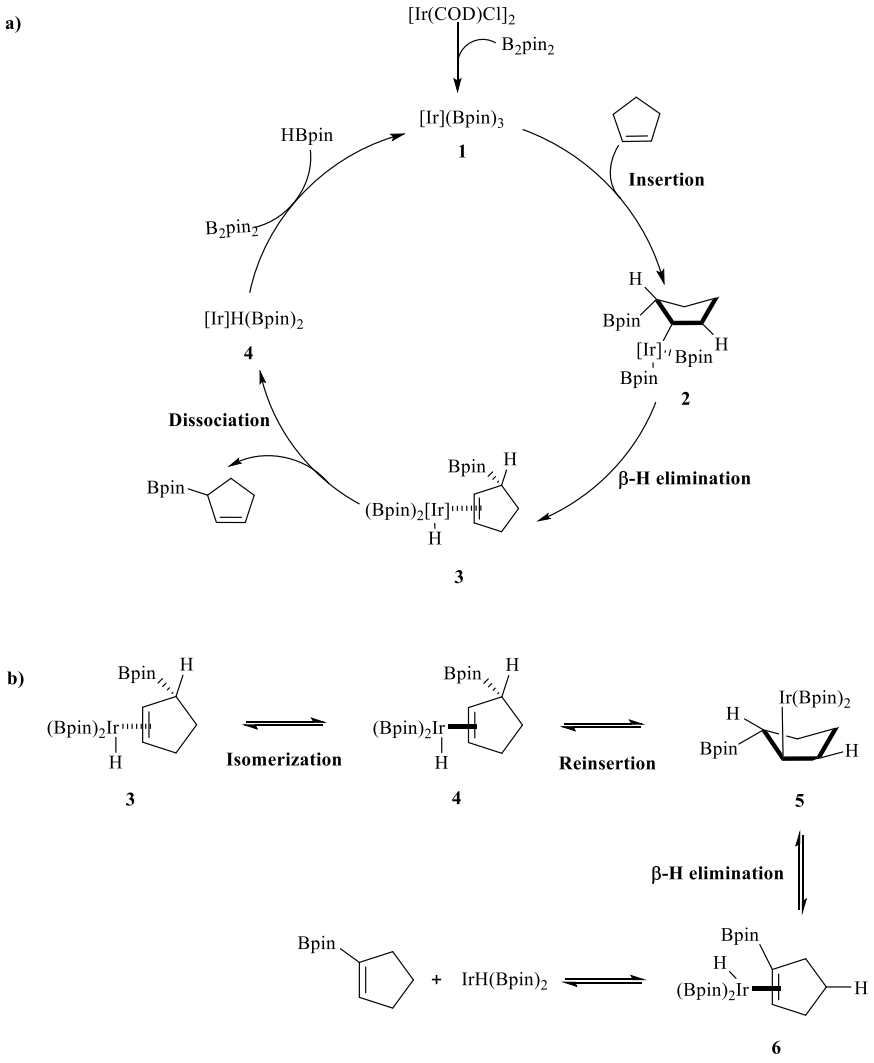

Figure 2.24. Iridium-catalysed dehydrogenative borylation mechanism of vinylarenes.

Because of the higher thermodynamic stability of the vinyl boronate then its isomeric allyl boronate, rearrangement of the initially formed cyclic allyl boronate to the corresponding vinyl boronate occurs. This isomerization of 3 occurs by dissociation of the iridium atom from the double bond followed by reassociation from the opposite face to give complex 4 then corresponding *syn*-β-H elimination gives the iridium-coordinated alkenyl boronate 6. After that, the alkenyl boronate product left the iridium-hydride complex.

Dehydrogenative borylation of acyclic olefins also proceeded through a similar mechanism.[54, 56]

In 2008, Miyaura et al. reported that one-step borylation of a vinylic C-H bond produces cyclic VBEs in the presence of the $[Ir(COD)(OMe)]_2$/dtbpy complex (Fig 2.25).[57]

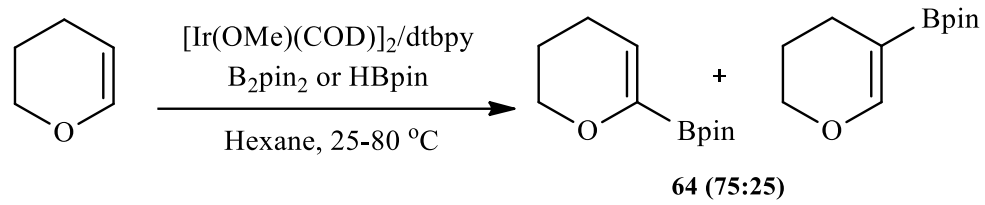

Figure 2.25. Iridium-catalysed dehydrogenative borylation of cyclic vinyl ethers.

According to the report by Ishiyama and co-workers, DHB reactions of cycloalkene-1-carboxylate derivatives with B_2pin_2 over $[Ir(COD)(OMe)]_2/AsPh_3$ catalyst system, VBEs were obtained with yields up to 96% (Fig 2.26).[58]

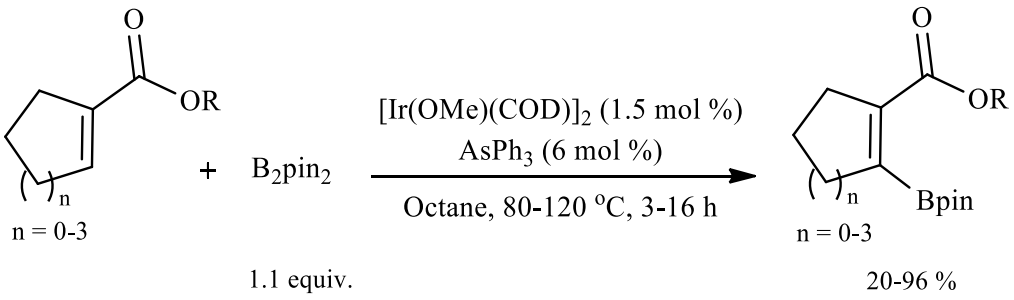

Figure 2.26. Iridium-catalysed dehydrogenative borylation of cycloalkene-1-carboxylate derivatives.

The Suzuki-Miyaura cross-coupling reaction is an exceptionally useful cross-coupling process that has been widely applied in synthetic chemistry, and boronic acids served as an effective coupling partner. Olson and Szabo showed that allyl silanes and dienes can be synthesized in one-pot process by borylation of terminal olefins with the $[Ir(COD)Cl]_2$ catalyst, followed by Suzuki reaction with an aryl or alkenyl halide (Fig 2.27).[59]

The palladium-catalysed Suzuki-Miyaura reaction between alkenyl boronic acids and free halides were also exemplified by Parkan et al. The method was used in synthesis of C-glycosylation and is successfully applied in the total synthesis of bergenin with antioxidant and antilithiatic agent (Fig 2.28).[60]

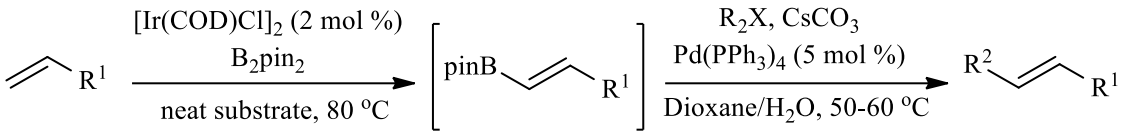

R^1 = CH_2SiMe_3, $CH(OMe)_2$, COOMe, COMe, OBu
R^2 = Aryl, Alkenyl, $CH{=}CHSiMe_3$
X = I, Br

Figure 2.27. One-pot borylation/cross-coupling reactions of terminal olefins.

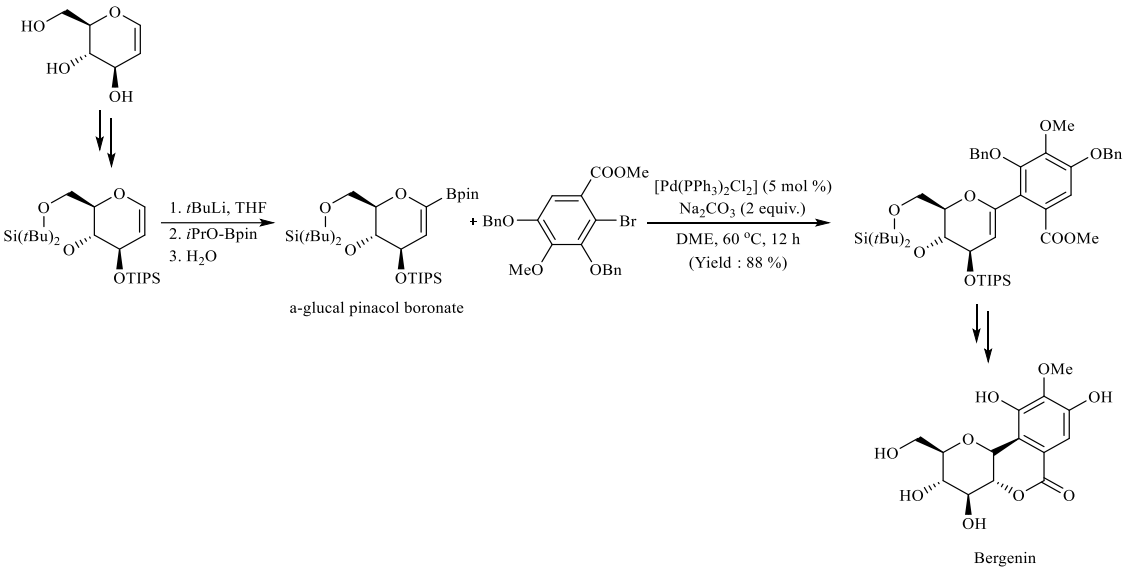

Figure 2.28. Synthesis of bergenin by Suzuki-Miyaura cross-coupling reaction.

CHAPTER 3

EXPERIMENTAL

3.1 General Information

CPME was used without any purification. THF and MTBE were dried from $LiAlH_4$ under nitrogen gas. Dioxane was distilled from benzophenone-ketyl under nitrogen gas. Acetone was distilled over $CaSO_4$. DCE was distilled over CaH_2. Distilled solvents were stored on a 4Å molecular sieve in the dark. Hexane, Cyclohexane, Toluene, Benzene, Acetonitrile, IPA, NMP and DMF were dried over 4Å molecular sieve at least 24 h. Methanol was dried over 3Å molecular sieve at least 24 h. Molecular sieves were activated by keeping at 400 °C for 12 hours prior to use. Purification of synthesized reagents were performed using column chromatography with 200-400 mesh silica gel.

3.2 Synthesis of Catalyst Complexes

3.2.1 Synthesis of $[Ir(COD)Cl]_2$

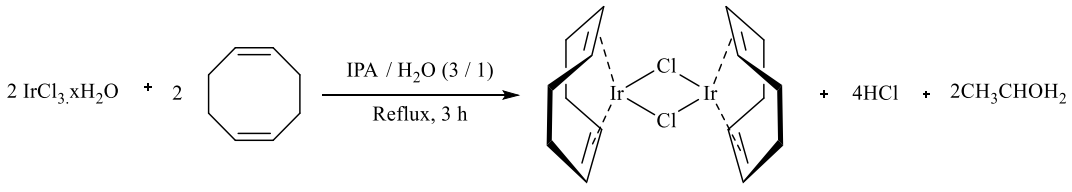

Figure 3.1. Synthesis of $[Ir(COD)Cl]_2$

$IrCl_3 \cdot XH_2O$ (2.0 g) is added into a 50-mL two-necked, round-bottomed flask charged with 1-propanol and water mixture (30 mL) with a ratio of 3/1. 1,5-Cyclooctadiene (4 mL) is dropwise added to the solution. The resulting solution is stirred in the air for 5 min. Then one neck of the flask is equipped with a water condenser, the other neck is connected to nitrogen gas. The resulting mixture is refluxed with vigorous stirring at 90 °C for 3 h, during which yellow-red solid particles are formed. After cooling the suspension to room temperature, it is concentrated, filtered, and washed with a small amount of cold methanol to remove unreacted 1,5-Cyclooctadiene, and dried under vacuum for 24 hours to afford $[Ir(COD)Cl]_2$ (red solid, yield: 1.16 g, 58 %).[61]

3.2.2 Synthesis of $[Ir(COD)OMe]_2$

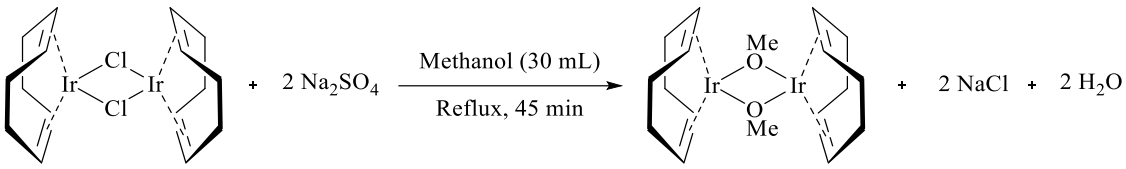

Figure 3.2. Synthesis of $[Ir(COD)OMe]_2$.

An excess of anhydrous Na_2CO_3 (1.20 g) is added into a 100-mL two-necked, round-bottomed flask charged with methanol (30 mL), and $[Ir(COD)Cl]_2$ (1.20 g) under nitrogen atmosphere. The resulting solution is refluxed with vigorous stirring at 60 °C for 45 min without boiling to prevent partial decomposition. Heating is stopped when the yellow particles turn brown. After cooling the suspension to room temperature, it is filtered and washed with water (6 x 5 mL) and a small amount of cold methanol under nitrogen atmosphere to get a yellow precipitate. Finally, it is dried under vacuum for 24 hours and stored in an inert atmosphere to afford $[Ir(COD)OMe]_2$ (yellow solid, yield: 1.13 g, 97 %).[61]

3.2.3 Synthesis of *N*-Hetero Carbene Complexes

3.2.3.1 Preparation of HCl Solution (4 M) in Dioxane

Acetyl chloride (2.84 mL) was added into a 50-mL round bottomed flask containing dry dioxane (10 mL). MeOH (1.6 mL) was dropwise added to the solution to obtain 4 M of HCl solution in Dioxane.[62]

3.2.3.2 Synthesis of Imidazole Salts

3.2.3.2.1 Method 1

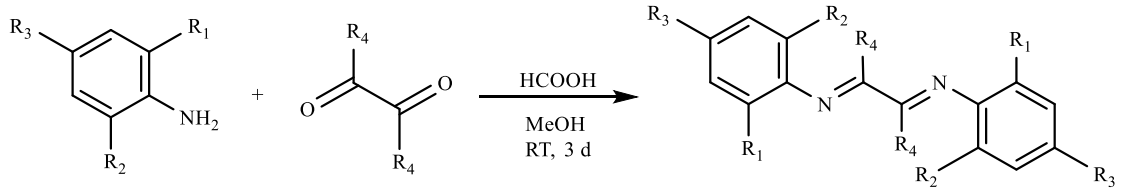

R_1, R_2, R_3, R_4 = Me, Me, Me, H
R_1, R_2, R_3, R_4 = i-Pr, i-Pr, H, H
R_1, R_2, R_3, R_4 = Me, Me, H, H
R_1, R_2, R_3, R_4 = Me, H, H, H
R_1, R_2, R_3, R_4 = Me, Me, H, Me

R_1, R_2, R_3, R_4 = Me, Me, Me, H
R_1, R_2, R_3, R_4 = i-Pr, i-Pr, H, H
R_1, R_2, R_3, R_4 = Me, Me, H, H
R_1, R_2, R_3, R_4 = Me, H, H, H
R_1, R_2, R_3, R_4 = Me, Me, H, Me

Figure 3.3. Synthesis of diimine derivatives.

Aniline derivative (16.9 mmol, 2.0 equiv) was added into a 50-mL round-bottomed flask containing methanol (16.3 mL). The solution was cooled to 0 °C, then a solution of 40% glyoxal in water (975 µL, 8.45 mmol, 1.0 equiv) and one drop of formic acid were added. The solution was warmed to ambient temperature and stirred for two or three days and controlled with TLC. The suspension was filtrated over PTFE, washed with a small amount of methanol, and diethyl ether to afford *N*,*N*'-dimesitylethanediimine (yellow powder, yield: 1.72g, 68.8%), *N*,*N*'-bis(2,6-diisopropylphenyl)ethane-1,2-

diimine (yellow powder, yield: 1.91 g, 60%), *N*,*N*'-bis(2,6-dimethylphenyl)ethane-1,2-diimine (yellow powder, yield: 1.42 g, 63.5%), *N*,*N*'-bis(o-methylphenyl)ethane-1,2-diimine (yellow-orange powder, yield: 1.22 g, 61%), *N*,*N*'-bis(2,6-dimethylphenyl)butane-2,3-diimine (69%).[63]

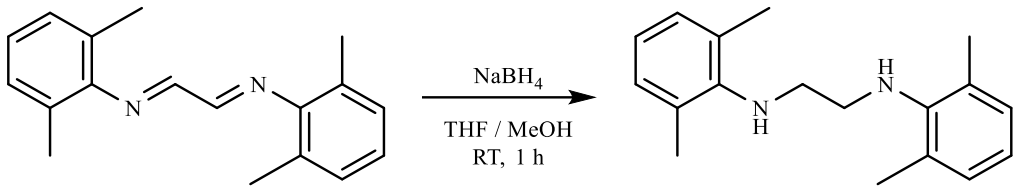

Figure 3.4. Synthesis of diamine complex.

N,*N*'-bis(2,6-dimethylphenyl)ethane-1,2-diimine (1.0 mmol) was added into a 25 mL round-bottomed flask containing THF (6 mL) and MeOH (4 mL). The solution was cooled to 0 °C, then $NaBH_4$ (8.0 mmol) was added in a period of 1 hour. The solution was warmed to ambient temperature and stirred for 1 hour and controlled with TLC. It was quenched with saturated NH_4Cl solution (10.0 mL). Extraction process was applied with diethyl ether and the solvent dried under reduced pressure to obtain *N*,*N'*-bis(2,6-dimethylphenyl)ethane-1,2-diamine (light yellow solid, yield: g, 96%).[64]

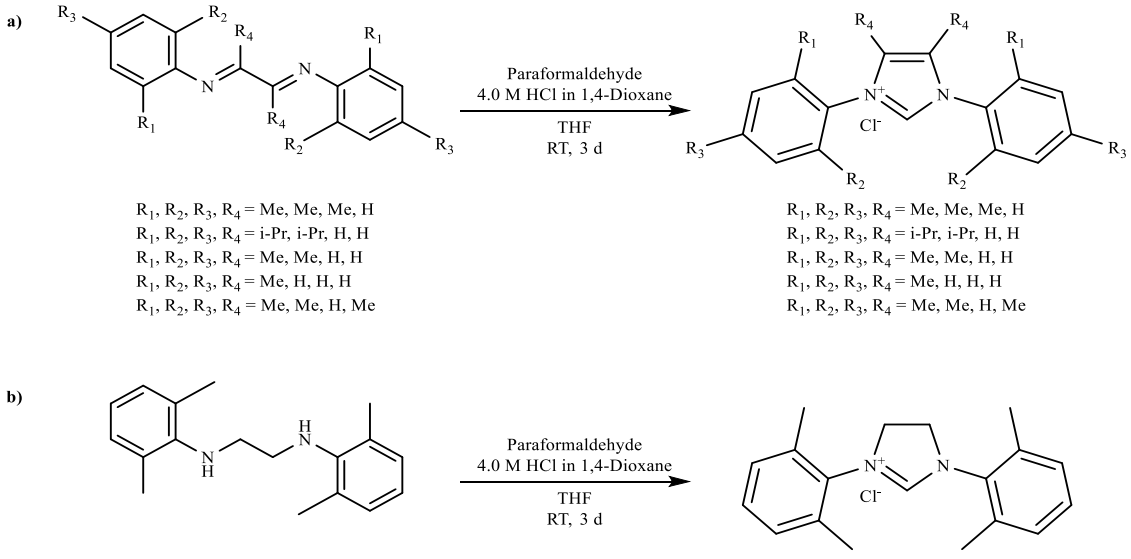

Figure 3.5. Synthesis of imidazole salts by method 1.

Paraformaldehyde (119.5 mg, 3.98 mmol, 1.0 equiv) was added into a 50-mL round-bottomed flask containing solution of 4M Hydrochloric acid in dioxane (1.80 mL, 7.16 mmol, 1.8 equiv) and stirred until the white solid was completely dissolved. THF (30 mL) and diimine derivative (3.98 mmol, 1.0 equiv) were added slowly. The solution

was stirred at 40 °C for three days and controlled with TLC. Then the suspension was cooled to room temperature and the precipitate was collected by filtration over PTFE, washed with THF and diethyl ether to afford 1,3-bis-(2,4,6-trimethylphenyl)imidazole-3-ium chloride (off-white powder, yield: 630.1 mg, 51.8%), 1,3-bis-(2,6-diisopropylphenyl) imidazole-3-ium chloride (white powder, yield: 812.4 mg, 47%), 1,3-bis-(2,6-dimethylphenyl)imidazole-3-ium chloride (off-white powder, yield: 452.6 mg, 41%), 1,3-bis-(o-methylphenyl)imidazole-3-ium chloride (brown powder, yield: 623.4 g, 55%), 1,3-bis(2,6-dimethylphenyl)-4,5-dimethyl-1H-imidazol-3-ium chloride (off-white powder, yield: 272.8 mg, 20%), 1,3-bis(2,6-dimethylphenyl)-4,5-dihydro-1H-imidazol-3-ium chloride (light brown solid, 64%).[63]

3.2.3.2.2 Method 2

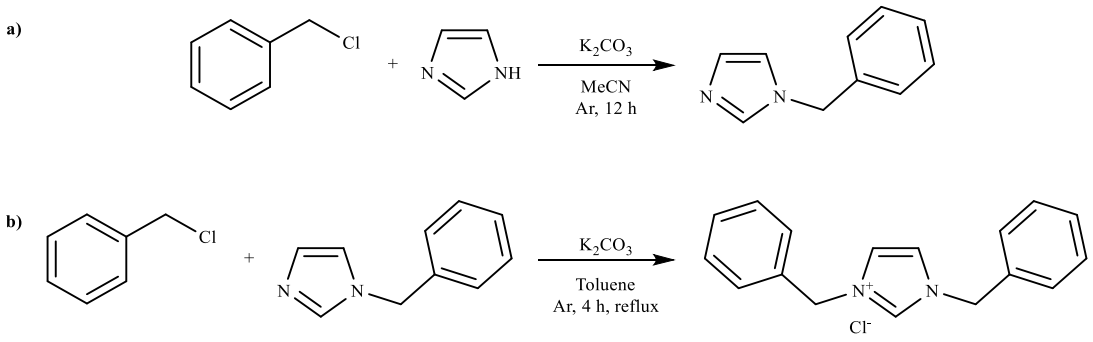

Figure 3.6. Synthesis of 1-benz1,3-dibenzyl-1H-imidazol-3-ium chloride yl-1H-imidazole.

Imidazole (340 mg, 5 mmol, 1.0 equiv) and K_2CO_3 (760 mg, 11 mmol, 2.2 equiv) was added into a 50-mL two-necked, round-bottomed flask containing MeCN (10 mL) and stirred at ambient temperature for 1 h. Benzyl chloride (633 mg, 5 mmol, 1.0 equiv) was added to the solution and stirred under reflux conditions for 12 h. The mixture was filtered, and dried under reduced pressure to obtain 1-benzyl-1H-imidazole (474.6 mg, 60% yield).

The obtained crude product was added into a 50-mL two-necked, round-bottomed flask containing toluene (5 mL). Additional benzyl chloride (633 mg, 5 mmol, 1.0 equiv) was added and stirred at reflux conditions for 4 h. After cooling to room temperature, the

solution concentrated as yellow oil, washed with diethyl ether (2 × 20 mL), and dried under reduced pressure to obtain 1,3-dibenzyl-1H-imidazol-3-ium chloride (358 mg, 1.25 mmol, 48% yield).[65]

3.2.3.3 Synthesis of Ir-NHC Complexes:

3.2.3.3.1 Method 1

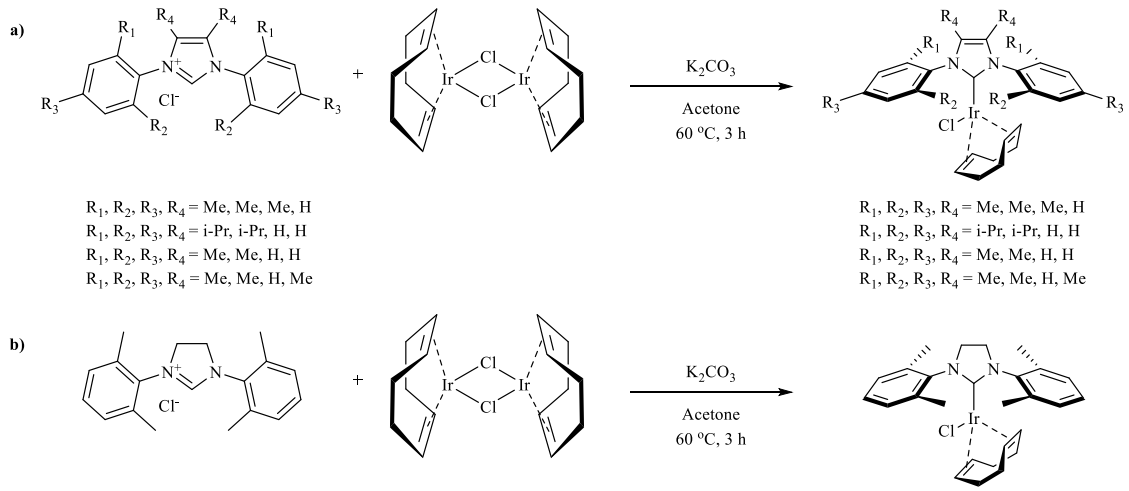

Figure 3.7. Synthesis of Ir-NHC complexes with method 1.

A mixture of imidazolium chloride salt derivative (0.178 mmol, 2.0 equiv), $[Ir(COD)Cl]_2$ (60 mg, 0.089 mmol, 1.0 equiv) and K_2CO_3 (74 mg, 0.534 mmol, 6.0 equiv) was added into a vial, under dry air. Acetone (3.0 mL) was added to the mixture and stirred at 60 °C for 20 h and controlled with TLC. After reaction completed the solvent was removed in vacuo and DCM was added (3 mL). The mixture was filtered through a pad of silica and washed with DCM until the filtrate becomes colourless. The solvent was removed under reduced pressure to obtain Ir(COD)(IMes)Cl (yellow-orange microcrystalline solid, yield: 55.4 mg, 48.3%), Ir(COD)(IPr)Cl (orange microcrystalline solid, yield: 69.7 mg, 53.8%), Ir(COD)(IXy)Cl (yellow microcrystalline solid, yield: 42.7 mg, 39.1%), Ir(COD)(SIXy)Cl (orange microcrystalline solid, yield: 91.1 mg, 84%), Ir(COD)(IXy^{Me})Cl (orange microcrystalline solid, 62.4 mg, 62%).[66]

3.2.3.3.2 Method 2

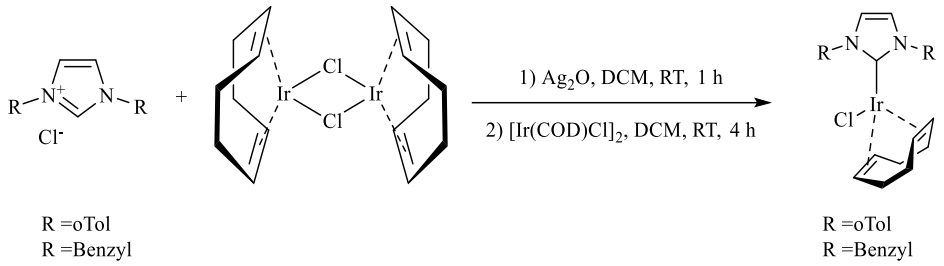

Figure 3.8. Synthesis of Ir-NHC complexes with method 2.

A mixture of imidazolium chloride salt derivative (0.08 mmol, 2.0 equiv) and Ag_2O (0.04 mmol, 9.5 mg, 1.0 equiv) was added into a vial containing DCM (2 mL) and stirred at ambient temperature for 1 h shielded from light. Then $[Ir(COD)Cl]_2$ (0.04 mmol, 25 mg, 1.0 equiv) was added to the suspension and stirred at ambient temperature for additional 4 h and controlled with TLC. The mixture was filtered through Celite. The obtained solid was washed with DCM (2 × 2 mL) and the solvent was removed in vacuo. The residue was purified by column chromatography on silica gel with DCM to obtain Ir(COD)(IBz)Cl (yellow solid, yield: 58.7 mg, 76%), Ir(COD)(Io-Tol)Cl (yellow crystalline solid, yield: 30.0 mg, 60.4%).[67]

3.2.4 Synthesis of Ir(COD)(Phen)Cl

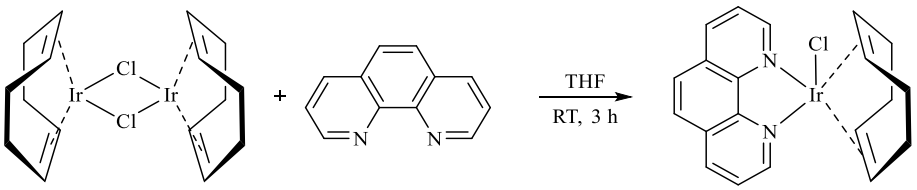

Figure 3.9. Synthesis of Ir(COD)(Phen)Cl.

$[Ir(COD)Cl]_2$ (50 mg, 0.074 mmol) and Phenanthroline (27 mg, 0.148 mmol) were added into 25 mL round-bottomed flask containing THF (5 mL) under nitrogen atmosphere. The reaction mixture was stirred at ambient temperature for 3 hours. The

solvent was removed under reduced pressure to obtain Ir(COD)(Phen)Cl (dark purple solid, yield: 76.2 mg, 99%).[68]

3.3 General Procedure of Borylation Reaction

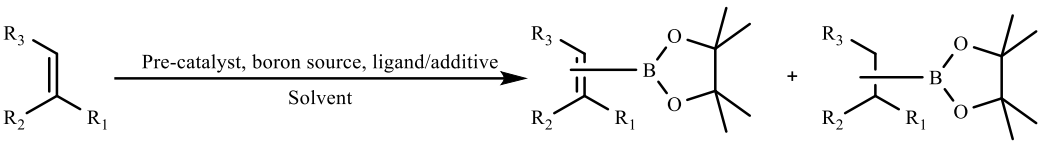

1a = R_1, R_2, R_3 = Me, H, H
1b = R_1, R_2, R_3 = Me, Me, H
1c = R_1, R_2, R_3 = H, H, H
1d = R_1, R_2, R_3 =H, Cyh.
1e = R_1, R_2, R_3 = C_8H_{17}, H, H
1f = R_1, R_2, R_3 = Ph, H, H

Figure 3.6. General borylation reaction.

3.3.1 Method with Reactor System (M1)

Figure 3.7. Reactor system used in M1.

In a glovebox system, B_2pin_2, ligand, base and pre-catalyst were added into a pyrex insert of reactor. After addition of the solvent, the mixture was stirred magnetically for 3 minutes at ambient temperature for pre-activation of catalyst. Then the glass insert

was placed in a 25 mL stainless steel reactor was sealed and taken out of glovebox. Then the reactor was attached to an olefin tank through a quick disconnect apparatus and pressurized with propylene or ethylene gas, The reaction mixture was stirred in a preheated oil bath for 16 h. At the end of the reaction, it was cooled to the ambient temperature and an internal standard was added. If the reaction conditions included a base, extraction process was applied with EtOAc or DCM. Calculations for conversion and yield are performed with an internal standard on GC.

3.3.2 Method Using Sealed Cap in Glovebox (M2)

A 50-mL round-bottomed flask was purged with 6 grade argon and solvent was added into it. Then, it was cooled to -60 °C with an immersion cooler. A 50-mL three-necked, round-bottomed flask was purged with argon and cooled to -60 °C with an immersion cooler and gaseous reactant was liquefied in this flask by continuous argon flow. Required amount of liquified olefin was transferred to the flask containing cold solvent using a syringe. Syringe was washed twice with the liquified olefin prior to final drawing the olefin to achieve required coldness before transfer. The prepared olefin solution was placed in a box containing molecular sieve stored at -20 °C.

In a glovebox system, HBpin, base and pre-catalyst were added into a 10 mL thick-wall-sealed cap glass tube. After addition of the solvent, the tube was capped with a septum and then the mixture was stirred for 3 minutes at ambient temperature for pre-activation of catalyst. After it was taken out of glovebox, the reaction tube was cooled to -20 °C with an immersion cooler, the olefin solution was added to the tube at -20 °C, and finally the septum was removed and the tube was sealed with a teflon lined screw cap immediately. The reaction mixture was stirred magnetically in a preheated oil bath for 16 h. At the end of the reaction, it was cooled to ambient temperature and an internal standard was added. If the reaction conditions included a base, an extraction process was applied with EtOAc or DCM. Calculations for conversion and yield were determined by internal standard method on GC.

3.3.3 Method Using Sealed Cap out Glovebox (M3)

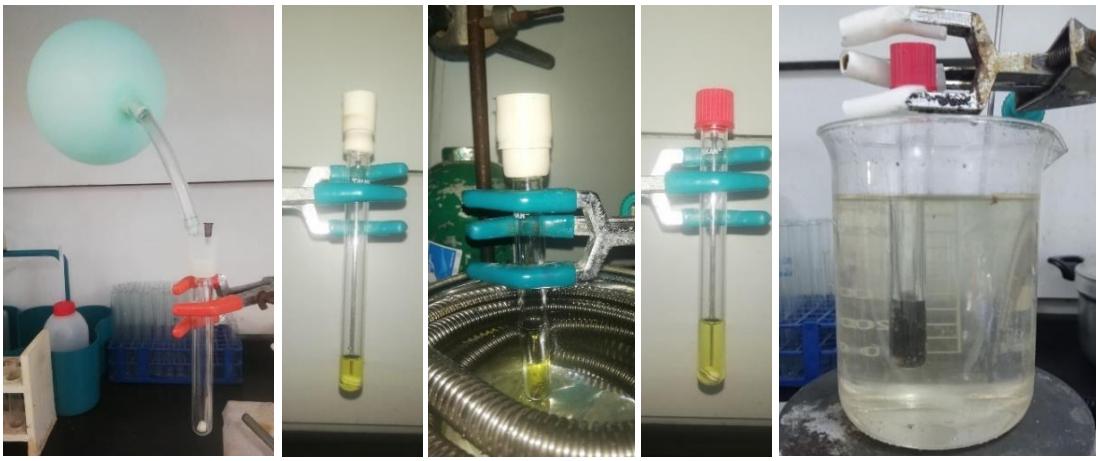

Figure 3.8. System used in M3.

B_2pin_2, ligand, base and pre-catalyst were added into a 10 mL thick-wall-sealed cap glass tube or 4 mL vial, capped with a septum, and purged with 6 grade argon through a septum. After addition of the solvent, the mixture was stirred for 3 minutes at ambient temperature for pre-activation of catalyst with argon flow. The reaction tube was cooled to -20 °C with an immersion cooler. Then, the reactant solution was added to the tube at -20 °C through the septum by precooled syringe and the tube was sealed with a teflon lined screw cap immediately promptly. The reaction mixture was stirred magnetically in a preheated oil bath for 16 h. At the end of the reaction, it was cooled to ambient temperature and an internal standard was added. Calculations for conversion and yield were determined by internal standard method on GC.

No cooling process was performed for the reaction systems comprising olefins that were liquid at ambient temperature.

3.4. Suzuki Reaction of 2ba with 4-Iodoanisole

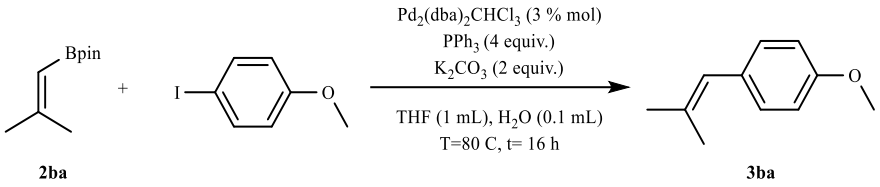

Figure 3.9. Suzuki coupling reaction with 4-Iodoanisole.

At the end of the borylation reaction of isobutylene, the glass tube was opened and charged with charged with $Pd_2(dba)_3CHCl_3$ (7.9 mg, 0.0075 mmol), PPh_3 (8.0 mg, 0.30 mmol) and K_2CO_3 (69.1 mg, 0.50 mmol) under argon atmosphere. THF (1.0 mL), water (0.1 mL) and 4-Iodoanisole (58.5 mg, 0.25 mmol) was added into the mixture. The tube was sealed, and the reaction mixture was stirred in a preheated oil bath for 16 h. Analysis was performed on GC/MS.

3.5. Suzuki Reaction of 2ba with 4-Bromoacetophenone

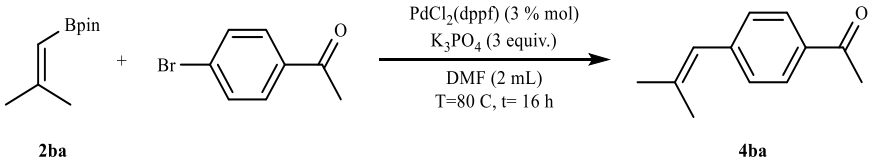

Figure 3.10. Suzuki coupling reaction with 4-Bromoacetophenone.

At the end of the borylation reaction of isobutylene, the glass tube was opened and charged with $PdCl_2(dppf)$ (5.3 mg, 0.0075 mmol) and K_3PO_4 (162.5 mg, 0.75 mmol). DMF (2.0 mL), and 4-Bromoacetophenone (52.6 mg, 0.25 mmol) consecutively under argon atmosphere. The tube was sealed, and the reaction mixture was stirred in a preheated oil bath for 16 h. Analysis was performed on GC/MS.[52]

3.6 Characterization Techniques

3.6.1 GC Method

The samples were analysed by GC (Thermo Scientific TRACE 1300 GC or Shimadzu GC2010 Plus on a 30 m, 0.25 mm capillary column, 5% dimetylsiloxane, 95% phenyldimethylsiloxane with a 0.25 μm film thickness and FID detector) and GC/MS (HP GC/MS 6890/5973N on a HP-5MS, 30 m, 0.25 mm capillary column, 5% phenylmethoxysiloxane, 95% dimethylpolysiloxane with 0.25 μm film thickness). The GC program was applied during the analysis: the column temperature was 40 °C at the start of the program and it was heated at a rate of 10 °C/min up to 300 °C with the split ratio of 20 to 1, then it was kept at this temperature for 15 min.

3.6.2 Calculation of Reactant and Product Amounts on GC

To calculate the amount of remaining reactant and obtained product, the response factor [5] was determined individually. To determine the RF, a known amount of standard compound and internal standard were dissolved in DCM and analysed by GC. After the analysis, the RF of that compound was calculated by using the following equation (3.1).

$$RF = \frac{\text{Internal standard area}}{\text{Compound area}} \times \frac{\text{Compound amount}}{\text{Internal standard amount}} \quad (3.1)$$

Some amount of sample was taken from the reaction vessel which contains dodecane or hexadecane as an internal standard. The sample diluted with DCM and analysed with GC. After the analysis, the amount of compound was calculated by using the following equation (3.2).

$$\text{Amount of compound} = \frac{\text{Internal standard amount}}{\text{Internal standard area}} \times \text{RF} \times \text{Compound area} \quad (3.2)$$

3.6.3 Calculation of Yield on GC

Yield of the product was calculated by using the following equation (3.3). Where $(n, product)_f$ is the mmol of the product calculated after the reaction and $(n, reactant)_i$ is the mmol of the reactant at the beginning of the reaction.

$$\text{Yield \%} = \frac{(n, product)_f}{(n, reactant)_i} \times 100 \quad (3.3)$$

3.6.4 NMR Method

NMR analyses were recorded by Varian VnmrJ 400 spectrometer in deuterated chloroform or deuterated DMSO. Chemical shifts are reported in ppm downfield from Me_4Si.

3.7 Spectral Data for the Prepared Compounds

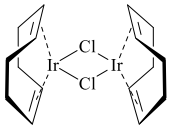

Bis(1,5-cyclooctadiene)diiridium(I) dichloride: ^{1}H NMR (400 MHz, $CDCl_3$) δ: 4.36 – 4.09 (m, 8H, C*H*$_2$cod), 2.37 – 2.16 (m, 8H, C*H*cod), 1.58 – 1.49 (m, 8H, C*H*$_2$cod); ^{13}C NMR (100 MHz, $CDCl_3$) δ: 62.18, 31.75.

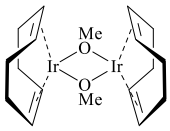

(1,5-Cyclooctadiene)(methoxy)iridium(I) dimer: ^{1}H NMR (400 MHz, $CDCl_3$) δ: 3.56 – 3.41 (m, 8H, C*H*cod), 3.22 (s, 6H, Me), 2.20 (m, 8H, CH_2cod), 1.35 (m, 8H, CH_2cod); ^{13}C NMR (100 MHz, $CDCl_3$) δ: 56.34, 31.36.

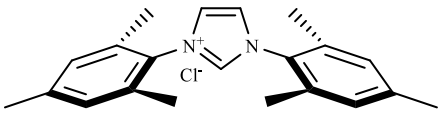

1,3-dimesityl-1H-imidazol-3-ium chloride: ^{1}H NMR (400 MHz, $CDCl_3$) δ: 10.95 (s, 1H), 7.61 (s, 1H), 7.26 (s, 1H), 7.01 (s, 2H), 2.33 (s, 3H), 2.17 (s, 6H).; ^{13}C NMR (100 MHz, $CDCl_3$) δ: 138.33, 131.92, 129.87, 125.96, 20.72, 19.24.

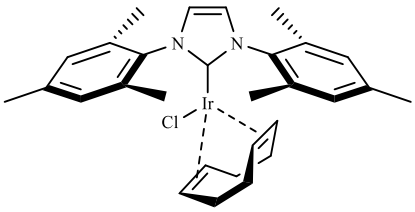

Ir(COD)(IMes)Cl: ^{1}H NMR (400 MHz, $CDCl_3$) δ: 6.99 (br, 2H, *H*Ar), 6.95 (br, 2H, *H*Ar), 6.93 (s, 2H, NC*H*), 4.12 (m, *J* = 4.5, 2.6 Hz, 2H, *H*cod), 2.98 – 2.91 (m, *J* = 5.1 Hz, 2H, *H*cod), 2.33 (s, 12H, Me), 2.14 (s, 6H, Me), 1.78 – 1.55 (m, 5H, *H*cod), 1.38 – 1.16 (m, 7H *H*cod).

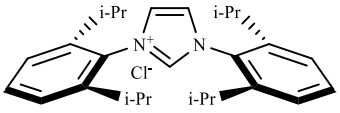

1,3-bis(2,6-diisopropylphenyl)-1H-imidazol-3-ium chloride: ^{1}H NMR (400 MHz, $CDCl_3$) δ: 9.97 (s, 1H), 8.12 (s, 2H), 7.55 (t, *J* = 7.8 Hz, 2H), 7.32 (d, *J* = 7.8 Hz, 4H), 2.41 (dt, *J* = 13.7, 6.8 Hz, 4H), 1.26 (d, *J* = 6.8 Hz, 12H), 1.21 (d, *J* = 6.9 Hz, 12H); ^{13}C NMR (101 MHz, $CDCl_3$) δ: 144.96, 138.33, 132.15, 129.80, 126.80, 124.70, 29.10, 24.73, 23.70.

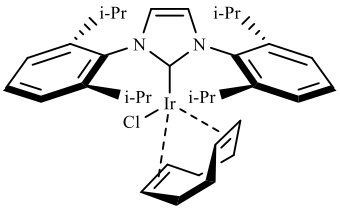

Ir(COD)(IPr)Cl: ^{1}H NMR (400 MHz, $CDCl_3$) δ: 7.45 (t, *J* = 7.7 Hz, 2H, *H*Ar), 7.24 (d, *J* = 27.5 Hz, 4H, *H*Ar), 6.99 (s, 2H, NC*H*), 4.23 – 4.10 (m, 2H, *H*cod), 3.41 (br, 2H, C*H*(CH3)2), 2.89 – 2.84 (m, 2H, *H*cod), 2.68 (br, 2H, C*H*(CH3)2), 1.74 – 1.60 (m, 2H, *H*cod), 1.58 – 1.15 (m, 21H, *H*cod + Me), 1.10 (d, *J* = 6.8 Hz, 12H, CH(C*H*3)2).

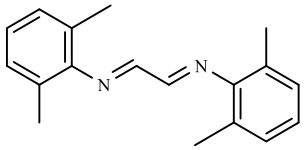

N1,N2-bis(2,6-dimethylphenyl)ethane-1,2-diimine: ^{1}H NMR (400 MHz, $CDCl_3$) δ: 8.12 (s, 2H), 7.10 (d, *J* = 7.7 Hz, 4H), 7.01 (t, *J* = 8.2, 6.7 Hz, 2H), 2.19 (s, 12H).

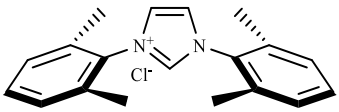

1,3-bis(2,6-dimethylphenyl)-1H-imidazol-3-ium chloride: ^{1}H NMR (400 MHz, $CDCl_3$) δ: 11.13 (s, 1H), 7.60 (s, 2H), 7.34 (t, 2H), 7.20 (d, J = 7.6 Hz, 2H), 2.21 (s, 12H).

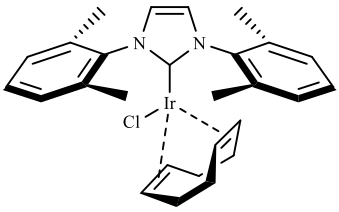

Ir(COD)(IXy)Cl: ^{1}H NMR (400 MHz, $CDCl_3$) δ: 7.28 (t, *J* = 7.6 Hz, 2H), 7.22 – 7.12 (m, 4H), 6.98 (s, 2H), 4.17 – 4.06 (m, 2H, C*H*cod), 2.97 – 2.88 (m, 2H, C*H*cod), 2.38 (s,

6H), 2.19 (s, 6H), 1.65 (m, *J* = 28.2, 15.6, 9.5 Hz, 4H, C*H*$_2$cod), 1.37 – 1.19 (m, 4H, C*H*$_2$cod).

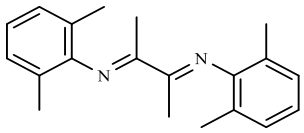

N2,N3-bis(2,6-dimethylphenyl)butane-2,3-diimine: ^{1}H NMR (400 MHz, $CDCl_3$) δ: 7.06 (d, *J* = 7.7 Hz, 4H), 7.06 – 6.80 (m, 2H), 2.02 (d, *J* = 0.8 Hz, 18H).

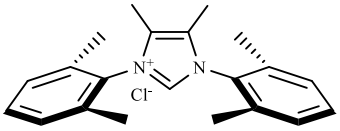

1,3-bis(2,6-dimethylphenyl)-4,5-dimethyl-1H-imidazol-3-ium chloride: ^{1}H NMR (400 MHz, $CDCl_3$) δ: 10.76 (s, 1H), 7.41 – 7.30 (m, 2H), 7.22 (d, J = 7.6 Hz, 4H), 2.14 (s, 10H), 2.05 (s, 5H).

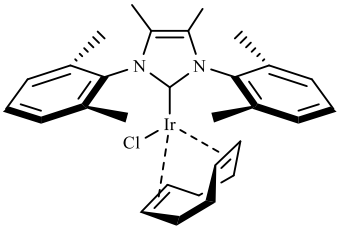

Ir(COD)(IXy^{Me})Cl: ^{1}H NMR (400 MHz, $CDCl_3$) δ: 7.28 (t, *J* = 7.5 Hz, 2H), 7.17 (dd, *J* = 14.6, 7.4 Hz, 4H), 4.05 – 3.98 (m, 2H), 3.03 – 2.95 (m, 2H), 2.33 (s, 6H), 2.07 (s, 6H), 1.82 (s, 6H), 1.62 – 1.51 (m, 4H), 1.29 – 1.16 (m, 4H).

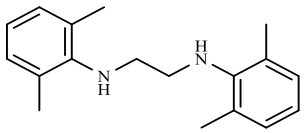

N1,N2-bis(2,6-dimethylphenyl)ethane-1,2-diamine: ^{1}H NMR (400 MHz, $CDCl_3$) δ: 7.00 (d, J = 7.6 Hz, 4H), 6.83 (t, 2H), 3.20 (s, 4H), 2.30 (s, 12H).

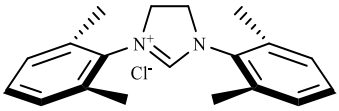

1,3-bis(2,6-dimethylphenyl)-4,5-dihydro-1H-imidazol-3-ium chloride: ^{1}H NMR (400 MHz, $CDCl_3$) δ: 9.39 (s, 1H), 7.25 (dd, J = 8.8, 6.4 Hz, 2H), 7.14 (d, J = 7.6 Hz, 4H), 4.61 (s,4H), 2.44 (s, 12H).

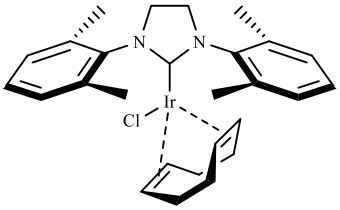

Ir(COD)(SIXy)Cl: ^{1}H NMR (400 MHz, $CDCl_3$) δ: 7.42 – 6.91 (m, 2H), 7.15 (dd, *J* = 12.5, 7.1 Hz, 4H), 4.26 – 4.01 (m, 2H), 3.93 (s, 4H), 3.25 – 2.98 (m, 2H), 2.59 (s, 6H), 2.38 (s, 6H), 1.66 – 1.53 (m, 4H), 1.36 – 1.17 (m, 4H).

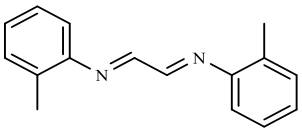

N1,N2-di-o-tolylethane-1,2-diimine: ^{1}H NMR (400 MHz, $CDCl_3$) δ: 8.30 (s, 2H, C*H*N), 7.37 – 7.12 (m, 6H, arom), 7.00 (dd, *J* = 7.6, 1.4 Hz, 2H, arom), 2.39 (s, 6H, CH_3).

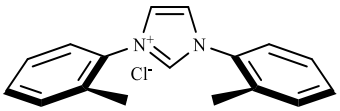

1,3-di-o-tolyl-1H-imidazol-3-ium chloride: ^{1}H NMR (400 MHz, DMSO-d_6) δ: 9.93 (s, 1H), 8.34 (s, 2H), 7.65 (d, *J* = 4.4 Hz, 2H), 7.50 (d, *J* = 24.1 Hz, 6H), 2.30 (s, 6H).

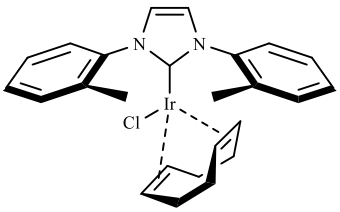

Ir(COD)(Io-Tol)Cl: ^{1}H NMR (400 MHz, $CDCl_3$) δ: 8.08 (s, 2H), 7.47 (m, *J* = 16.7, 14.8, 7.2, 1.9 Hz, 6H), 7.09 (s, 2H), 4.30 – 4.18 (m, 2H), 2.57 – 2.48 (m, 2H), 2.23 (s, 6H), 1.72 - 1.51 (m, 4H), 1.49 – 1.09 (m, 4H).

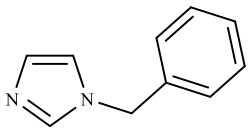

1-benzyl-1H-imidazole: ^{1}H NMR (400 MHz, $CDCl_3$) δ: 7.54 (s, 1H, *H*Ar), 7.40 – 7.29 (m, 3H, *H*Ar), 7.18 – 7.11 (m, 2H, *H*Ar), 7.09 (t, *J* = 1.0 Hz, 1H, *H*imi), 6.90 (t, *J* = 1.3 Hz, 1H, *H*imi), 5.12 (s, 2H, C*H*2).

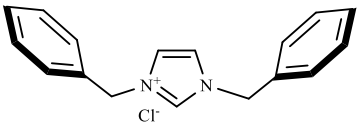

1,3-dibenzyl-1H-imidazol-3-ium chloride: ^{1}H NMR (400 MHz, $CDCl_3$) δ: 10.92 (s, 1H), 7.41 (dd, *J* = 6.6, 2.8 Hz, 4H), 7.41 (dd, J = 6.6, 2.9 Hz, 6H), 7.22 (d, *J* = 1.5 Hz, 2H), 5.50 (s, 4H).

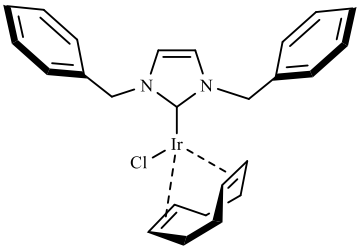

Ir(COD)(IBz)Cl: ^{1}H NMR (400 MHz, $CDCl_3$) δ: 7.39 – 7.27 (m, 10H, *H*Ar), 6.65 (s, 2H, C=C*H*N), 5.76 (d, *J* = 14.8 Hz, 2H, ArCH_2N), 5.59 (d, *J* = 14.8 Hz, 2H, ArCH_2N),

4.64 (dd, J = 5.2, 2.3 Hz, 2H, *H*cod), 2.99 – 2.90 (m, 2H, *H*cod), 2.26 – 2.05 (m, 4H, *H*cod), 1.75 – 1.66 (m, 2H, *H*cod), 1.59 – 1.49 (m, 4H, *H*cod).

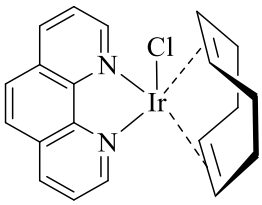

Ir(COD)(Phen)Cl: ^{1}H NMR (400 MHz, $CDCl_3$) δ: 8.65 (dd, J = 5.3, 1.3 Hz, 2H), 8.50 (dd, J = 8.1, 1.3 Hz, 2H), 7.93 (s, 2H), 7.79 (dd, J = 8.1, 5.3 Hz, 2H), 3.93 – 3.88 (m, 4H), 2.48 − 2.40 (m, 4H), 1.98 – 1.57 (m, 4H).

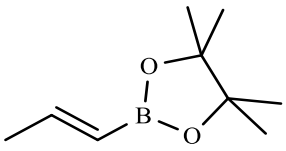

2aa

(E)-4,4,5,5-tetramethyl-2-(prop-1-en-1-yl)-1,3,2-dioxaborolane: MS (EI, m/z): 168 (10), 154 (4), 153 (38), 152 (8), 111 (20), 110 (8), 109 (6), 95 (5), 85 (24), 83 (13), 82 (81), 70 (5), 69 (100), 68 (39), 67 (22), 59 (15), 58 (7), 57 (10), 56 (7), 55 (8).

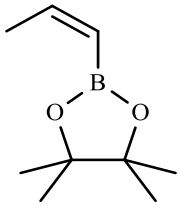

2ab

(Z)-4,4,5,5-tetramethyl-2-(prop-1-en-1-yl)-1,3,2-dioxaborolane: MS (EI, m/z): 168 (6), 153 (24), 152 (6), 111 (12), 110 (8), 109 (4), 97 (3), 95 (4), 85 (22), 83 (14), 82 (71), 70 (4), 69 (100), 68 (38), 67 (20), 59 (27), 58 (7), 57 (10), 55 (10), 53 (3).

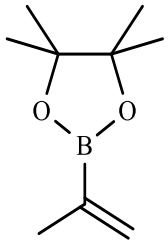

2ac

4,4,5,5-tetramethyl-2-(prop-1-en-2-yl)-1,3,2-dioxaborolane: MS (EI, m/z): 168 (14), 154 (5), 153 (68), 152 (17), 111 (33), 110 (12), 109 (6), 95 (8), 85 (33), 83 (12), 82 (100), 81 (5), 69 (92), 68 (31), 67 (36), 59 (36), 58 (12), 57 (16), 55 (14), 53 (5).

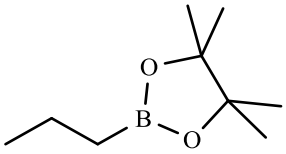

2ad

4,4,5,5-tetramethyl-2-propyl-1,3,2-dioxaborolane: MS (EI, m/z): 156 (7), 155 (81), 154 (16), 127 (7), 113 (18), 112 (7), 100 (4), 87 (11), 86 (7), 85 (44), 84 (67), 83 (19), 71 (100), 70 (40), 69 (32), 59 (49), 58 (27), 57 (18), 56 (7), 55 (18).

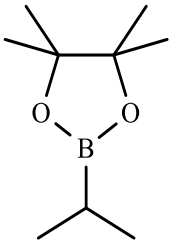

2ae

2-isopropyl-4,4,5,5-tetramethyl-1,3,2-dioxaborolane: MS (EI, m/z): 170 (6), 155 (56), 154 (13), 113 (10), 112 (23), 111 (8), 86 (7), 85 (75), 84 (100), 83 (60), 71 (67), 70 (68), 69 (40), 59 (62), 58 (19), 57 (22), 56 (30), 55 (30), 53 (8), 45 (7).

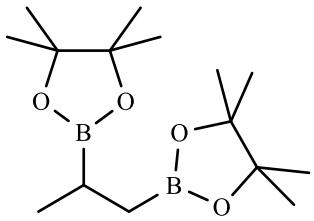

2af

2,2'-(propane-1,2-diyl)bis(4,4,5,5-tetramethyl-1,3,2-dioxaborolane): MS (EI, m/z): 294 (4), 279 (8), 237 (7), 236 (5), 194 (8), 193 (5), 179 (11), 178 (5), 153 (6), 113 (4), 101 (5), 85 (15), 84 (100), 83 (49), 80 (4), 69 (21), 67 (10), 59 (10), 57 (7), 55 (23).

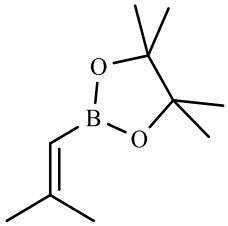

2ba

4,4,5,5-tetramethyl-2-(2-methylprop-1-en-1-yl)-1,3,2-dioxaborolane: MS (EI, m/z): 167 (21), 166 (5), 139 (8), 125 (29), 124 (17), 123 (4), 109 (5), 101 (7), 97 (8), 96 (24), 85 (13), 84 (5), 83 (100), 82 (36), 81 (10), 69 (3), 67 (5), 59 (13), 57 (7), 55 (10).

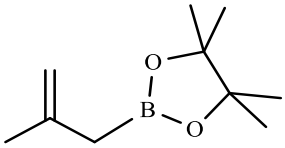

2bb

2-(tert-butyl)-4,4,5,5-tetramethyl-1,3,2-dioxaborolane: MS (EI, m/z): 167 (22), 125 (79), 124 (39), 123 (18), 109 (22), 97 (30), 96 (18), 85 (36), 84 (10), 83 (63), 82 (28), 81 (34), 69 (22), 67 (13), 59 (34), 58 (13), 57 (22), 56 (23), 55 (100), 54 (9).

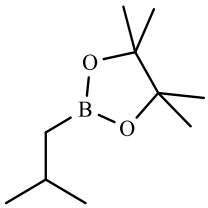

2bc

2-isobutyl-4,4,5,5-tetramethyl-1,3,2-dioxaborolane: ^{1}H NMR (400 MHz, $CDCl_3$) δ: 1.82 (dt, *J* = 15.7, 6.8 Hz, 1H), 1.21 (s, 12H), 0.89 (d, *J* = 6.6 Hz, 6H), 0.70 (d, *J* = 7.2 Hz, 2H), ^{13}C NMR (101 MHz, $CDCl_3$) δ: 82.75, 25.17, 24.81, 24.77, ^{11}B NMR (128 MHz, $CDCl_3$) δ: 34.06; MS (EI, m/z): 169 (51), 168 (12), 129 (86), 128 (20), 127 (13), 125 (9), 113 (18), 101 (18), 98 (16), 87 (56), 86 (19), 85 (100), 84 (43), 83 (49), 69 (47), 59 (50), 58 (23), 57 (84), 56 (33), 55 (28).

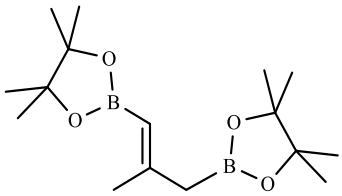

2bd

2,2'-(2-methylpropane-1,2-diyl)bis(4,4,5,5-tetramethyl-1,3,2-dioxaborolane): MS (EI, m/z): 251 (17), 250 (15), 207 (8), 166 (26), 151 (7), 127 (35), 126 (9), 123 (10), 109 (10), 108 (7), 101 (7), 95 (7), 84 (16), 83 (100), 82 (7), 81 (16), 69 (16), 67 (8), 57 (7), 55 (32).

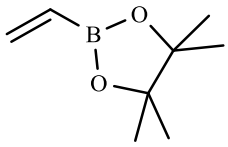

2ca

4,4,5,5-tetramethyl-2-vinyl-1,3,2-dioxaborolane: MS (EI, m/z): 139 (22), 138 (8), 112 (10), 111 (6), 110 (4), 97 (11), 96 (7), 95 (7), 87 (6), 85 (18), 81 (3), 69 (12), 68 (100), 67 (10), 59 (22), 58 (12), 57 (10), 55 (48), 54 (13), 53 (3).

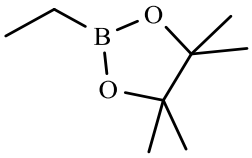

2cb

2-ethyl-4,4,5,5-tetramethyl-1,3,2-dioxaborolane: 142 (6), 141 (83), 140 (24), 99 (14), 98 (10), 97 (3), 86 (3), 85 (35), 84 (3), 83 (13), 70 (31), 69 (8), 67 (2), 59 (58), 58 (39), 57 (100), 56 (31), 55 (13), 53 (2), 45 (2).

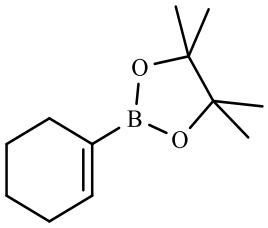

2da

2-(cyclohex-1-en-1-yl)-4,4,5,5-tetramethyl-1,3,2-dioxaborolane: MS (EI, m/z): 123 (32), 122 (49), 109 (58), 108 (40), 107 (32), 101 (10), 93 (10), 85 (85), 84 (100), 83 (15), 81 (32), 80 (42), 79 (29), 78 (13), 69 (21), 67 (33), 59 (18), 57 (12), 55 (23), 53 (11).

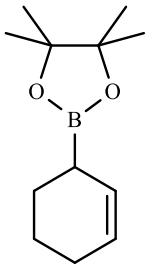

2db

2-(cyclohex-2-en-1-yl)-4,4,5,5-tetramethyl-1,3,2-dioxaborolane: MS (EI, m/z): 123 (23), 122 (18), 109 (14), 108 (16), 107 (18), 101 (10), 85 (72), 84 (100), 83 (23), 81 (34), 80 (35), 79 (24), 78 (10), 77 (6), 69 (23), 67 (26), 59 (9), 57 (11), 55 (20), 53 (8).

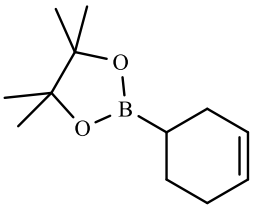

2dc

2-(cyclohex-3-en-1-yl)-4,4,5,5-tetramethyl-1,3,2-dioxaborolane: MS (EI, m/z): 123 (20), 122 (11), 108 (7), 107 (10), 101 (8), 86 (8), 85 (100), 84 (40), 83 (13), 81 (15), 80 (36), 79 (20), 78 (11), 69 (17), 67 (15), 66 (6), 59 (12), 57 (12), 55 (17), 53 (6).

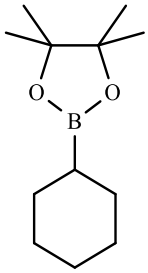

2dd

2-cyclohexyl-4,4,5,5-tetramethyl-1,3,2-dioxaborolane: MS (EI, m/z): 195 (20), 129 (21), 125 (9), 124 (100), 111 (17), 110 (33), 109 (29), 87 (22), 86 (10), 84 (16), 83 (31), 82 (48), 81 (27), 69 (90), 68 (13), 67 (15), 59 (24), 57 (14), 55 (32).

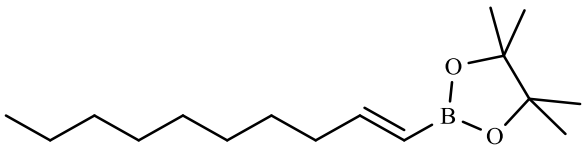

2ea

2-(dec-1-en-1-yl)-4,4,5,5-tetramethyl-1,3,2-dioxaborolane: MS (EI, m/z): 153 (100), 152 (28), 111 (45), 110 (43), 109 (32), 101 (40), 97 (28), 96 (51), 95 (55), 85 (93), 84 (78), 83 (86), 82 (54), 81 (53), 69 (76), 68 (64), 67 (52), 59 (31), 57 (57), 55 (91).

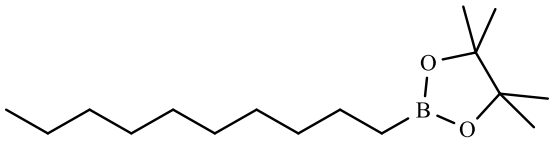

2eb

2-decyl-4,4,5,5-tetramethyl-1,3,2-dioxaborolane: MS (EI, m/z): 253 (18), 129 (99), 128 (27), 127 (17), 111 (18), 101 (22), 97 (48), 96 (13), 87 (54), 86 (21), 85 (100), 84 (32), 83 (42), 71 (18), 70 (12), 69 (45), 59 (41), 57 (4), 56 (14), 55 (38).

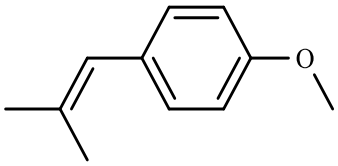

3ba

1-methoxy-4-(2-methylprop-1-en-1-yl)benzene: MS (EI, m/z): 163 (15), 162 (100), 161 (13), 148 (11), 147 (80), 146 (6), 132 (8), 131 (16), 129 (9), 121 (20), 119 (9), 117 (13), 115 (19), 104 (5), 103 (12), 91 (35), 77 (15), 65 (7), 63 (6), 51 (6).

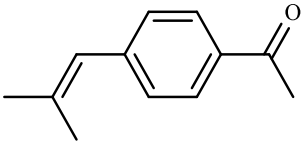

4ba

1-(4-(2-methylprop-1-en-1-yl)phenyl)ethan-1-one: MS (EI, m/z): 174 (18), 160 (13), 159 (100), 132 (3), 131 (21), 129 (20), 128 (5), 116 (14), 115 (15), 105 (3), 103 (3), 91 (19), 90 (6), 89 (7), 77 (5), 63 (4), 65 (3), 51 (3), 43 (11), 39 (4).

CHAPTER 4

RESULTS AND DISCUSSION

In this study, optimization studies for borylation of petroleum cracking products were examined. Experiments were performed with abovementioned methods and different combinations of boron source, pre-catalyst, ligand, and solvent under thermal conditions.

4.1 Borylation of Propene

The first trials were performed to determine whether some of the literature works[55, 70] (Table 4.1, entries 1 and 2) can be applicable for the borylation of propene. Some modifications were made to accommodate the natural properties of propene and thus, **M1** was applied. Each individual product was determined with its standard sample by using GC.

Table 4.1. First trials for the borylation of propene and its variations.

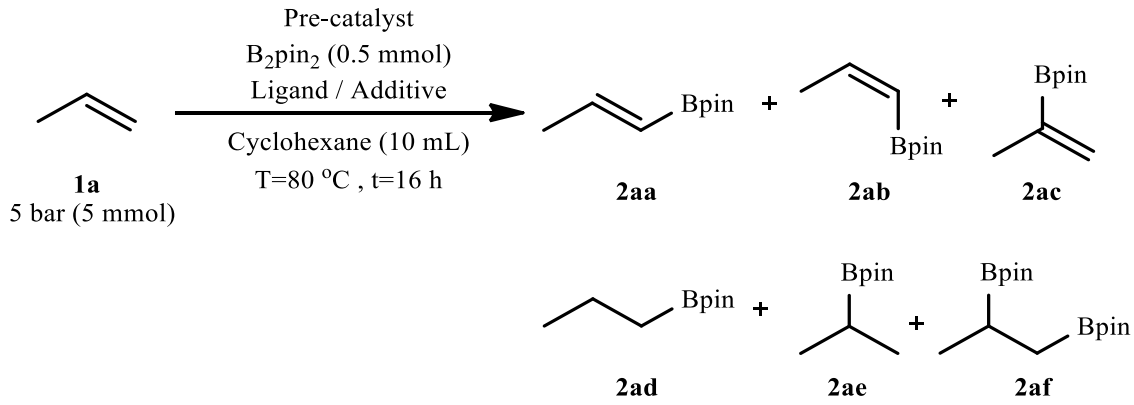

Entry	Pre-catalyst	Ligand / Additive[b]	Yield%[a]						
			2aa	2ab	2ac	2ad	2ae	2af	Total
1	$[Ir(COD)Cl]_2$	-	91	14	13	31	3	37	189
2	$[Ir(COD)Cl]_2$	DBU	0	15	7	9	55	6	92
3	$[Ir(COD)Cl]_2$	TMP	2	19	27	1	6	0	55
4	$[Ir(COD)Cl]_2$	TMP, KO^tBu	2	0	23	61	3	0	89
5	$[Ir(COD)OMe]_2$	-	109	16	27	23	0	4	179
6	$[Ir(COD)OMe]_2$	DBU	49	8	12	14	1	5	89
7	$[Ir(COD)OMe]_2$	TMP	22	5	42	71	2	2	144
8	$[Ir(COD)OMe]_2$	TMP, KO^tBu	20	4	35	82	3	0	144
9[c]	$[Ir(COD)OMe]_2$	TMP, KO^tBu	13	3	49	57	1	0	123
10[c, d]	$[Ir(COD)OMe]_2$	TMP, KO^tBu	0	0	30	51	1	0	82

a) Determined by GC technique using dodecane as the internal standard.
b) 5 % mol DBU, 10 % mol TMP, 1 equivalent of KO^tBu used.
c) Benzene was used as a solvent.
d) H_2O (0.5 mmol) was used as an additive.

Resulting from these trials, it was evident that when $[Ir(COD)Cl]_2$ or $[Ir(COD)OMe]_2$ complexes can used without requirement of any additive in the reaction medium, in these reactions, alkenylboron **2aa** was predominantly obtained. However, addition of DBU, TMP or KO^tBu, either caused a decrease in the yield of **2aa** and/or led to promote formation of other borylated products. Specifically, having a base in reaction medium resulted in mainly hydroboration of propene, producing **2ad** mainly (Table 4.1,

entries 4, 8 and 9). The presence of water was detrimental for the reaction and decreased the amount of **2ac**; however, it did not affect the selectivity (Table 4.1, entry 10). When benzene was used as a solvent, in addition to the borylative and hydroboration products, borylated benzene products were also observed to form (Table 4.1, entries 9 and 10).

Table 4.2. Effects of temperature on the borylation of propene.

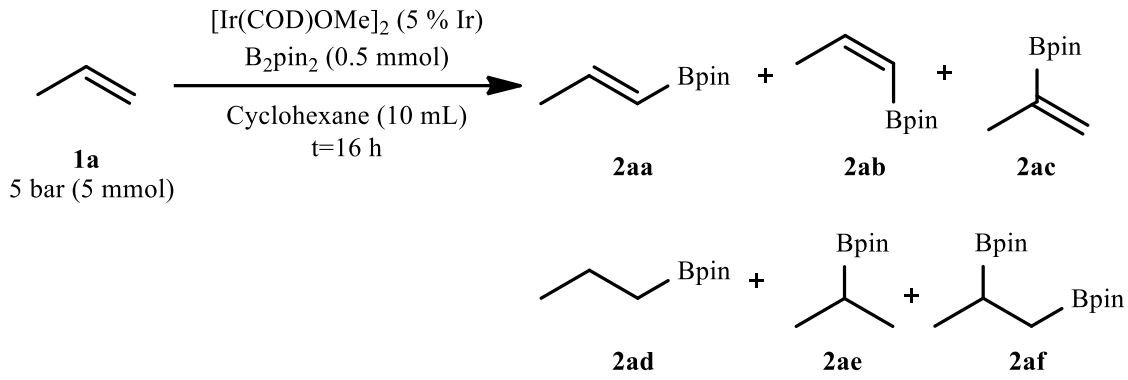

Entry	T (°C)	Yield%[a]						
		2aa	**2ab**	**2ac**	**2ad**	**2ae**	**2af**	**Total**
1	80	109	16	27	23	0	4	179
2	100	120	20	28	19	0	0	187
3	120	93	18	23	19	0	0	153

a) Determined by GC technique using dodecane as the internal standard.

The optimum reaction temperature is determined to be 100 °C. At this reaction temperature, **2aa** formation was in the highest possible yield (Table 4.2).

Table 4.3. Effect of amount of reactant on the borylation of propene.

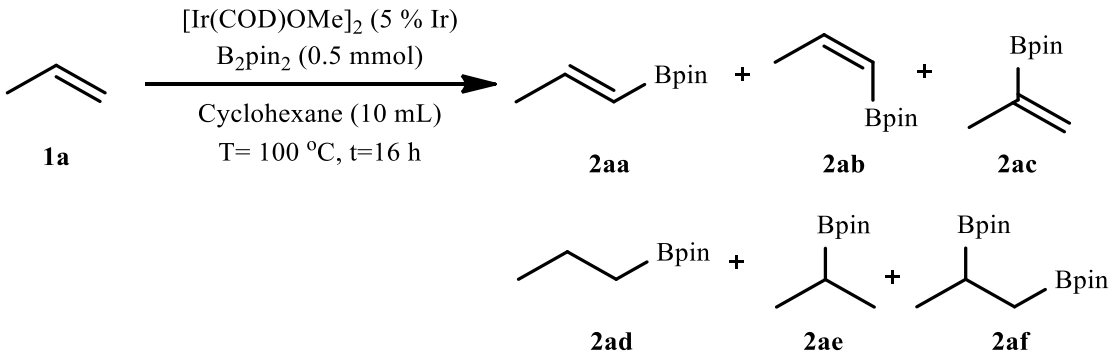

Entry	Propene Amount	Yield%[a]						
		2aa	2ab	2ac	2ad	2ae	2af	Total
1	2 bar (2 mmol)	82	15	19	24	0	6	146
2	5 bar (5 mmol)	120	20	28	19	0	0	187
3	10 bar (10 mmol)	102	18	25	12	0	3	160

a) Determined by GC technique using dodecane as the internal standard.

To determine the optimum amount of reactant used, the propene amount was varied (Table 4.3). The amount of propene charged was maintained with the pressure of the reactor before the experiment started. The weight of propene charged was calculated by ideal gas equation ignoring the solubility in cyclohexane initially.

Table 4.4. Effect of solvents on the borylation of propene.

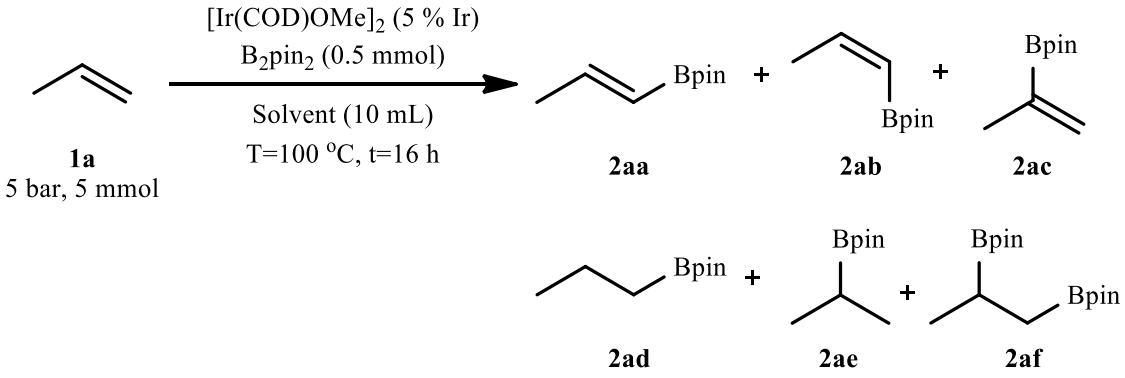

Entry	Solvent	Yield%[a]						
		2aa	2ab	2ac	2ad	2ae	2af	Total
1	Cyclohexane	120	20	28	19	0	0	187
2	1,4-Dioxane	113	19	18	21	1	6	178
3[b]	1,4-Dioxane	47	7	7	16	0	1	78

(cont. on the next page)

(Con. of. Table 4.4)

4	THF	72	13	25	12	0	4	126
5	MTBE	55	10	23	16	0	3	107
6	DMF	45	8	10	6	0	2	71

a) Determined by GC technique using dodecane as the internal standard.
b) Experiment was done with M2 (microwave method).

Even tough generally nonpolar solvents are preferred for Ir-catalysed borylation reactions, some polar solvent were used in the reaction. However, the use of polar solvents led to decrease of the yield of the desired product (Table 4.4). Only 1,4-dioxane produced a comparable result with cyclohexane. Since 1,4-dioxane has microwave-active properties, an experiment was also performed via microwave heating under **M2** conditions (Table 4.4, entry 3). However, the microwave heating showed no beneficial effect for the method.

Table 4.5. Effect of ligands and additives on the borylation of propene.

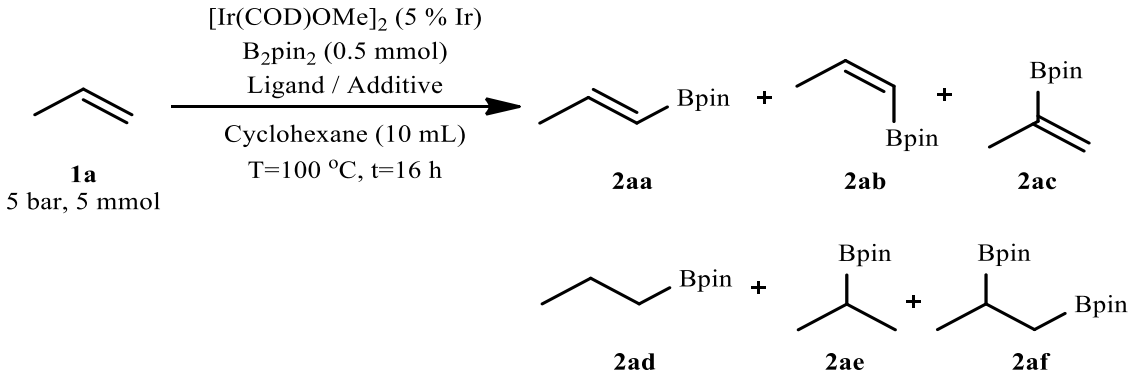

Entry	Ligand/Additive	Yield%[a]						
		2aa	**2ab**	**2ac**	**2ad**	**2ae**	**2af**	**Total**
1	-	120	20	28	19	0	0	187
2[b]	PPh_3	106	19	53	14	0	2	191
3[b]	$AsPh_3$	104	18	28	19	0	8	177

(cont. on the next page)

(Con. of. Table 4.5)

4[c]	DPPE	100	20	26	10	0	7	163
5[c]	DPPB	60	11	28	16	0	6	121
6[d]	2-Norbornene	56	10	16	10	4	0	96
7[e]	Cyclohexanone	32	6	18	8	0	2	66

a) Determined by GC technique using dodecane as the internal standard.
b) 10% ligand was used.
c) 5% ligand was used.
d) 2 equivalent of 2-Norbornene was used.
e) 5 equivalent of cyclohexanone was used.

Phosphines are generally the preferred choice of ligands in the transition-metal-mediated processes. Thus, the activity of ligands combined with $[Ir(COD)OMe]_2$ was investigated. Using simple monodentate ligand, PPh_3, increased the total formation of borylated products. However, the selectivity of the method was somewhat diminished and the formation of **2ac** was enhanced (Table 4.5, entry 2). Similarly, the ligand $AsPh_3$ resulted in a decrease of borylated yields (Table 4.5, entry 3). Using bidentate ligands instead of monodentate ligands also resulted with lower yields (Table 4.5, entries 4 and 5).

Significant amount of hydroboration product **2ad** is usually exist among the borylation products. It has been shown that using sacrificial alkene can reduce the hydroboration product.[47, 49] To eliminate **2ad**, 2-norbornene and cyclohexanone were used sacrificial alkene, but these attempts led to inferior results (Table 4.5, entries 6 and 7).

Table 4.6. Effect of different iridium complexes on the borylation of propene.

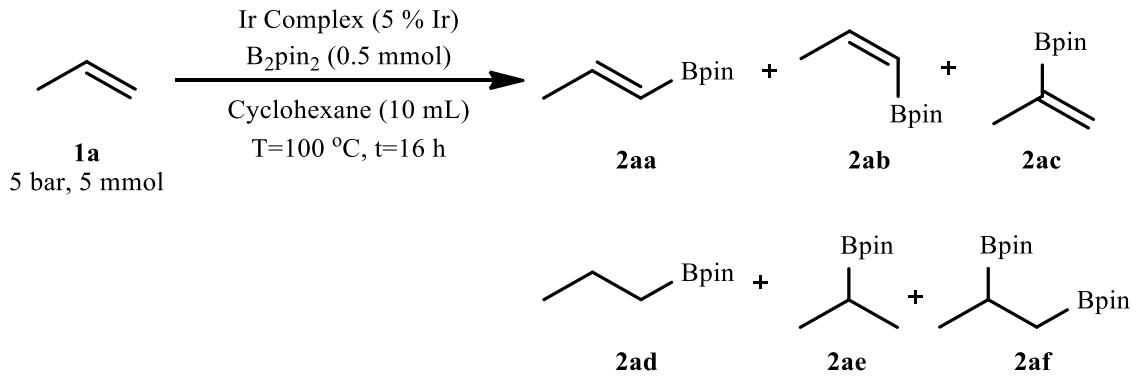

Entry	Pre-catalyst	Yields %[a]						
		2aa	2ab	2ac	2ad	2ae	2af	Total
1	$[Ir(COD)OMe]_2$	120	20	28	19	0	0	187
2	Ir(COD)(IMes)Cl	120	23	17	26	0	6	192
3[b]	$Ir(COD)(IBz(iPr)_3)Cl$	107	20	18	32	1	5	183
4[c]	$Ir(COD)(IBz(CF_3)^{PhCl})Cl$	105	19	21	23	0	6	174
5	$IrCl_3.xH_2O$	68	9	5	38	6	35	161

a) Determined by GC technique using dodecane as the internal standard.

b)

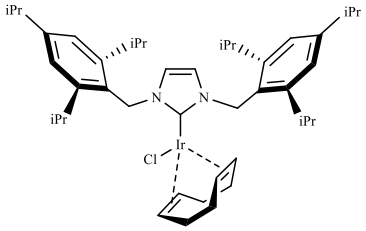

c)

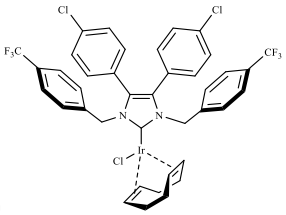

A number of N-hetero carben (NHC) ligated iridium complexes (Ir-NHC) complexes were also tested for their activities (Table 4.6).[71-73] A comparable result was obtained with Ir(COD)(IMes)Cl, and somewhat lower yields could be obtained with benzyl-substituted Ir-NHC complexes (Table 4.6, entry 2-4). However, the catalytic activity of $IrCl_3$ was insufficient (Table 4.6, entry 5).

Table 4.7. Effect of different rhodium complexes on the borylation of propene.

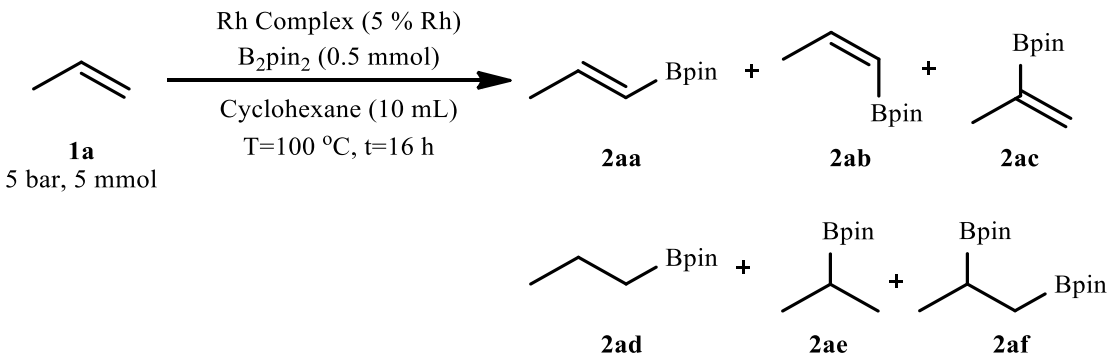

Entry	Pre-catalyst	Yield%[a]						
		2aa	2ab	2ac	2ad	2ae	2af	Total
1	$RhCl_3.xH_2O$	46	8	1	16	1	7	79
2[d]	$Rh(COD)_2BF_4$	82	15	5	51	3	45	201
3	$Rh(PPh_3)_3Cl$	59	10	3	40	2	15	129
4	$RhCp^*Cl_2$	88	16	7	29	1	11	152
5[b]	$[Rh(COD)OH]_2$	73	11	3	81	1	26	195
6[b]	$[Rh(COD)Cl]_2$	59	7	2	39	1	12	120
7[b, c]	$[Rh(COD)Cl]_2$	102	16	9	58	2	20	207
8[b, c]	$[Rh(COD)OMe]_2$	56	89	3	83	1	39	189
9	$[Rh(COD)OMe]_2$	48	8	3	92	1	26	178
10[e]	$Rh(COD)(IBz(iPr)_3)Cl$	49	17	1	55	5	91	218
11	Rh(COD)(IMes)Cl	29	5	2	26	1	112	175

a) Determined by GC technique using dodecane as the internal standard.
b) Reaction temperature is 80 °C
c) 5% TMP used as additive.

d)

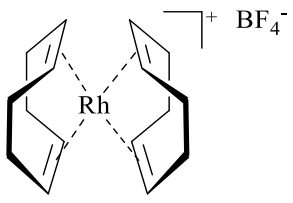

e)

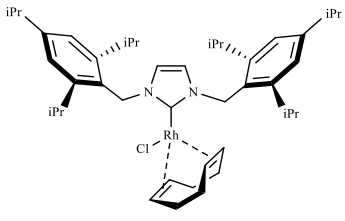

In addition to Ir complexes, other metal complexes can also be used in borylation reactions. Because of its Ir-like nature, Rh complexes was also tested in the reaction.

Experiment with $RhCl_3$ did not give an effective result (Table 4.7, entry 1). When $Rh(COD)_2BF_4$ was used as the catalyst, even though there was a significant increase in the total yield, there was no selective formation of the borylated product (Table 4.7, entry 2). The reaction with Wilkinson's catalyst resulted in lower yield (Table 4.7, entry 3). Changing catalyst to $RhCp^*Cl_2$ did not improve selectivity or yield (Table 4.7, entry 4).

Optimization studies were also proceeded with rhodium catalysts containing functional groups with different electronic effects. Results obtained with $[Rh(COD)OH]_2$ was not so selective (Table 4.7, entry 5). Even though $[Rh(COD)Cl]_2$ gave a similar result, the addition of TMP caused a significant increase in the yield of **2aa** (Table 4.7, entries 6 and 7). The catalytic activity of $[Rh(COD)OMe]_2$ was insufficient with or without TMP (Table 4.7, entries 8 and 9).

N-heterocarben (NHC) ligated rhodium complexes (Rh-NHC) complexes directed to the diborylation products (Table 4.7, entries 10 and 11).

4.2 Borylation of Isobutene

Propene contains a double bond with a single methyl substituent and has many open positions for dehydrogenative borylation or hydroboration. Because of these properties of propene, the selectivity of borylation was not ideal for this procedure and several by-products formed. To reduce the number of by-products, a more sterically hindered reactant was used. For this, the preferred choice was isobutene.

To achieve more controllable conditions for reactant amount, a suitable method to prepare reactant solution was established. If the reaction conditions included an air sensitive reagent; such as $[Ir(COD)OMe]_2$, HBpin, KO^tBu; **M2** was the method of choice. Other reactions were carried out under the conditions of **M3** method.

Table 4.8. First trials for the borylation of isobutene and its variations.

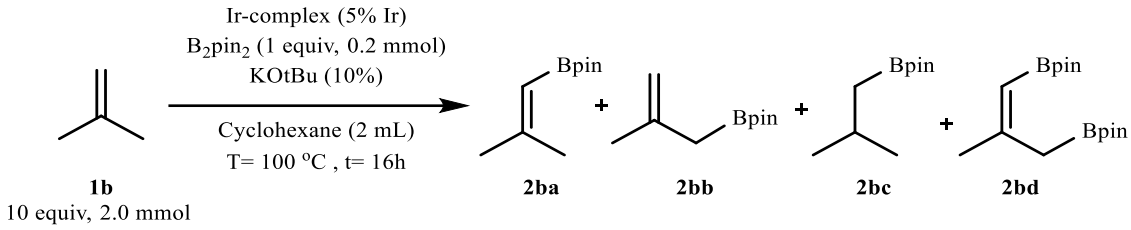

Entry	Pre-catalyst	Additive	Yield%[a]				
			2ba	2bb	2bc	2bd	Total
1	$[Ir(COD)OMe]_2$	-	47	1	19	7	74
2	$[Ir(COD)Cl]_2$	-	66	2	23	21	112
3	$[Ir(COD)Cl]_2$	KO^tBu	45	1	25	4	75
4	Ir(COD)(IMes)Cl	-	35	1	32	3	68
5	Ir(COD)(IMes)Cl	KO^tBu	14	0	39	4	57
6[b]	Ir(COD)(IMes)Cl	KO^tBu	2	0	58	2	62

a) Determined by GC technique using dodecane as the internal standard.
b) 0.4 mmol HBpin was used instead of 0.2 mmol B_2pin_2 while using the same amount of Ir-complex. Thus, Iridium amount in the reaction became 2.5 %.

The first trial for borylation reaction for isobutene was done under the conditions optimized for the borylation of propene (Table 4.8, entry 1). Under this condition, the main product was the corresponding terminal dehydrogenative borylation molecule and the hydroboration and diborylated molecules were the by-products of the reaction as determined by GC/MS and NMR analyses.

Changing the pre-catalyst from $[Ir(COD)OMe]_2$ to $[Ir(COD)Cl]_2$ resulted in 40% increase in the yield of **2ba** (Table 4.8, entry 2). Using Ir(COD)(IMes)Cl caused to decrease **2ba** formation and increase the formation of **2bb** (Table 4.11, entry 4). This can be explained by higher hydrogen transfer activity of Ir(COD)(IMes)Cl. Similar results were also obtained when KO^tBu was used as an additive (Table 4.8, entries 3 and 5).

It was observed that Ir(COD)(IMes)Cl and KO^{t}Bu led to the formation of hydroboration product **2bb** selectively, when HBpin was used as the boron source (Table 4.8, entry 6).

Table 4.9. Effect of solvent on borylation of isobutene.

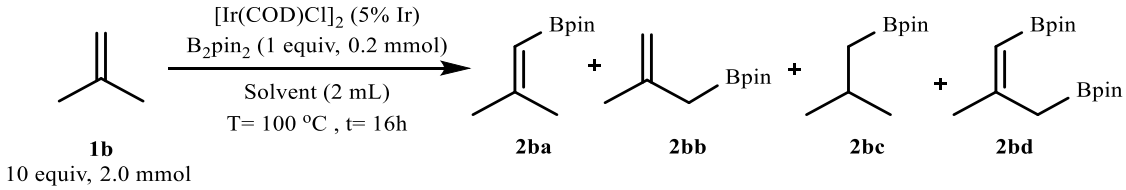

Entry	Solvent	Yield%[a]				
		2ba	**2bb**	**2bc**	**2bd**	**Total**
1	Cyclohexane	66	2	23	21	112
2	Toluene	104	5	27	28	164
3	DCE	104	6	26	17	153
4	Benzene	98	4	27	25	154
5	MTBE	94	6	23	8	131
6	CPME	86	3	23	5	117
7	Acetone	28	0	16	0	44
8	IPA	27	1	6	0	34
9	NMP	10	2	9	0	21
10	MeCN	3	4	38	1	46
11	THF	38	1	75	3	117

a) Determined by GC technique using dodecane as the internal standard.

Similar to the effects of solvent in borylation of propene, non-polar solvents afforded higher amount of dehydrogenative borylation products (Table 4.9, entries 2-4). Polar solvents resulted in lower production of **2ba**. Specifically, MeCN and THF provided a higher yield of **2bb**. With toluene and DCE solvents, with which the highest yields of dehydrogenative borylation product **2ba** could be achieved, the effect of pre-catalyst and additive were also investigated (Tables 4.10 and 4.11).

Table 4.10. Effect of pre-catalyst and additive on borylation of isobutene using toluene or DCE solvents.

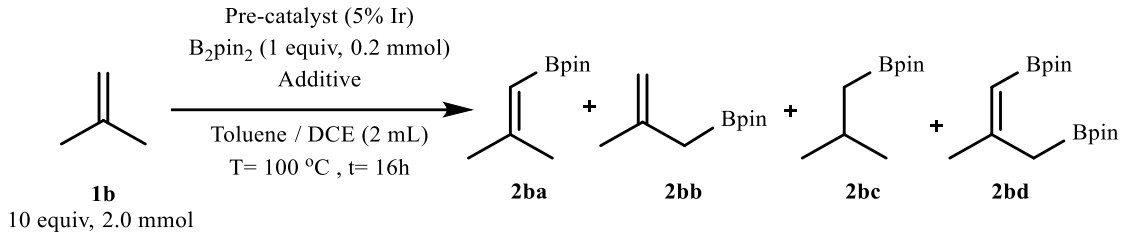

Entry	Solvent	Pre-catalyst	Additive	Yield%[a]				
				2ba	2bb	2bc	2bd	Total
1[b]	Toluene	$[Ir(COD)Cl]_2$	Acetone	92	23	3	2	120
2[b]	Toluene	$[Ir(COD)Cl]_2$	IPA	75	20	2	2	99
3[b]	Toluene	$[Ir(COD)Cl]_2$	Benzal-dehyde	13	27	0	12	52
4	Toluene	Ir(COD)(IMes)Cl	-	34	33	1	1	69
5	Toluene	Ir(COD)(Phen)Cl	-	14	20	2	1	37
6[c]	Toluene	Ir(COD)(Phen)Cl	HBpin	11	14	4	2	31
7[c]	DCE	$[Ir(COD)Cl]_2$	MeCN	100	6	28	14	148

(cont. on the next page)

(Con. of. Table 4.10)

8[b]	DCE	Ir(COD)(IMes)Cl	Acetone	101	5	24	10	140
9	DCE	$[IrCp^*Cl_2]_2$	-	12	0	0	0	12

a) Determined by GC technique using dodecane as the internal standard.
b) 2 equiv. additive was used
c) 5% additive was used.

When using toluene as the solvent, acetone and benzaldehyde were used as sacrificial reagents to reduce the formation of hydroboration products. Also, IPA was used as a hydrogen atom source to enhance the production of **2bb**. These trials resulted in lower activity of iridium complex (Table 4.10, entries 1-3). Ir(COD)(IMes)Cl and Ir(COD)(Phen)Cl resulted in lower yields (Table 4.10, entries 4-9). When using DCE as a solvent, the use of MeCN and acetone for the promotion of the yield of **2bb** failed. Also, $[IrCp^*Cl_2]_2$ resulted in a decreased yield (Table 4.10, entries 7-9). Optimization studies continued with using DCE as the solvent, because of the by-products detected which were formed by borylation of toluene.

Table 4.11. Effect of temperature on borylation of isobutene.

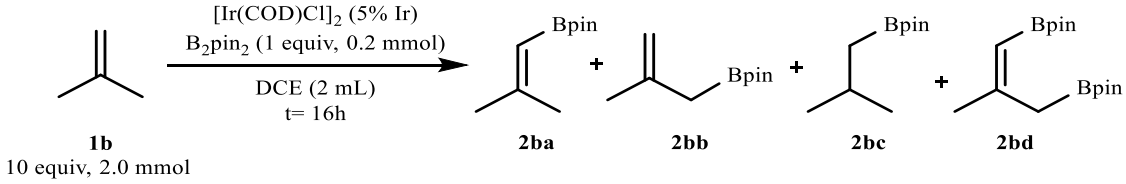

1b
10 equiv, 2.0 mmol

2ba **2bb** **2bc** **2bd**

Entry	**T (°C)**	**Yield%[a]**				
		2ba	**2bb**	**2bc**	**2bd**	**Total**
1	50	78	3	35	4	120
2	70	107	3	28	4	142

(cont. on the next page)

(Con. of. Table 4.11)

3[b]	70	91	4	30	34	159
4	100	104	6	26	17	153
5[c]	120	90	6	20	11	127

a) Determined by GC technique using dodecane as the internal standard.
b) 0.4 mmol B_2pin_2 was used.
c) Reaction time was 6 hours.

The reaction at lower temperature of 70 °C resulted in similar outcome. Decreasing reaction temperature to 50 °C or increasing to 120 °C showed negative impact (Table 4.11).

Table 4.12. Effects of ligands on borylation of isobutene.

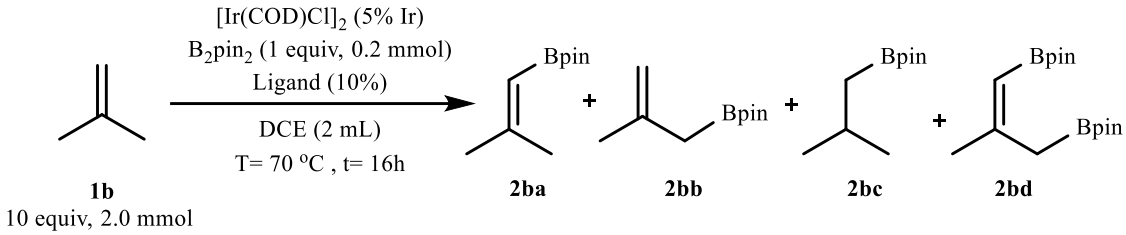

No	Ligand (%)	Yield%[a]				
		2ba	2bb	2bc	2bd	Total
1	$P(Ph(CF_3))_3$	0	0	0	0	0
2	$P(Ph(CF_3)_2)_3$	0	0	0	0	0
3	PPh_3	0	0	0	0	0
4	$AsPh_3$	0	0	0	0	0

a) Determined by GC technique using dodecane as the internal standard.

Effects of ligands were investigated at 70 °C, in these trials both ligands with electron donating ability and electron withdrawing ability caused activity of iridium complex to disappear (Table 4.12).

Table 4.13. Effect of pre-catalyst amount on borylation of isobutene.

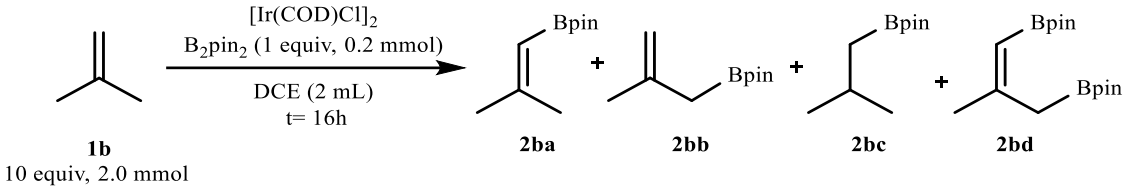

Entry	T (°C)	Pre-catalyst Amount (Ir%)	Yield%[a]				
			2ba	2bb	2bc	2bd	Total
1	70	5.0	107	3	28	4	142
2	70	2.5	95	1	27	3	126
3	100	5.0	104	6	26	17	153
4	100	2.5	107	2	19	2	130
5	100	1.0	69	4	11	2	86

a) Determined by GC technique using dodecane as the internal standard.

The price of the pre-catalyst covers the significant amount of the process expenses. Because of that, trials to decrease the amount of pre-catalyst were carried out. At 70 °C, decrease on products was observed. However, at 100 °C, slight increase on **2ba** was detected. Decreasing the amount of the catalyst some more did not accomplish any advancement (Table 4.13).

Table 4.14. Effect of solvent amount on borylation of isobutene.

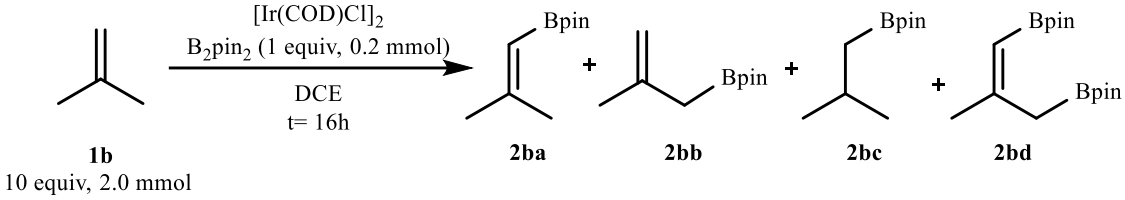

Entry	T (°C)	Pre-catalyst Amount (Ir%)	DCE Amount (mL)	Yield%[a]				
				2ba	2bb	2bc	2bd	Total
1	70	5.0	3.0	104	3	23	3	133
2	70	5.0	2.0	107	3	28	4	142
3	70	5.0	1.0	96	3	24	22	145
4	100	2.5	3.0	97	5	18	3	123
5	100	2.5	2.0	107	2	19	2	130
6	100	2.5	1.0	116	6	28	15	165
7	100	2.5	0.6	110	6	31	19	166

a) Determined by GC technique using dodecane as the internal standard.

Because of the similar results with 5% Ir at 70 °C, and 2.5% Ir at 100 °C, the trials to find out the effect of solvent amount were performed on both conditions. Changing the solvent amount at 70 °C, did not yield any improvement (Table 4.14, entries 1-3). The optimal amount of solvent at 100 °C was established as 1.0 mL (Table 4.14, entries 4-7).

Table 4.15. Effect of isobutene and B_2pin_2 amount on borylation of isobutene.

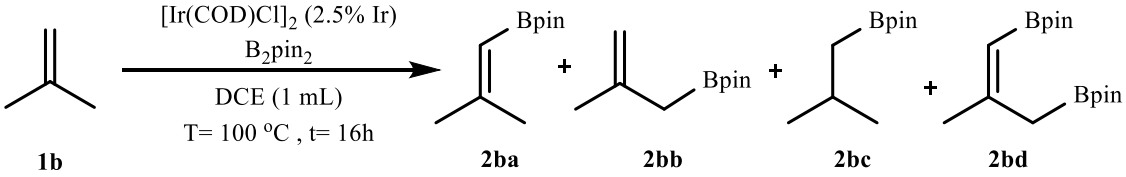

Entry	B_2pin_2 Amount (mmol)	Isobutene Amount	Yield%[a]				
			2ba	2bb	2bc	2bd	Total
1	0.1	10 equiv	65	3	18	1	87
2	0.2	3.3 equiv	87	5	21	12	125
3	0.2	5 equiv	90	5	21	9	125
4	0.2	8.3 equiv	104	4	20	3	131
5	0.2	10 equiv	116	6	28	15	165
6	0.2	15 equiv	110	6	27	13	156
7	0.3	10 equiv	93	5	20	8	126
8	0.4	10 equiv	77	4	19	21	121

a) Determined by GC technique using dodecane as the internal standard.

Effect of reactant amount was also investigated. It was observed that it is possible to increase the amount of isobutene to 15 equivalent (3 mmol), but lowering it yielded inferior results. Also, similar changes of B_2pin_2 had no effect on the reaction positively (Table 4.15).

Table 4.16. Effect of time on borylation of isobutene.

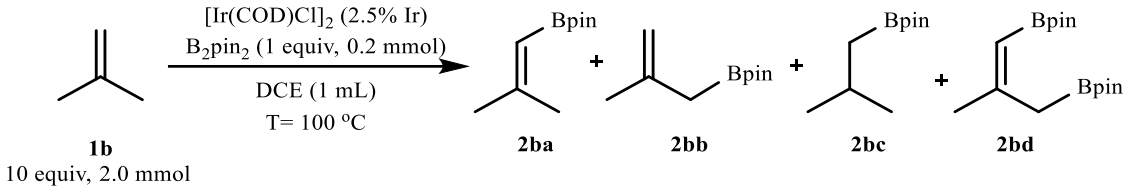

Entry	t (h)	Yield%[a]				
		2ba	2bb	2bc	2bd	Total
1	2	75	18	5	15	113
2	3	83	22	6	15	126
3	5	93	25	6	19	143
4	9	100	26	6	21	153
5	16	116	6	28	15	165

a) Determined by GC technique using dodecane as the internal standard.

In the last part of the optimization of dehydrogenative borylation of isobutene, effect of reaction period was examined. It was observed that significant amount of borylation was occurred in the first two hours of reaction. The reaction further continued till 16 hours with a slowed rate and after 16 hours (Table 4.16), it was observed that B_2pin_2 has completely consumed.

4.3 Hydroboration of Isobutene

In aforementioned dehydroborylation studies, it was observed that, Ir(COD)(IMes)Cl as a pre-catalyst improved the relative formation of the corresponding hydroboration product. THF and MeCN were the solvents that favoured the formation of the hydroboration product. To achieve selective formation of hydroboration product,

initial studies were performed using these reagents. HBpin was used as the boron source instead of B_2pin_2, because HBpin can also act as a hydrogen atom source.

Table 4.17. Effects of solvent on hydroboration of isobutene

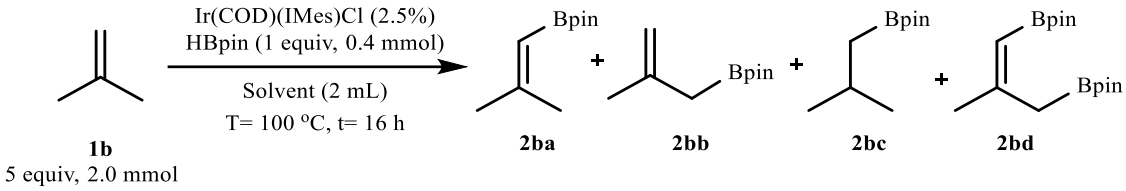

Entry	Solvent	Yield%[a]				
		2ba	2bb	2bc	2bd	Total
1	MeCN	0	0	54	0	54
2	THF	3	0	86	1	90
3[b]	THF	4	0	62	3	69

a) Determined by GC technique using dodecane as the internal standard.
b) 0.05 % Ir(COD)(IMes)Cl was used.

The hydroboration product **2bb** was obtained with a moderate yield and with a high selectivity when MeCN was used as the solvent. Significantly higher yield of **2bb** was produced in THF solvent (Table 4.17, entries 1 and 2). Thus, THF became the preferred solvent for hydroboration of isobutene. When the Ir(COD)(IMes)Cl amount reduced to 0.05%, there was a decrease on the yield to a moderate level (Table 4.17, entry 3).

Table 4.18. Effect of temperature on hydroboration of isobutene in the presence of 0.05% of Ir(COD)(IMes)Cl.

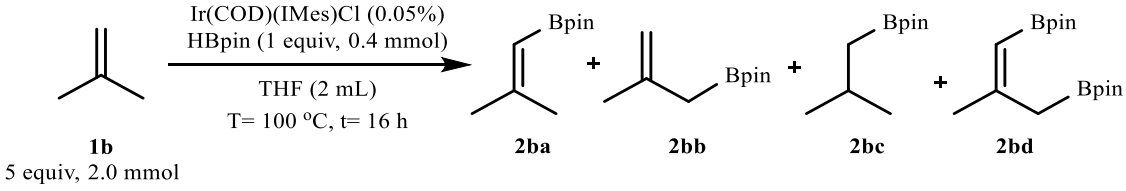

Entry	T (°C)	Yield%[a]				
		2ba	2bb	2bc	2bd	Total
1	80	2	0	56	3	61
2	100	4	0	62	3	69
3[b]	100	0	0	6	0	6
4	120	3	0	60	2	65

a) Determined by GC technique using dodecane as the internal standard.
b) 5% KOH was used as additive.

It was determined that the reaction the temperature of 100 °C is optimal for the formation of **2bb** (Table 4.18, entry 2). The presence of KOH base almost completely destroyed catalytic activity of the iridium complex (Table 4.18, entry 3). There was apparent decrease in the yield when the reaction is performed at lower temperature (Table 4.18, entry 1) and application of higher temperature was useless (Table 4.18, entry 120).

Table 4.19. Effect of pre-catalyst on hydroboration of isobutene in the presence of 0.05% iridium.

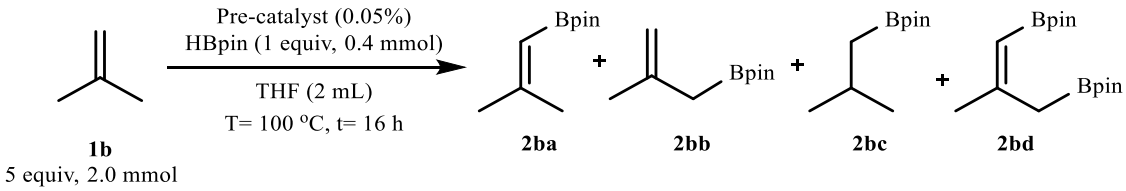

Entry	Pre-catalyst	Yield%[a]				
		2ba	2bb	2bc	2bd	Total
1	Ir(COD)(IMes)Cl	4	0	62	3	69
2	Ir(COD)(IPr)Cl	2	0	42	1	45

(cont. on the next page)

(Con. of. Table 4.19)

3	Ir(COD)(IBz)Cl	5	2	59	7	73
4[b]	Ir(COD)(IBz(iPr)$_3$)Cl	2	0	37	1	40
5	Ir(COD)(IoTol)Cl	3	0	46	1	50
6	Ir(COD)(IXy)Cl	4	0	84	2	90
7	Ir(COD)(IXy^{Me})Cl	5	3	73	6	87
8	Ir(COD)(SIXy)Cl	4	0	105	1	109

a) Determined by GC technique using dodecane as the internal standard.
b) 2.5% pre-catalyst was used.

Effect of various NHC ligated pre-catalyst complexes was investigated with varying steric and electronic properties. 2,6-Diisopropyl substituted NHC ligated iridium complex afforded lower yield of **2bb**, indicating that increased steric factors had negative effect for the method. (Table 4.19, entry 2). A comparable result was obtained with an alkyl substituted NHC ligated complex (Table 4.19, entry 3). Similarly, increased steric factors with 2,4,6-triisopropyl benzene attached alkyl substituted NHC ligated complex, decreased the yield of the experiment (Table 4.19, entry 4). Mono- and di-methyl substituted Ir-NHC complexes was also tested and found that Ir(COD)(IXy)Cl gave improved results (Table 4.19, entries 5-6). To enhance the yield, modifications on Ir(COD)(IXy)Cl was established. The catalyst system, with the NHC ligand having methyl groups on the imidazole ring, gave an unfavourable result (Table 4.19, entry 7). However, the best result could be acquired with saturated NHC ligated complex, Ir(COD)(SIXy)Cl with significant increase on the amount of **2bb** (Table 4.19, entry 8).

Table 4.20. Effect of Ir(COD)(SIXy)Cl amount on hydroboration of isobutene.

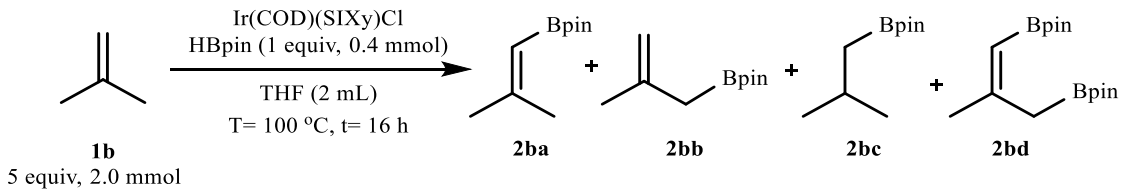

Entry	Ir(COD)(SIXy)Cl (%)	Yield%[a]				
		2bc	2bb	2ba	2bd	Total
1	0.01	3	0	107	1	111
2[b]	0.01	3	0	73	1	77
3[c]	0.01	3	1	60	1	65
4	0.005	2	0	31	0	33
5	0.001	0	0	3	0	3

a) Determined by GC technique using dodecane as the internal standard.
b) Experiment temperature is 80 C.
c) Experiment time is 6 hours.

Experiments with a lower amount of Ir(COD)(SIXy)Cl were also performed. Experiment with 0.01% pre-catalyst had no significant influence on the yield (Table 20, entry 1). When the reaction temperature decreased to 80 °C, the reaction was resulted with a lower yield (Table 20, entry 2). Also, decreasing the reaction time to 6 hours resulted with an inferior yield (Table 20, entry 3). Lowering the pre-catalyst loading further more decreased the yield significantly (Table 4.20, entries 4 and 5).

Table 4.21. Effect of isobutene amount on hydroboration of isobutene while using 0.01% Ir(COD)(SIXy)Cl.

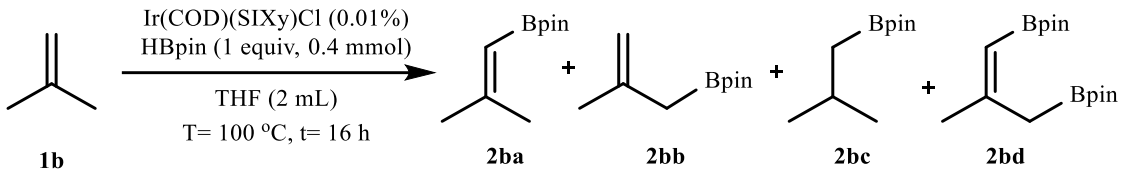

Entry	Isobutene Amount	Yield%[a]				
		2ba	2bb	2bc	2bd	Total
1	2.5 equiv	3	0	85	1	89
2	5 equiv	4	0	107	1	112
3	7.5 equiv	0	0	6	0	6

a) Determined by GC technique using dodecane as the internal standard.

In the last part of the optimization of hydroboration of isobutene, the effect of isobutene amount was examined (Table 4.21). Particularly the use of higher amount of isobutene was highly detrimal (Table 4.21, entry 3).

4.4 Proposed Catalytic Cycles

In the catalytic cycle of dehydrogenative borylation of isobutene, firstly transmetallation phase takes place with Ir (I) pre-catalyst and B_2pin_2, and active catalyst **A** that is tris-boryl Ir[3] complex form. The reactant **1b** coordinates to the metal center of Iridium complex (**B**). Then, insertion phase takes place, with oxidative addition of vinylic C-H bond to **A,** complex **C** is formed. **D** is produced as a result of β-hydrogen elimination of **C**, and dissociation of **D** produces Ir-hydride complex **E** and product **2ba**. Lastly, oxidative addition of B_2pin_2 replenishs active complex **A** and forms HBpin (Figure 4.1).

In the catalytic cycle of hydroboration of isobutene, similarly transmetallation phase takes place with Ir (I) pre-catalyst and HBpin, and active catalyst **F** that is bis-boryl hydride Ir [3] complex forms. The coordination of reactant **1b** forms iridium complex **G**. In the insertion step, **H** is formed from oxidative addition of vinylic C-H bond. In the dissociation step, product **2bb** and iridium complex **I** is formed. Oxidative addition of HBpin replenishs the active complex **F** and completes the catalytic cycle (Figure 4.2).

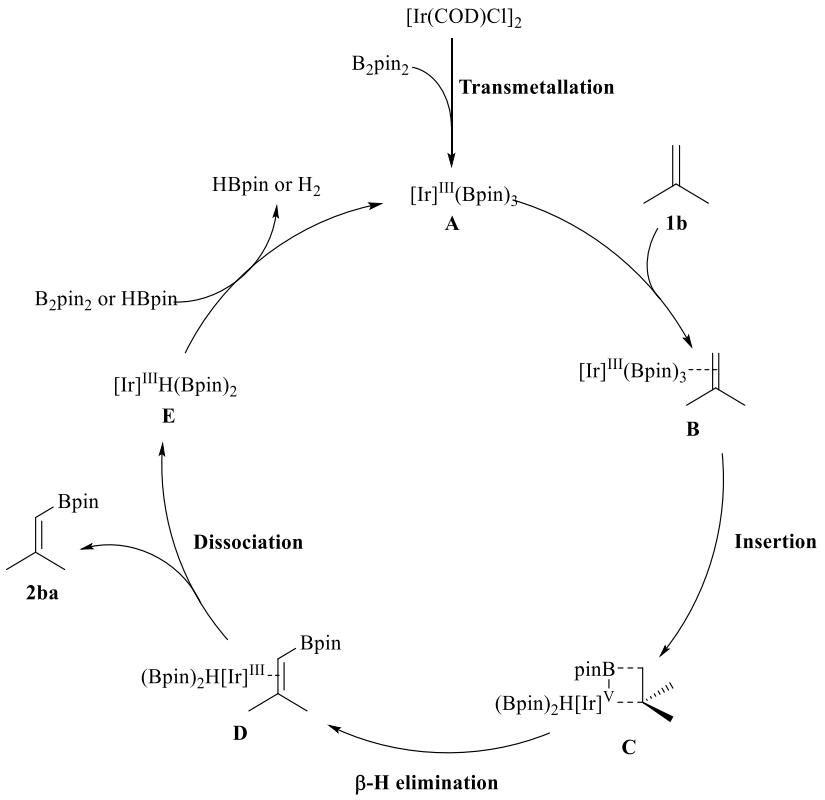

Figure 4.1. Proposed mechanism for dehydrogenative borylation of isobutene.

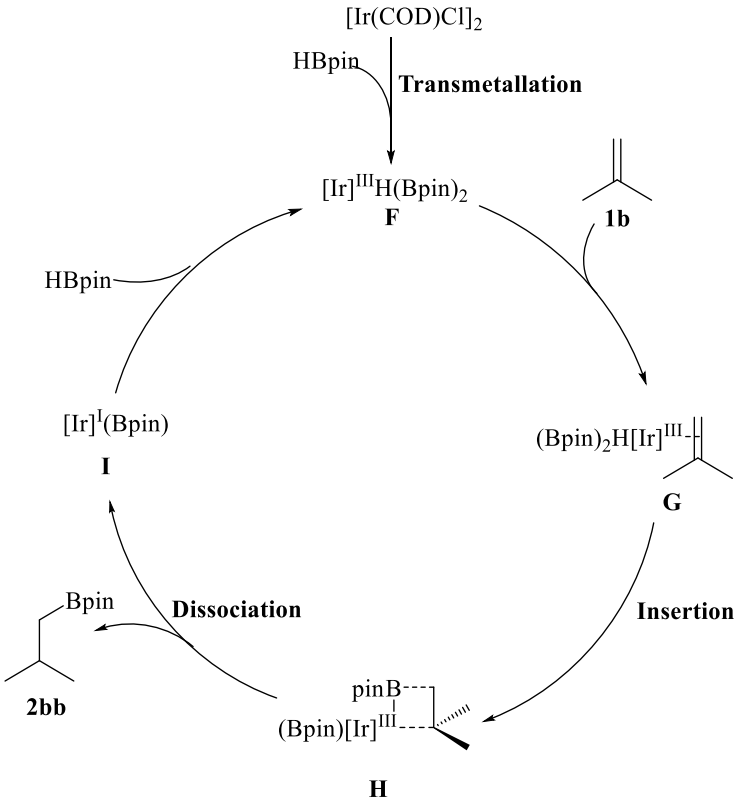

Figure 4.2. Proposed mechanism for hydroboration of isobutene.

4.5 Substrate Scope of Borylation Reactions

The scope of the hydroboration and dehydrogenative borylation methods on several internal and terminal alkenes was investigated. The optimal conditions for the borylation of propene, as determined, involve the use of $[Ir(COD)OMe]_2$, cyclohexane solvent, 100 °C of reaction temperature, and 16 hours of reaction period. The optimal conditions for the hydroboration of isobutene includes the combination of HBpin and Ir(COD)(SIXy)Cl in THF as the solvent, 100 °C of reaction temperature, and 16 hours of reaction period. Also, the optimal dehydrogenative borylation of isobutene condition includes the combination of B_2pin_2 and $[Ir(COD)Cl]_2$ in DCE, and same reaction time and temperature as above.

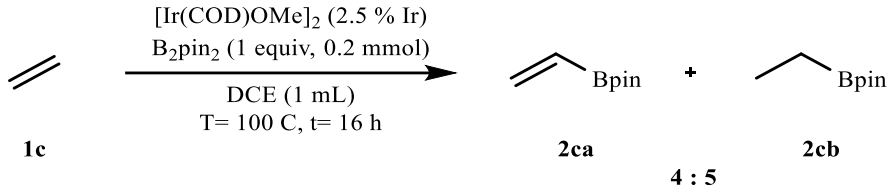

Figure 4.3. Borylation of ethene.

The **M1** method was employed for the borylation of the simplest olefin, ethene. The It was determined that the major product of the process was found to be hydroboration product instead of dehydrogenative borylation product with a ratio of **2ca**:**2cb** is 4:5.

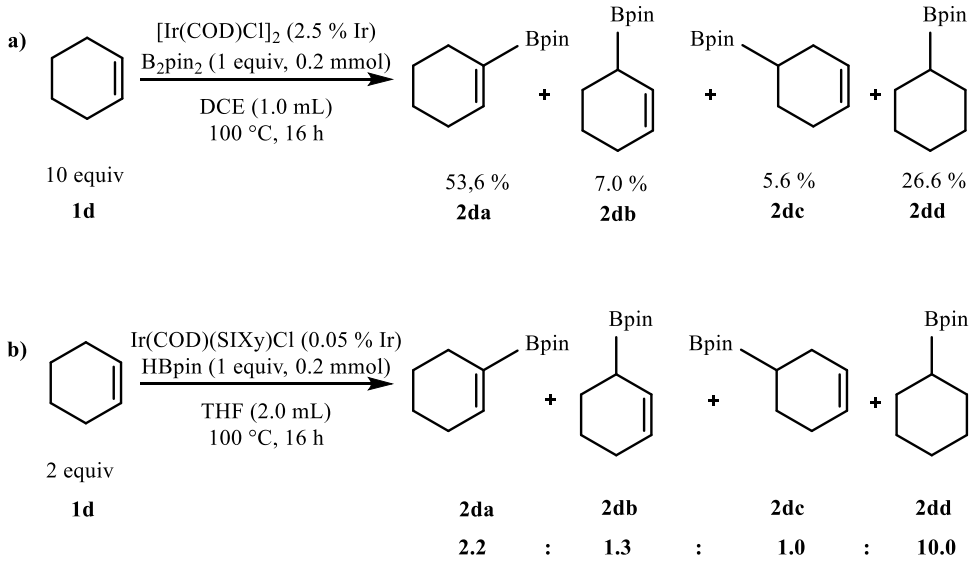

Figure 4.4. Borylation of cyclohexene.

Both dehydrogenative borylation and hydroboration methods were also applied on cyclohexane. The borylation reaction yielded three isomers of dehydroborylative producs; corresponding alkenylboron **2da** as the major product, allylboron **2db**, and homoallylboron 2dr and hydroboration product **2dd**. On the other hand, the hydroboration condition led the formation 2dd as the major product. When the hydroboration condition is applied, the expected product **2dd** was produced dominantly the ratio of products are as follows; 2.2:1.3:1:10.

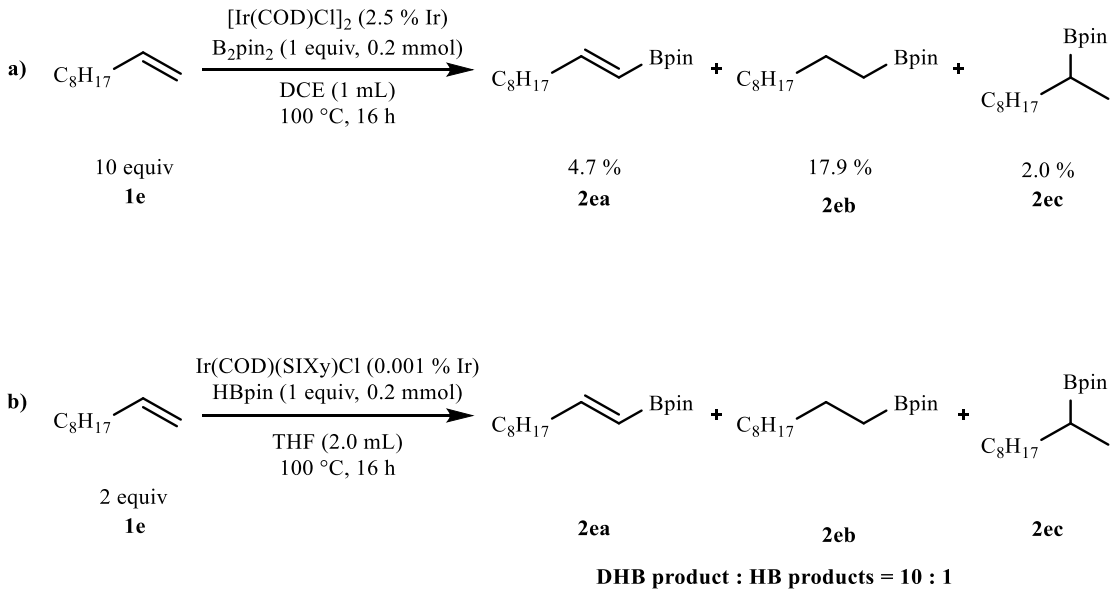

Figure 4.5. Borylation of 1-decene.

The reaction of 1-decene under the dehydrogenative borylation condition led to unexpected results. The yield of the desired product, **2ea**, is lower than hydroboration products **2eb**, **2ec**. When the hydroboration condition is applied, the expected anti-Markovnikov addition hydroboration product is obtained with a high regioselectivity (10:1).

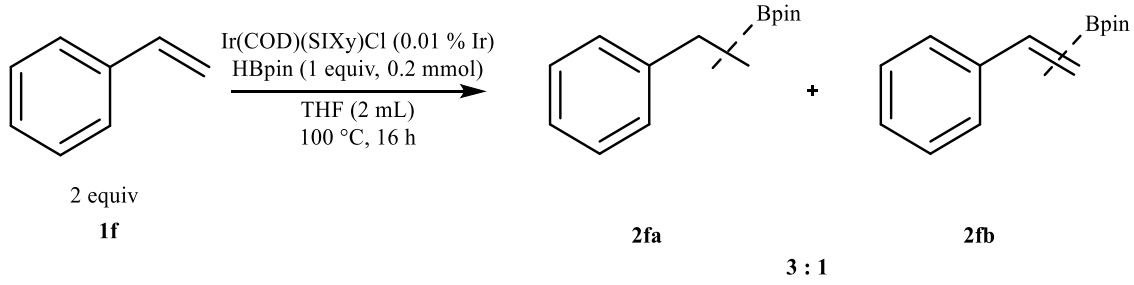

Figure 4.6. Borylation of styrene.

Hydroboration reaction of styrene was carried out under optimum condition, but no selective product was obtained (3:1).

4.6 Suzuki-Miyaura Coupling Reactions with Borylated Isobutene

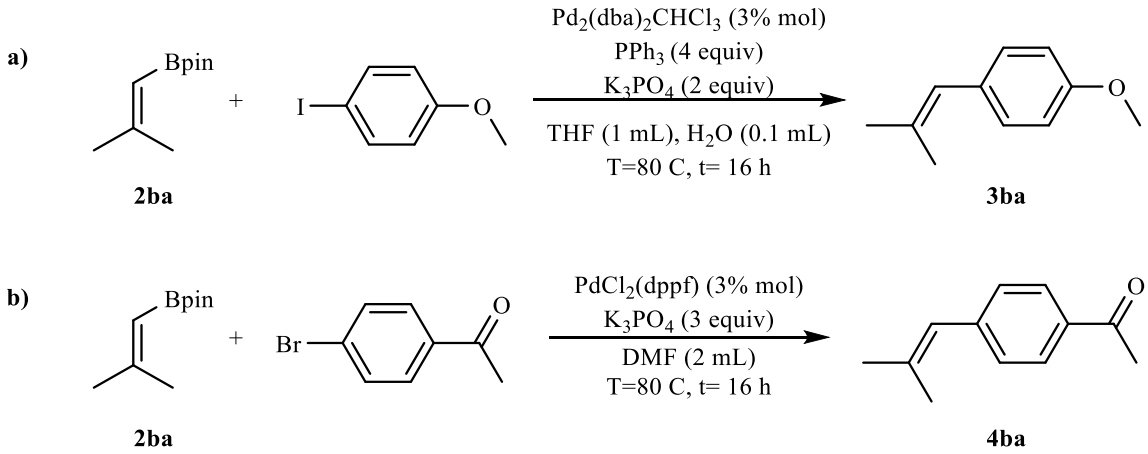

Figure 4.7. Suzuki-Miyaura coupling reaction of **2ba**.

The Suzuki-Miyaura coupling reaction was applied to **2ba** with a palladium catalyst in the presence of base and the formation of coupling reaction products, **3ba** and **4ba**, was detected by GC/MS analysis. The reaction was performed with one-pot method, no purification was applied to borylated isobutene product before the coupling reaction.

CHAPTER 5

CONCLUSION

In this thesis, metal catalysed borylation reaction strategies have been developed for the conversion of petroleum cracking olefinic products to high-added-value organoboron derivatives. These strategies, including hydroboration and dehydrogenative borylation reactions, can be applied to internal or external alkene derivatives. The selectivity of products can be enhanced with a number of substituent groups attached to alkene. Dehydrogenative borylation of petroleum cracking vinylic products was achieved with good yields. Additionally, hydroboration of these products was formed with high regioselectivity and high turn-over-number using N-hetero carbene ligated iridium complexes. The applicability of the method was investigated on various olefins. In accord to this study, further research will be carried out on petroleum cracking olefins to widen the scope of the method.

REFERENCES

1. Alfke, G., W. W. Irion, and O. S. Neuwirth. "Ullmann's encyclopedia of industrial chemistry: Oil refining." (2010).

2. Speight, James G. "Chapter 3-Refining Chemistry.'." *The Refinery of the Future (William Andrew Publishing: Boston)* (2011).

3. Smith, Kyle T., Simon Berritt, Mariano González-Moreiras, Seihwan Ahn, Milton R. Smith III, Mu-Hyun Baik, and Daniel J. Mindiola. "Catalytic borylation of methane." *Science* 351, no. 6280 (2016): 1424-1427.

4. Hu, Anhua, Jing-Jing Guo, Hui Pan, and Zhiwei Zuo. "Selective functionalization of methane, ethane, and higher alkanes by cerium photocatalysis." *Science* 361, no. 6403 (2018): 668-672.

5. Zbieg, Jason R., Eiji Yamaguchi, Emma L. McInturff, and Michael J. Krische. "Enantioselective CH crotylation of primary alcohols via hydrohydroxyalkylation of butadiene." *Science* 336, no. 6079 (2012): 324-327.

6. Yang, Yang, Shi-Liang Shi, Dawen Niu, Peng Liu, and Stephen L. Buchwald. "Catalytic asymmetric hydroamination of unactivated internal olefins to aliphatic amines." *Science* 349, no. 6243 (2015): 62-66.

7. Pagar, Vinayak Vishnu, and T. V. RajanBabu. "Tandem catalysis for asymmetric coupling of ethylene and enynes to functionalized cyclobutanes." *Science* 361, no. 6397 (2018): 68-72.

8. Lachance, Hugo, and Dennis G. Hall. "Allylboration of carbonyl compounds." *ChemInform* 12, no. 2 (2010): i.

9. Mkhalid, Ibraheem AI, Jonathan H. Barnard, Todd B. Marder, Jaclyn M. Murphy, and John F. Hartwig. "C− H activation for the construction of C− B bonds." *Chemical Reviews* 110, no. 2 (2010): 890-931.

10. Pelter, A. "Tilden lecture. Carbon–carbon bond formation involving boron reagents." *Chemical Society Reviews* 11, no. 2 (1982): 191-225.

11. Xu, Liang, Guanghui Wang, Shuai Zhang, Hong Wang, Linghua Wang, Li Liu, Jiao Jiao, and Pengfei Li. "Recent advances in catalytic C− H borylation reactions." *Tetrahedron* 73, no. 51 (2017): 7123-7157.

12. Yang, Chu-Ting, Zhen-Qi Zhang, Hazmi Tajuddin, Chen-Cheng Wu, Jun Liang, Jing-Hui Liu, Yao Fu et al. "Alkylboronic esters from copper-catalyzed borylation of primary and secondary alkyl halides and pseudohalides." *Angewandte Chemie* 124, no. 2 (2012): 543-547.

13. Itoh, Takahiko, Hayato Ishikawa, and Yujiro Hayashi. "Asymmetric aldol reaction of acetaldehyde and isatin derivatives for the total syntheses of ent-convolutamydine E and CPC-1 and a half fragment of madindoline A and B." *Organic letters* 11, no. 17 (2009): 3854-3857.

14. Silverio, Daniel L., Sebastian Torker, Tatiana Pilyugina, Erika M. Vieira, Marc L. Snapper, Fredrik Haeffner, and Amir H. Hoveyda. "Simple organic molecules as catalysts for enantioselective synthesis of amines and alcohols." *Nature* 494, no. 7436 (2013): 216-221.

15. Penner, Marlin, Vivek Rauniyar, Ludwig T. Kaspar, and Dennis G. Hall. "Catalytic asymmetric synthesis of palmerolide A via organoboron methodology." *Journal of the American Chemical Society* 131, no. 40 (2009): 14216-14217.

16. Lou, Sha, Philip N. Moquist, and Scott E. Schaus. "Asymmetric allylboration of acyl imines catalyzed by chiral diols." *Journal of the American Chemical Society* 129, no. 49 (2007): 15398-15404.

17. Brown, Herbert, and B. C. Rao. "Communications-Hydroboration of Olefins. A Remakably Fast Room-Temperature Addition of Diborane to Olefins." *The Journal of Organic Chemistry* 22, no. 9 (1957): 1136-1137.

18. Männig, Detlef, and Heinrich Nöth. "Catalytic hydroboration with rhodium complexes." *Angewandte Chemie International Edition in English* 24, no. 10 (1985): 878-879.

19. Westcott, Stephen A., Todd B. Marder, and R. Thomas Baker. "Transition metal-catalyzed addition of catecholborane to. alpha.-substituted vinylarenes: hydroboration vs dehydrogenative borylation." *Organometallics* 12, no. 3 (1993): 975-979.

20. Pereira, Schubert, and Morris Srebnik. "A study of hydroboration of alkenes and alkynes with pinacolborane catalyzed by transition metals." *Tetrahedron letters* 37, no. 19 (1996): 3283-3286.

21. Zhang, Lei, Dongjie Peng, Xuebing Leng, and Zheng Huang. "Iron-Catalyzed, Atom-Economical, Chemo-and Regioselective Alkene Hydroboration with Pinacolborane." *Angewandte Chemie* 125, no. 13 (2013): 3764-3768.

22. Su, Wei, Rui-Xiao Qiao, Yuan-Ye Jiang, Xiao-Li Zhen, Xia Tian, Jian-Rong Han, Shi-Ming Fan, Qiushi Cheng, and Shouxin Liu. "Ligand-free iron-catalyzed regioselectivity-controlled hydroboration of aliphatic terminal alkenes." *ACS Catalysis* 10, no. 20 (2020): 11963-11970.

23. Chen, Xu, Zhaoyang Cheng, and Zhan Lu. "Iron-catalyzed, Markovnikov-selective hydroboration of styrenes." *Organic letters* 19, no. 5 (2017): 969-971.

24. MacNair, Alistair J., Clement RP Millet, Gary S. Nichol, Alan Ironmonger, and Stephen P. Thomas. "Markovnikov-selective, activator-free iron-catalyzed vinylarene hydroboration." *ACS Catalysis* 6, no. 10 (2016): 7217-7221.

25. Touney, Eric E., Ryan Van Hoveln, Carl T. Buttke, Michael D. Freidberg, Ilia A. Guzei, and Jennifer M. Schomaker. "Heteroleptic nickel complexes for the Markovnikov-selective hydroboration of styrenes." *Organometallics* 35, no. 20 (2016): 3436-3439.

26. Li, Jiang-Fei, Zhen-Zhong Wei, Yong-Qiu Wang, and Mengchun Ye. "Base-free nickel-catalyzed hydroboration of simple alkenes with bis (pinacolato) diboron in an alcoholic solvent." *Green Chemistry* 19, no. 19 (2017): 4498-4502.

27. Kubota, Koji, Eiji Yamamoto, and Hajime Ito. "Copper (I)-catalyzed borylative exo-cyclization of alkenyl halides containing unactivated double bond." *Journal of the American Chemical Society* 135, no. 7 (2013): 2635-2640.

28. Hemming, David, Russell Fritzemeier, Stephen A. Westcott, Webster L. Santos, and Patrick G. Steel. "Copper-boryl mediated organic synthesis." *Chemical Society Reviews* 47, no. 19 (2018): 7477-7494.

29. Obligacion, Jennifer V., and Paul J. Chirik. "Bis (imino) pyridine cobalt-catalyzed alkene isomerization–hydroboration: a strategy for remote hydrofunctionalization with terminal selectivity." *Journal of the American Chemical Society* 135, no. 51 (2013): 19107-19110.

30. Palmer, W. Neil, Tianning Diao, Iraklis Pappas, and Paul J. Chirik. "High-activity cobalt catalysts for alkene hydroboration with electronically responsive terpyridine and α-diimine ligands." *Acs Catalysis* 5, no. 2 (2015): 622-626.

31. Yamamoto, Yasunori, Rhyou Fujikawa, Tomokazu Umemoto, and Norio Miyaura. "Iridium-catalyzed hydroboration of alkenes with pinacolborane." *Tetrahedron* 60, no. 47 (2004): 10695-10700.

32. Vijaykumar, Gonela, Mrinal Bhunia, and Swadhin K. Mandal. "A phenalenyl-based nickel catalyst for the hydroboration of olefins under ambient conditions." *Dalton Transactions* 48, no. 17 (2019): 5779-5784.

33. Wang, Guangzhu, Xinyi Liang, Lili Chen, Qian Gao, Jian-Guo Wang, Panke Zhang, Qian Peng, and Senmiao Xu. "Iridium-Catalyzed Distal Hydroboration of Aliphatic Internal Alkenes." *Angewandte Chemie International Edition* 58, no. 24 (2019): 8187-8191.

34. Zhang, Heyi, and Zhan Lu. "Dual-stereocontrol asymmetric cobalt-catalyzed hydroboration of sterically hindered styrenes." *ACS Catalysis* 6, no. 10 (2016): 6596-6600.

35. Smith, James R., Beatrice SL Collins, Matthew J. Hesse, Mark A. Graham, Eddie L. Myers, and Varinder K. Aggarwal. "Enantioselective rhodium (III)-catalyzed Markovnikov hydroboration of unactivated terminal alkenes." *Journal of the American Chemical Society* 139, no. 27 (2017): 9148-9151.

36. Tseng, Kuei-Nin T., Jeff W. Kampf, and Nathaniel K. Szymczak. "Regulation of iron-catalyzed olefin hydroboration by ligand modifications at a remote site." *Acs Catalysis* 5, no. 1 (2015): 411-415.

37. Zhang, Lei, Ziqing Zuo, Xuebing Leng, and Zheng Huang. "A Cobalt-Catalyzed Alkene Hydroboration with Pinacolborane." *Angewandte Chemie International Edition* 53, no. 10 (2014): 2696-2700.

38. Obligacion, Jennifer V., and Paul J. Chirik. "Highly selective bis (imino) pyridine iron-catalyzed alkene hydroboration." *Organic letters* 15, no. 11 (2013): 2680-2683.

39. Wu, Jessica Y., Benoît Moreau, and Tobias Ritter. "Iron-catalyzed 1, 4-hydroboration of 1, 3-dienes." *Journal of the American Chemical Society* 131, no. 36 (2009): 12915-12917.

40. Evans, David A., Gregory C. Fu, and Amir H. Hoveyda. "Rhodium (I)-and iridium (I)-catalyzed hydroboration reactions: scope and synthetic applications." *Journal of the American Chemical Society* 114, no. 17 (1992): 6671-6679.

41. Geier, Stephen J., and Stephen A. Westcott. "Dehydrogenative borylation: the dark horse in metal-catalyzed hydroborations and diborations?." *Reviews in Inorganic Chemistry* 35, no. 2 (2015): 69-79.

42. Brown, John M., and Guy C. Lloyd-Jones. "Vinylborane formation in rhodium-catalysed hydroborations; ligand-free homogeneous catalysis." *Journal of the Chemical Society, Chemical Communications* 9 (1992): 710-712.

43. Burgess, Kevin, Wilfred A. Van der Donk, Stephen A. Westcott, Todd B. Marder, R. Thomas Baker, and Joseph C. Calabrese. "Reactions of catecholborane with Wilkinson's catalyst: implications for transition metal-catalyzed hydroborations of alkenes." *Journal of the American Chemical Society* 114, no. 24 (1992): 9350-9359.

44. Murata, Miki, Shinji Watanabe, and Yuzuru Masuda. "Rhodium-catalyzed dehydrogenative coupling reaction of vinylarenes with pinacolborane to vinylboronates." *Tetrahedron letters* 40, no. 13 (1999): 2585-2588.

45. Brown, Alec N., Lev N. Zakharov, Tanya Mikulas, David A. Dixon, and Shih-Yuan Liu. "Rhodium-catalyzed B–H activation of 1, 2-azaborines: synthesis and characterization of BN isosteres of stilbenes." *Organic letters* 16, no. 12 (2014): 3340-3343.

46. Caballero, Ana, and Sylviane Sabo-Etienne. "Ruthenium-catalyzed hydroboration and dehydrogenative borylation of linear and cyclic alkenes with pinacolborane." *Organometallics* 26, no. 5 (2007): 1191-1195.

47. Morimoto, Masao, Tomoya Miura, and Masahiro Murakami. "Rhodium-Catalyzed Dehydrogenative Borylation of Aliphatic Terminal Alkenes with Pinacolborane." *Angewandte Chemie International Edition* 54, no. 43 (2015): 12659-12663.

48. Waltz, Karen M., Xiaoming He, Clare Muhoro, and John F. Hartwig. "Hydrocarbon functionalization by transition metal boryls." *Journal of the American Chemical Society* 117, no. 45 (1995): 11357-11358.

49. Wang, Chao, Caizhi Wu, and Shaozhong Ge. "Iron-catalyzed E-selective dehydrogenative borylation of vinylarenes with pinacolborane." *ACS Catalysis* 6, no. 11 (2016): 7585-7589.

50. Neeve, Emily C., Stephen J. Geier, Ibraheem AI Mkhalid, Stephen A. Westcott, and Todd B. Marder. "Diboron (4) compounds: from structural curiosity to synthetic workhorse." *Chemical Reviews* 116, no. 16 (2016): 9091-9161.

51. Mkhalid, I. A. I., R. B. Coapes, S. N. Edes, D. N. Coventry, F. E. S. Souza, and R. Thomas. "LI.; Hall, JJ; Bi, S.-W.; Lin, Z.; Marder, TB." *Dalton Trans* 1055 (2008).

52. Kondoh, Azusa, and Timothy F. Jamison. "Rhodium-catalyzed dehydrogenative borylation of cyclic alkenes." *Chemical communications* 46, no. 6 (2010): 907-909.

53. Selander, Nicklas, Benjamin Willy, and Kálmán J. Szabó. "Selective C□ H Borylation of Alkenes by Palladium Pincer Complex Catalyzed Oxidative Functionalization." *Angewandte Chemie* 122, no. 24 (2010): 4145-4147.

54. Takaya, Jun, Naohiro Kirai, and Nobuharu Iwasawa. "Efficient synthesis of diborylalkenes from alkenes and diboron by a new PSiP-pincer palladium-catalyzed dehydrogenative borylation." *Journal of the American Chemical Society* 133, no. 33 (2011): 12980-12983.

55. Olsson, Vilhelm J., and Kalman J. Szabo. "Functionalization of Unactivated Alkenes through Iridium-Catalyzed Borylation of Carbon− Hydrogen Bonds. Mechanism and Synthetic Applications." *The Journal of Organic Chemistry* 74, no. 20 (2009): 7715-7723.

56. Coapes, R. Benjamin, Fabio ES Souza, Rhodri Ll Thomas, Jonathan J. Hall, and Todd B. Marder. "Rhodium catalysed dehydrogenative borylation of vinylarenes and 1, 1-disubstituted alkenes without sacrificial hydrogenation—a route to 1, 1-disubstituted vinylboronates." *Chemical communications* 5 (2003): 614-615.

57. Kikuchi, Takao, Jun Takagi, Hironori Isou, Tatsuo Ishiyama, and Norio Miyaura. "Vinylic C-H Borylation of Cyclic Vinyl Ethers with Bis (pinacolato) diboron Catalyzed by an Iridium (I)-dtbpy Complex." *Chemistry–An Asian Journal* 3, no. 12 (2008): 2082-2090.

58. Sasaki, Ikuo, Hana Doi, Toshiya Hashimoto, Takao Kikuchi, Hajime Ito, and Tatsuo Ishiyama. "Iridium (i)-catalyzed vinylic C–H borylation of 1-cycloalkenecarboxylates with bis (pinacolato) diboron." *Chemical Communications* 49, no. 68 (2013): 7546-7548.

59. Olsson, Vilhelm J., and Kalman J. Szabo. "Synthesis of Allylsilanes and Dienylsilanes by a One-Pot Catalytic C− H Borylation− Suzuki− Miyaura Coupling Sequence." *Organic Letters* 10, no. 14 (2008): 3129-3131.

60. Parkan, Kamil, Radek Pohl, and Martin Kotora. "Cross-Coupling Reaction of Saccharide-Based Alkenyl Boronic Acids with Aryl Halides: The Synthesis of Bergenin." *Chemistry–A European Journal* 20, no. 15 (2014): 4414-4419.

61. Marigo, Mauro, Nazario Marsich, and Erica Farnetti. "Polymerization of phenylacetylene catalyzed by organoiridium compounds." *Journal of Molecular Catalysis A: Chemical* 187, no. 2 (2002): 169-177.

62. Boer, Stephanie A., Pei-Xi Wang, Mark J. MacLachlan, and Nicholas G. White. "Open pentiptycene networks assembled through charge-assisted hydrogen bonds." *Crystal Growth & Design* 19, no. 8 (2019): 4829-4835.

63. Beillard, Audrey, Thomas-Xavier Métro, Xavier Bantreil, Jean Martinez, and Frédéric Lamaty. "Cu (0), O 2 and mechanical forces: A saving combination for efficient production of Cu–NHC complexes." *Chemical science* 8, no. 2 (2017): 1086-1089.

64. Papadaki, Evanthia, and Victoria Magrioti. "Synthesis of pentafluorobenzene-based NHC adducts and their catalytic activity in the microwave-assisted reactions of aldehydes." *Tetrahedron Letters* 61, no. 4 (2020): 151419.

65. Gülcemal, Süleyman, Derya Gülcemal, George FS Whitehead, and Jianliang Xiao. "Acceptorless Dehydrogenative Oxidation of Secondary Alcohols Catalysed by Cp* IrIII–NHC Complexes." *Chemistry–A European Journal* 22, no. 30 (2016): 10513-10522.

66. Savka, R., and H. Plenio. "Facile synthesis of [(NHC) MX (cod)] and [(NHC) MCl (CO) 2](M= Rh, Ir; X= Cl, I) complexes." *Dalton Transactions* 44, no. 3 (2015): 891-893.

67. Gülcemal, Süleyman, Aytaç Gürhan Gökçe, and Bekir Çetinkaya. "Iridium (I) N-heterocyclic carbene complexes of benzimidazol-2-ylidene: effect of electron donating groups on the catalytic transfer hydrogenation reaction." *Dalton Transactions* 42, no. 20 (2013): 7305-7311.

68. Seechurn, Carin CC Johansson, Vilvanathan Sivakumar, Deepak Satoskar, and Thomas J. Colacot. "Iridium-Catalyzed C–H Borylation of Heterocycles Using an Overlooked 1, 10-Phenanthroline Ligand: Reinventing the Catalytic Activity by Understanding the Solvent-Assisted Neutral to Cationic Switch." *Organometallics* 33, no. 13 (2014): 3514-3522.

69. Schenck, Terry G., J. M. Downes, C. R. C. Milne, Peter B. Mackenzie, Terry G. Boucher, John Whelan, and B. Bosnich. "Bimetallic reactivity. Synthesis of bimetallic complexes containing a bis (phosphino) pyrazole ligand." *Inorganic Chemistry* 24, no. 15 (1985): 2334-2337.

70. Olsson, Vilhelm J., and Kalman J. Szabo. "Selective One-Pot Carbon–Carbon Bond Formation by Catalytic Boronation of Unactivated Cycloalkenes and Subsequent Coupling." *Angewandte Chemie* 119, no. 36 (2007): 7015-7017.

71. Özdemir, Ismail, Serpil Demir, and Bekir Çetinkaya. "Synthesis of novel rhodium–carbene complexes as efficient catalysts for addition of phenylboronic acid to aldehydes." *Journal of Molecular Catalysis A: Chemical* 215, no. 1-2 (2004): 45-48.

72. Yiğit, Murat, Ismail Özdemir, Bekir Çetinkaya, and Engin Çetinkaya. "Novel N-heterocyclic-carbene–rhodium complexes as hydrosilylation catalysts." *Journal of Molecular Catalysis A: Chemical* 241, no. 1-2 (2005): 88-92.

73. Neshat, Abdollah, Piero Mastrorilli, and Ali Mousavizadeh Mobarakeh. "Recent Advances in Catalysis Involving Bidentate N-Heterocyclic Carbene Ligands." *Molecules* 27, no. 1 (2021): 95.

APPENDIX A

1H-NMR AND 13C-NMR SPECTRA OF COMPOUNDS

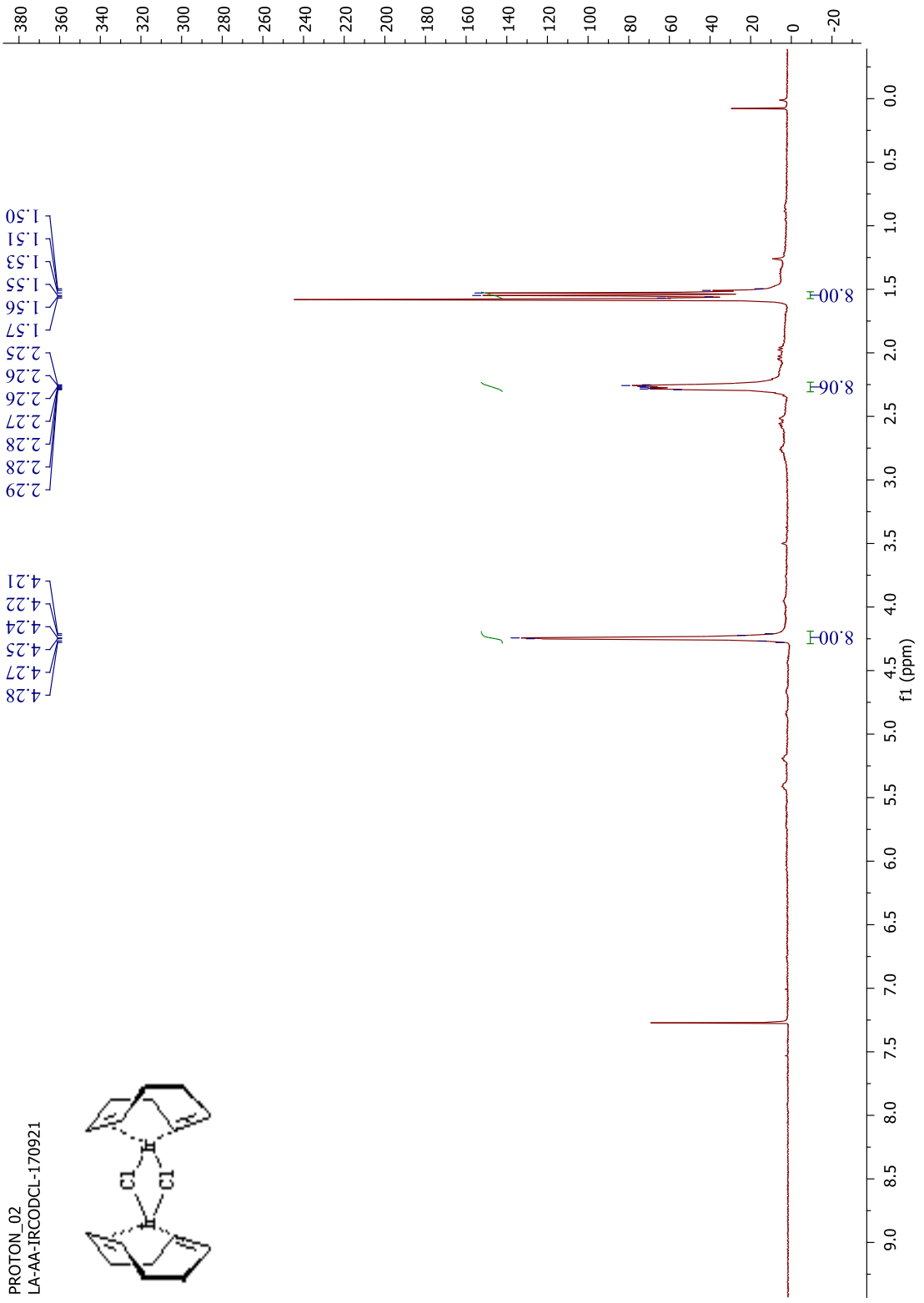
PROTON_02
LA-AA-IRCODCL-170921
Cl
Ir
Cl
Ir
1.50
1.51
1.53
1.55
1.56
1.57
2.25
2.26
2.26
2.27
2.28
2.28
2.29
4.21
4.22
4.24
4.25
4.27
4.28
8.00
8.06
8.00
f1 (ppm)

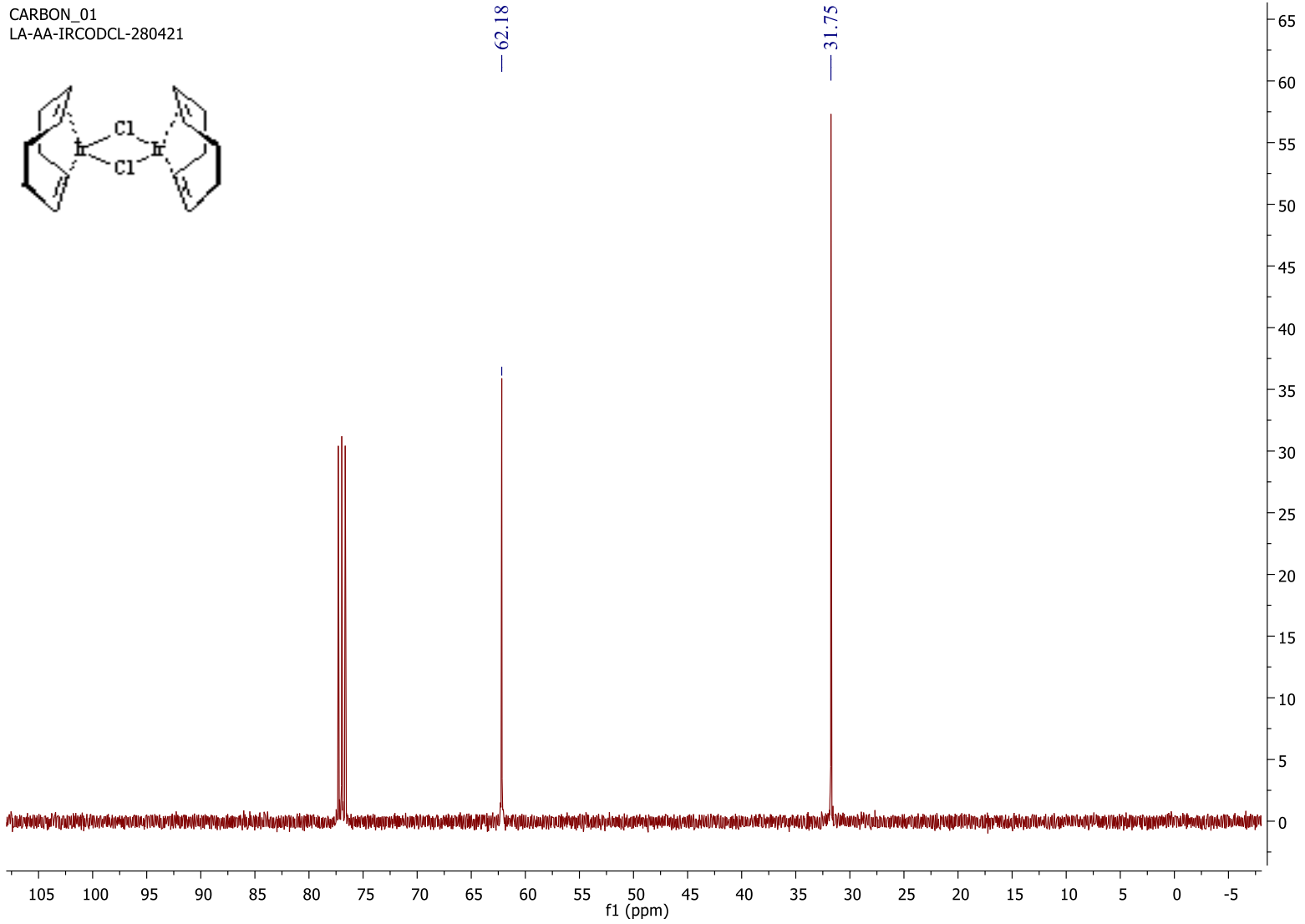
CARBON_01
LA-AA-IRCODCL-280421
Cl
Ir
Ir
Cl
62.18
31.75
f1 (ppm)

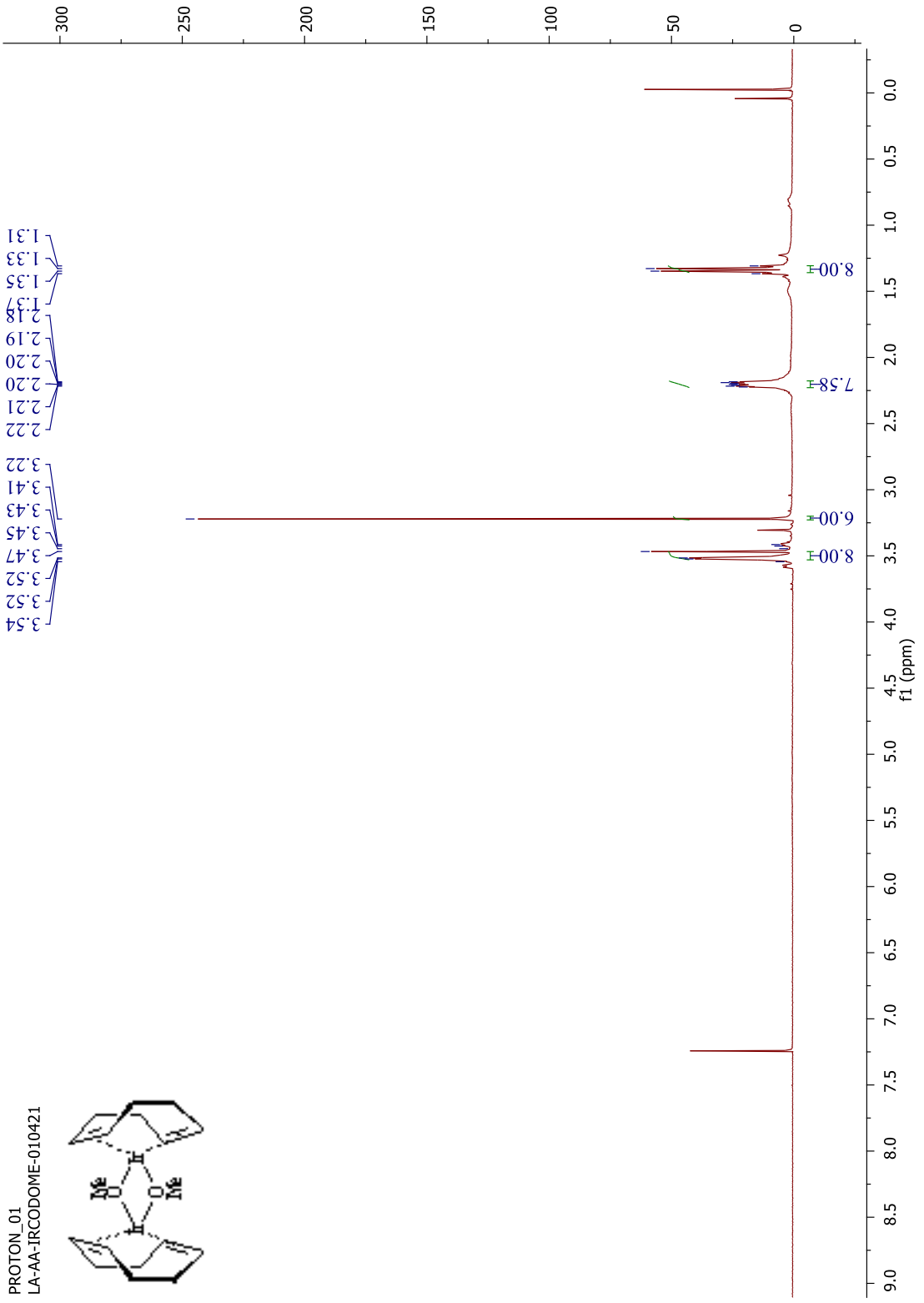
PROTON_01
LA-AA-IRCODOME-010421
Me
O
O
Me
Ir
Ir
1.31
1.33
1.35
1.37
2.18
2.19
2.20
2.20
2.21
2.22
3.22
3.41
3.43
3.45
3.47
3.52
3.52
3.54
8.00
7.58
6.00
8.00
f1 (ppm)

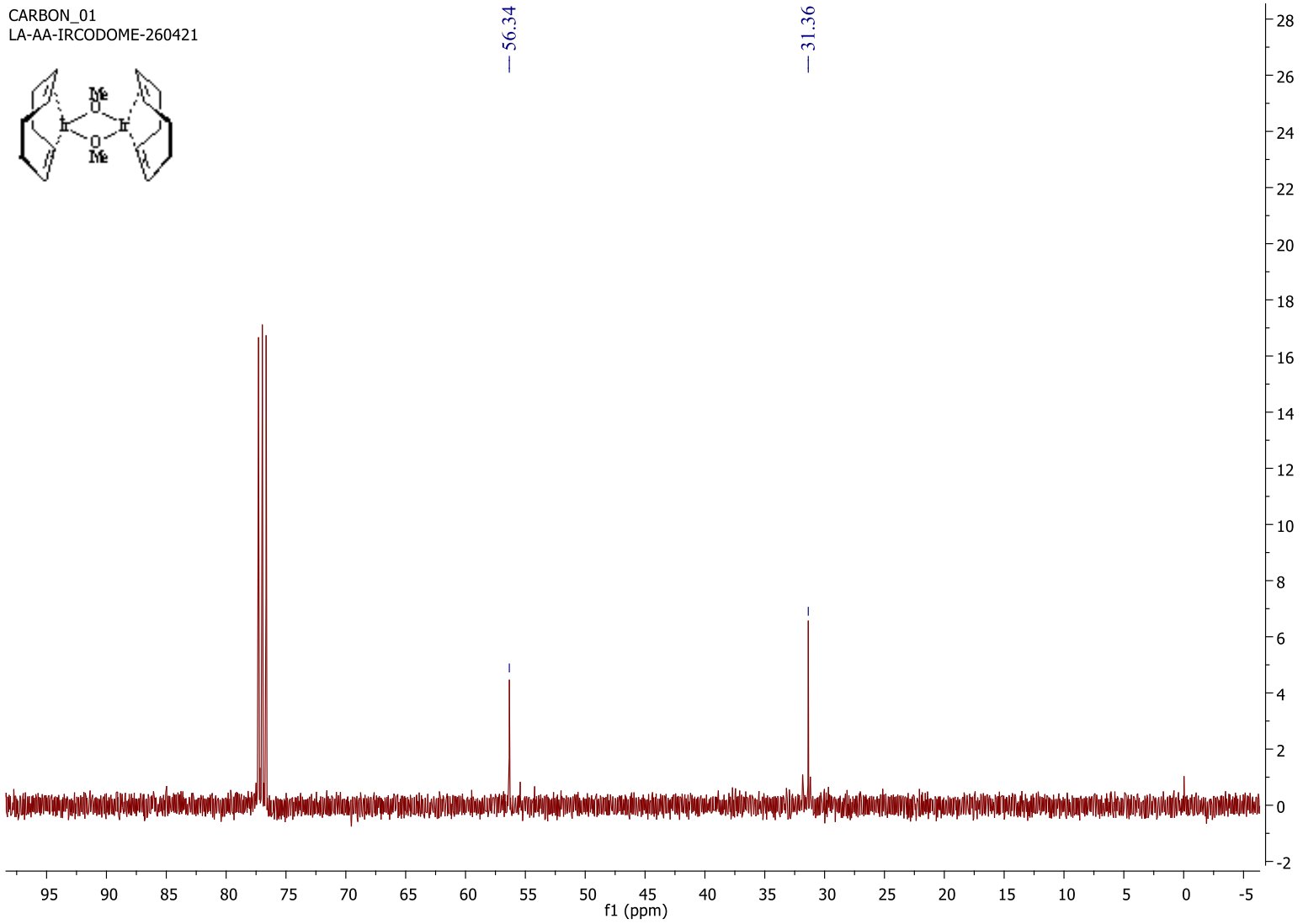
CARBON_01
LA-AA-IRCODOME-260421
56.34
31.36
f1 (ppm)

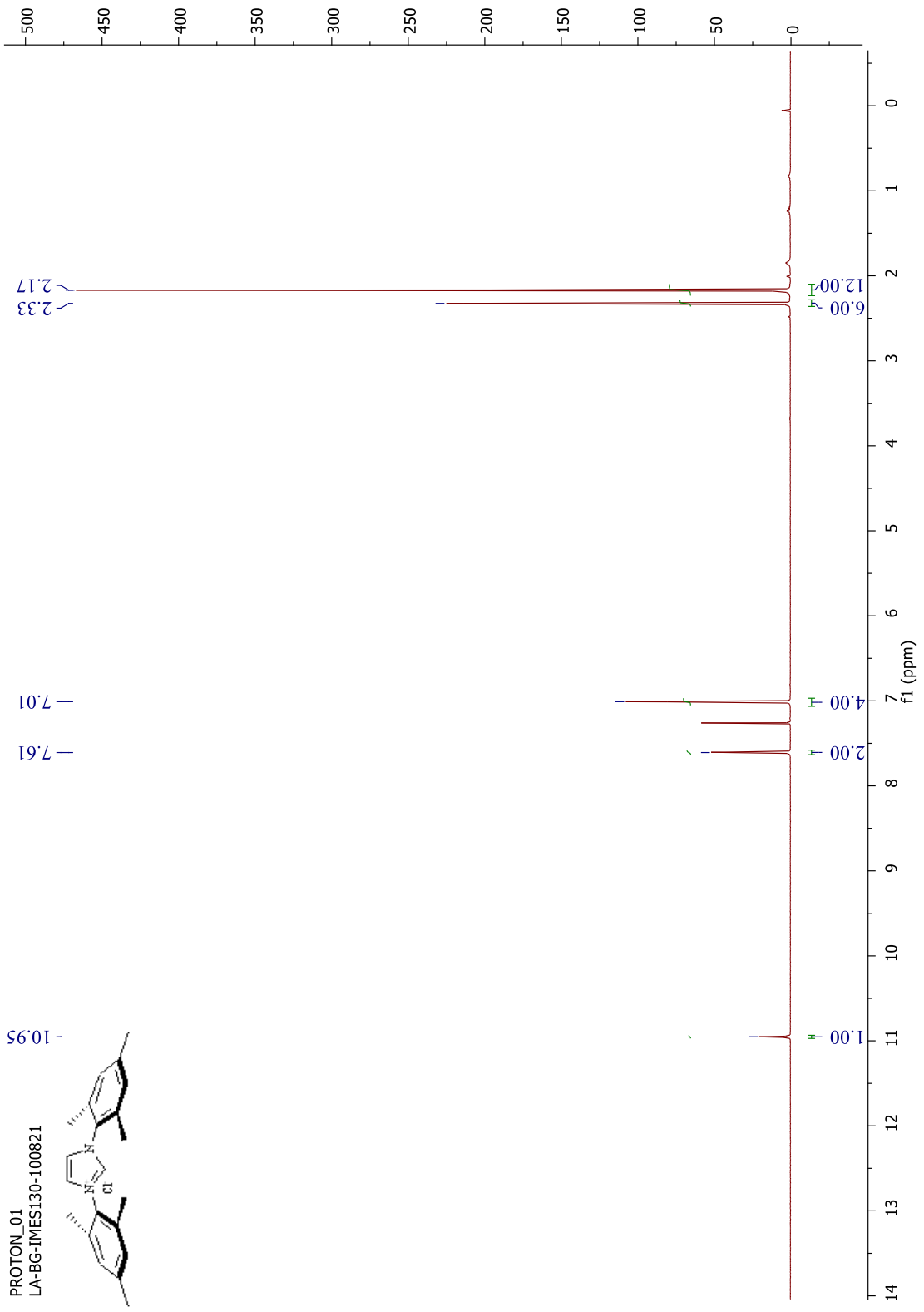
PROTON_01
LA-BG-IMES130-100821
10.95
7.61
7.01
2.33
2.17
1.00
2.00
4.00
6.00
12.00
f1 (ppm)

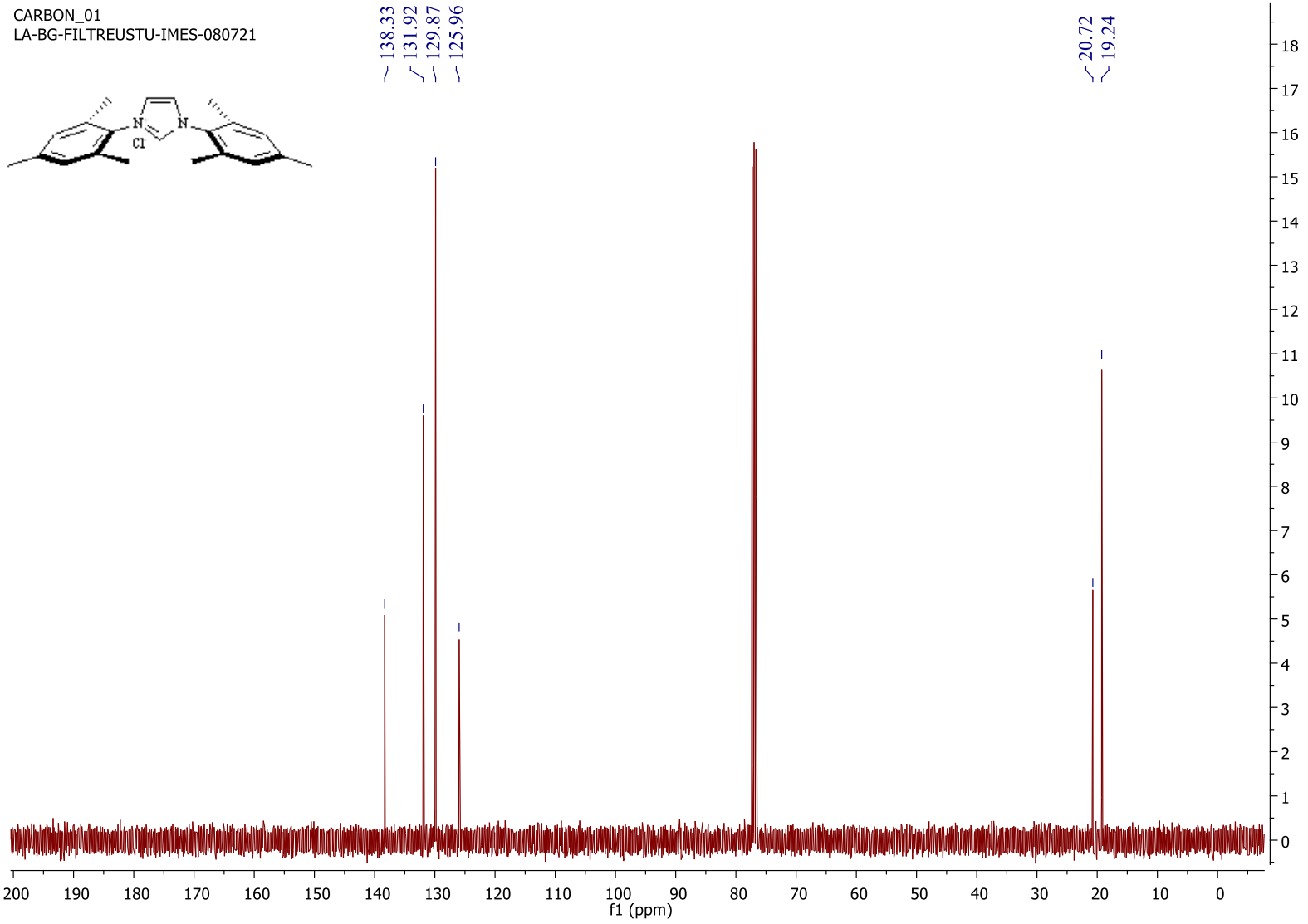
CARBON_01
LA-BG-FILTREUSTU-IMES-080721
138.33
131.92
129.87
125.96
20.72
19.24
N
N
Cl
f1 (ppm)

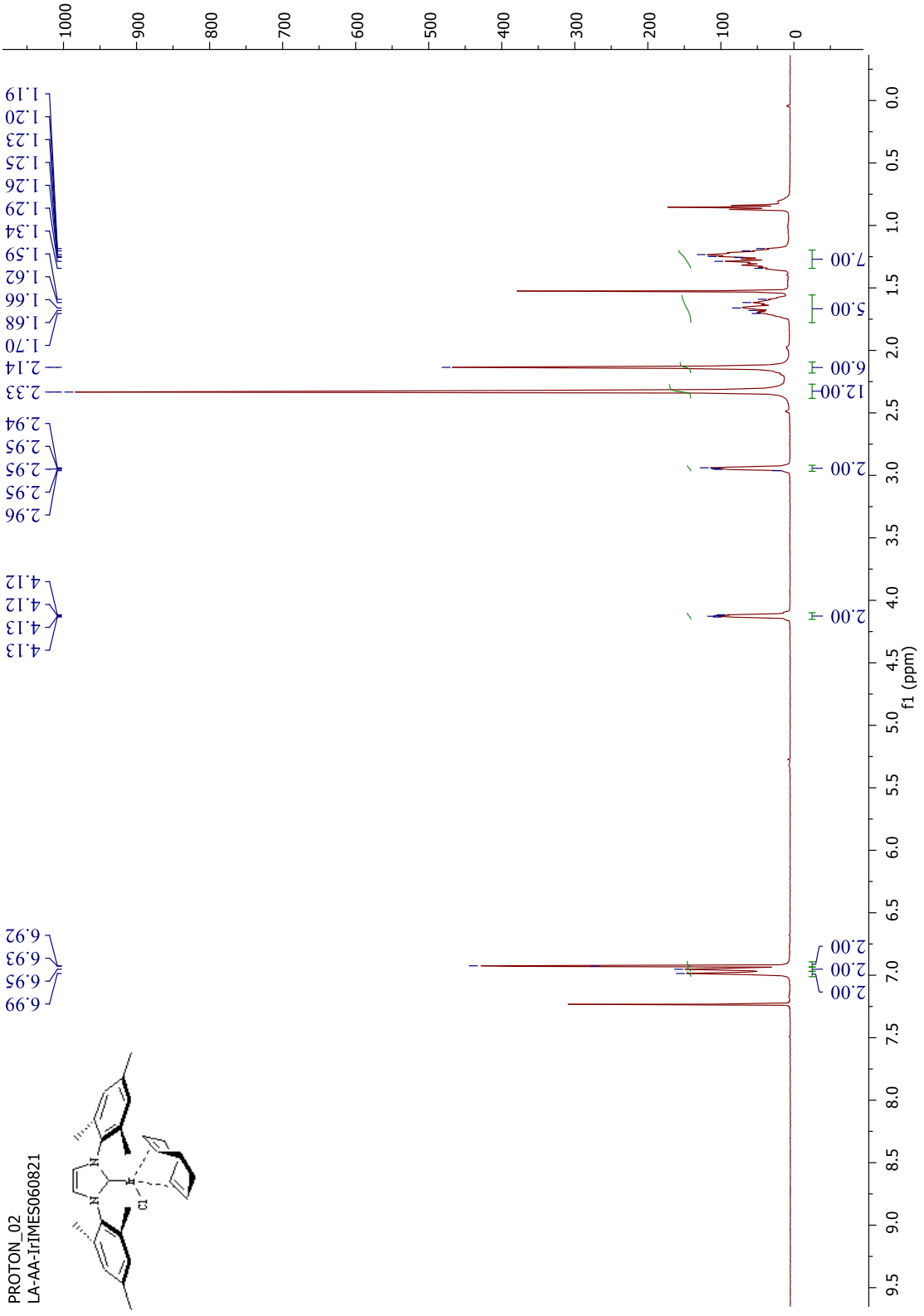
PROTON_02
LA-AA-IrIMES060821
f1 (ppm)

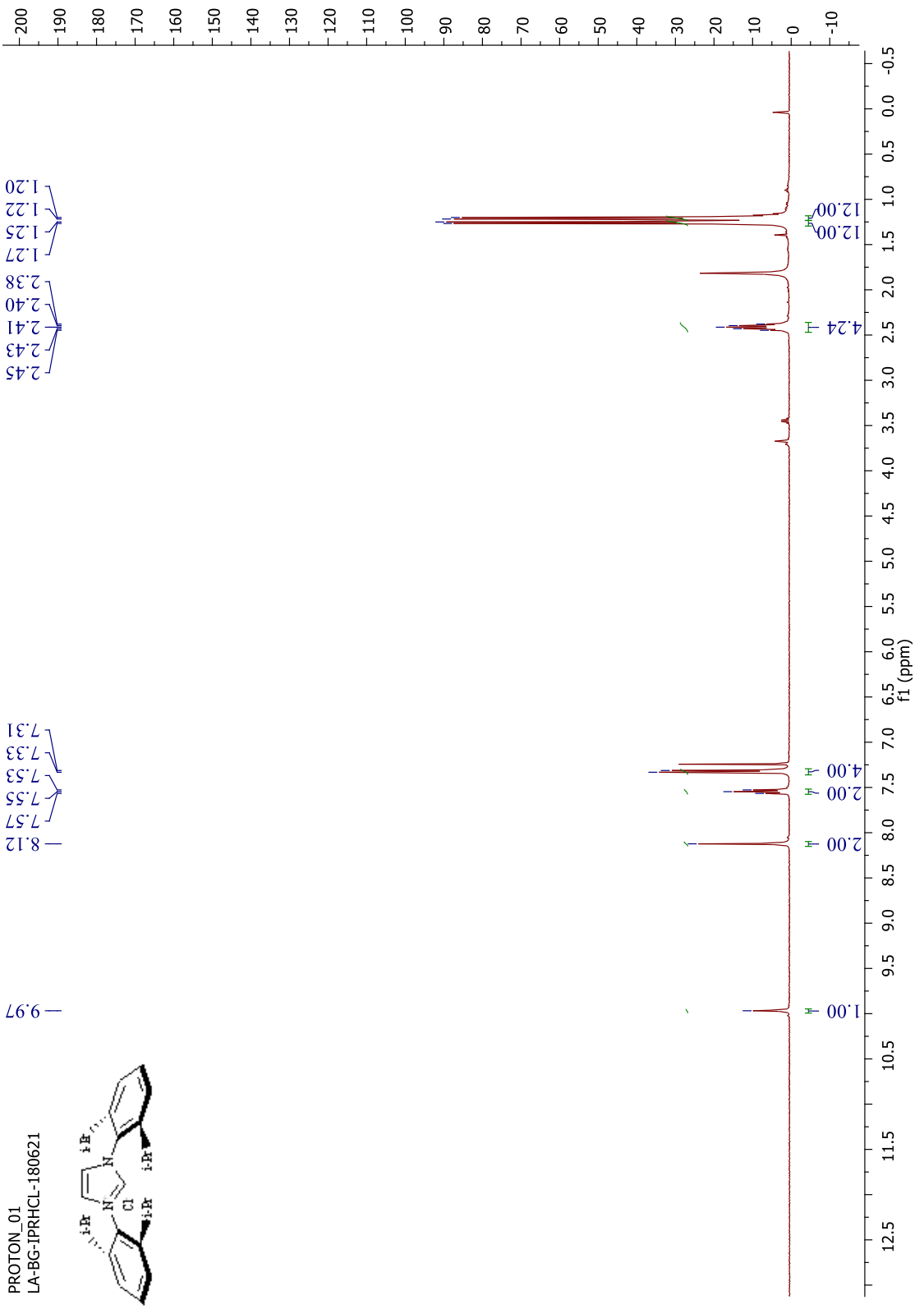
PROTON_01
LA-BG-IPRHCL-180621
i-Pr
i-Pr
N
Cl
N
i-Pr
i-Pr
9.97
8.12
7.57
7.55
7.53
7.33
7.31
2.45
2.43
2.41
2.40
2.38
1.27
1.25
1.22
1.20
1.00
2.00
2.00
4.00
2.00
4.24
12.00
12.00
f1 (ppm)

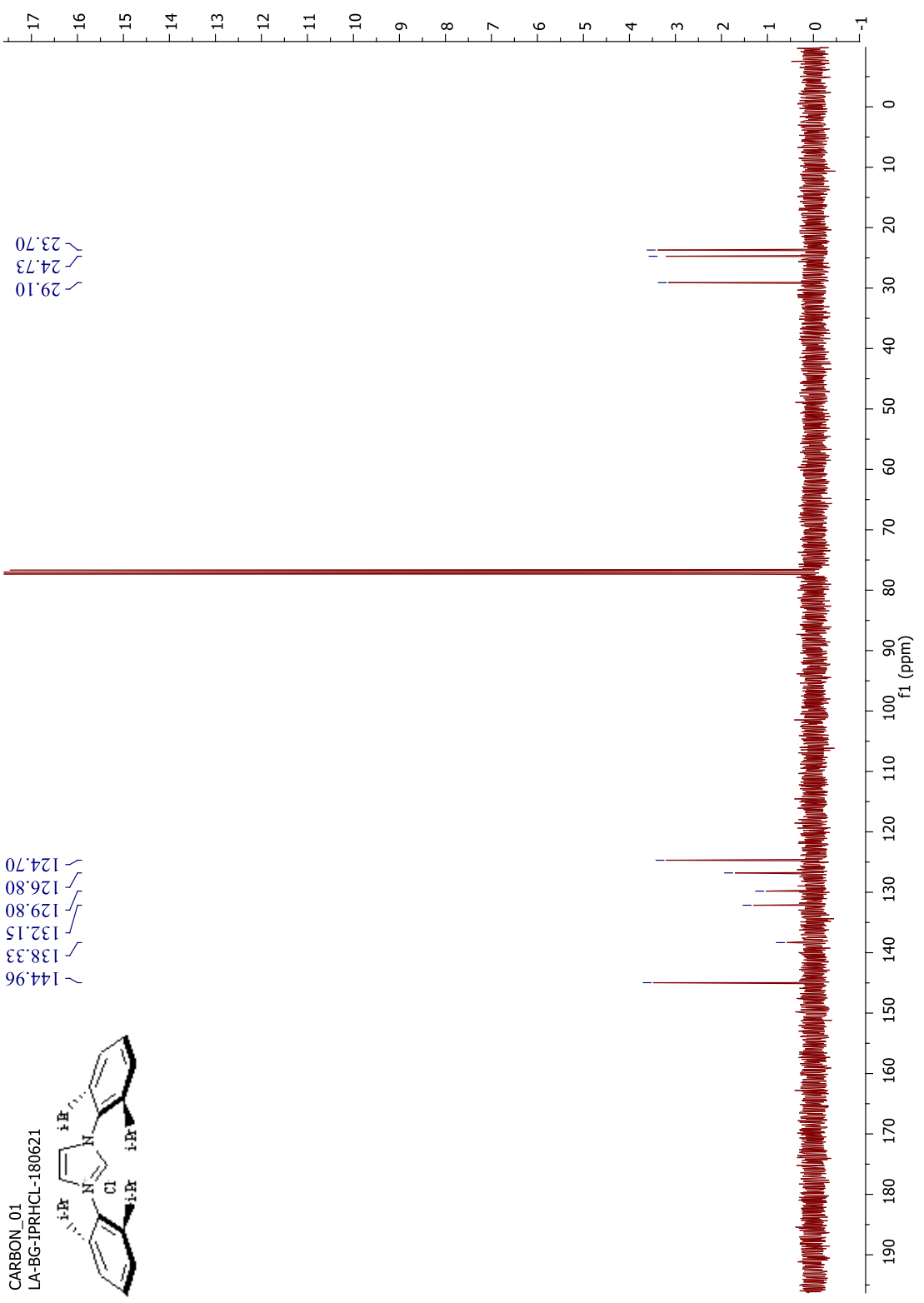
CARBON_01
LA-BG-IPRHCL-180621
144.96
138.33
132.15
129.80
126.80
124.70
29.10
24.73
23.70
f1 (ppm)

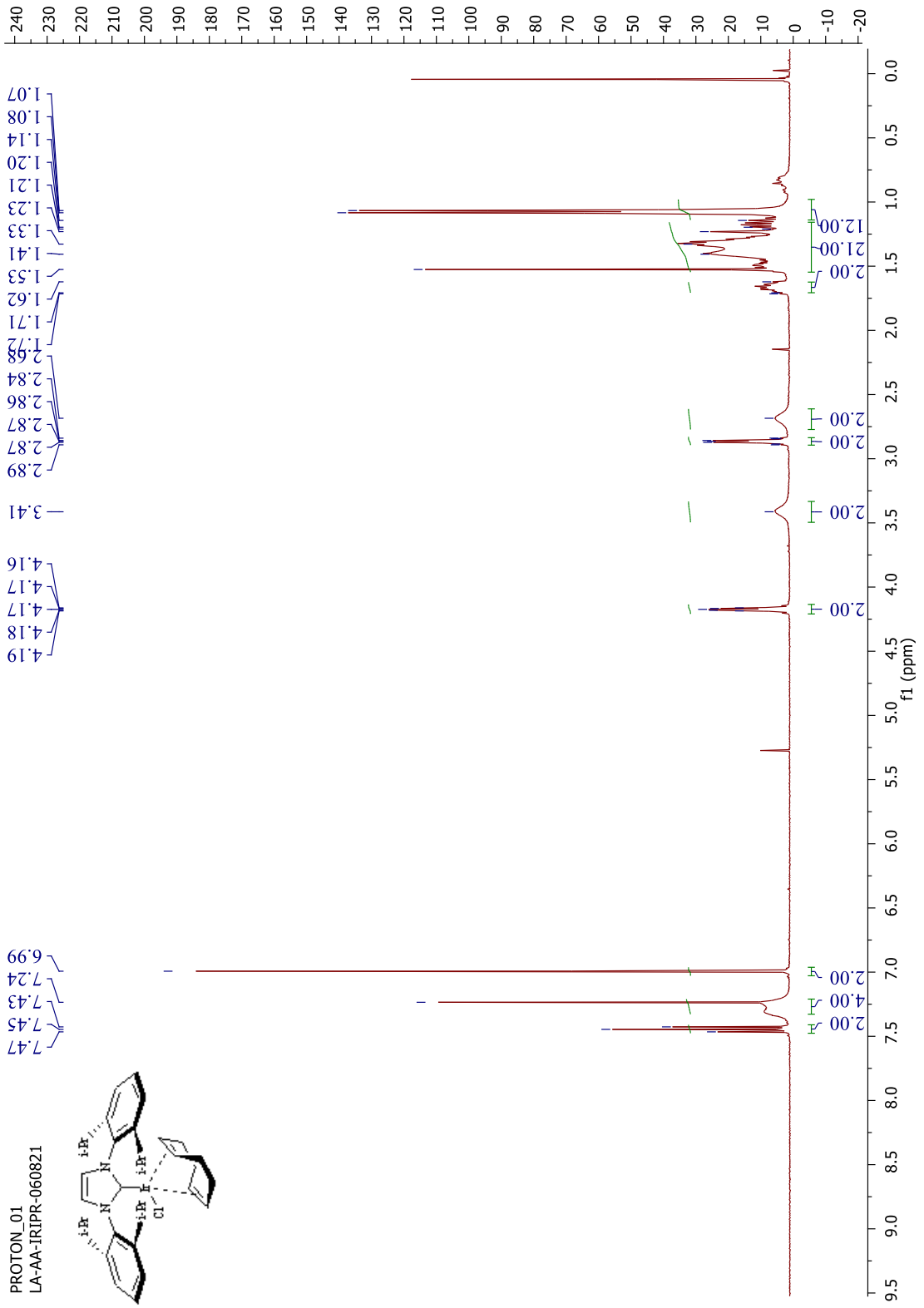
PROTON_01
LA-AA-IRIPR-060821
f1 (ppm)

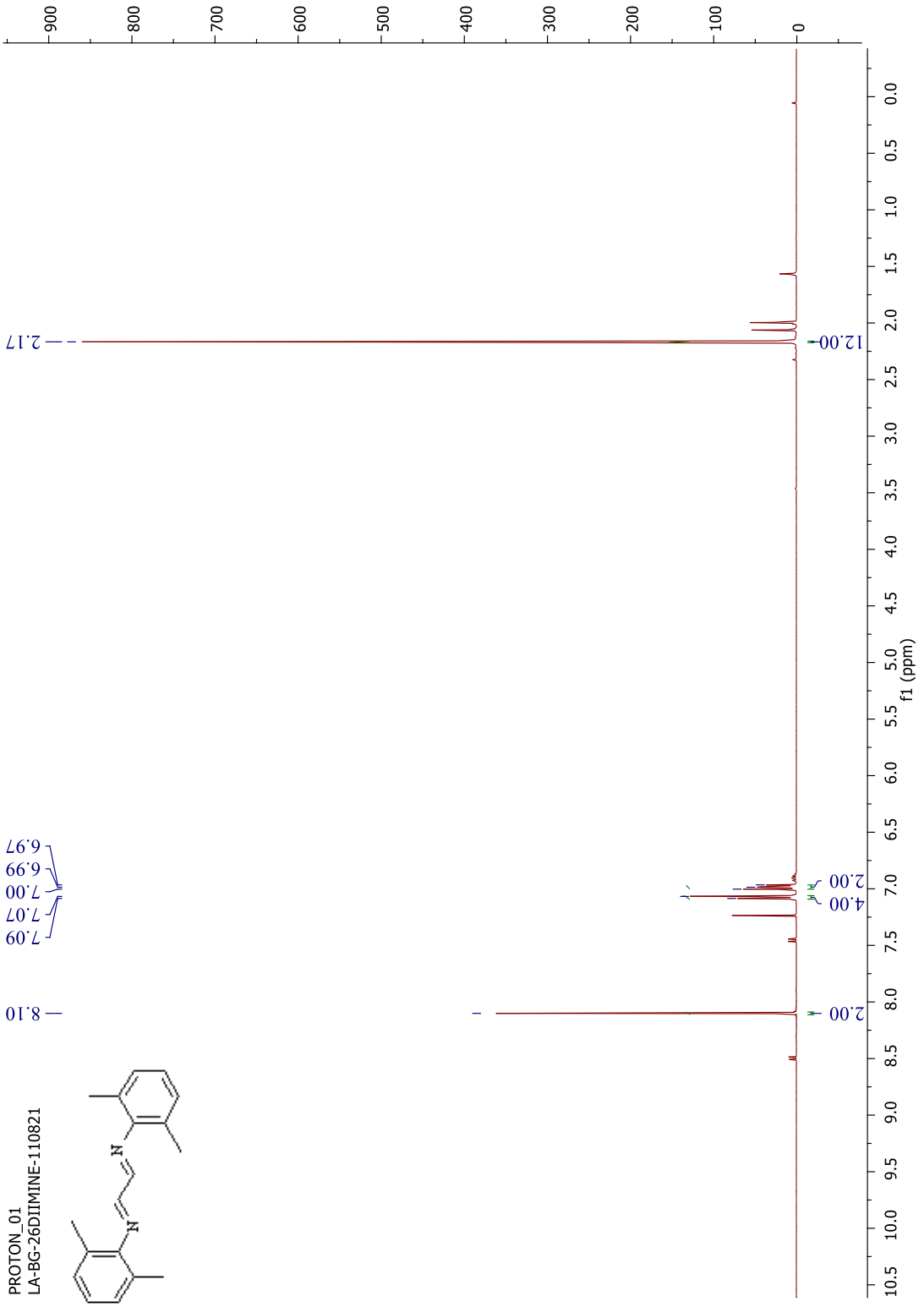
PROTON_01
LA-BG-26DIIMINE-110821
2.17
8.10
7.09
7.07
7.00
6.99
6.97
12.00
4.00
2.00
2.00
f1 (ppm)

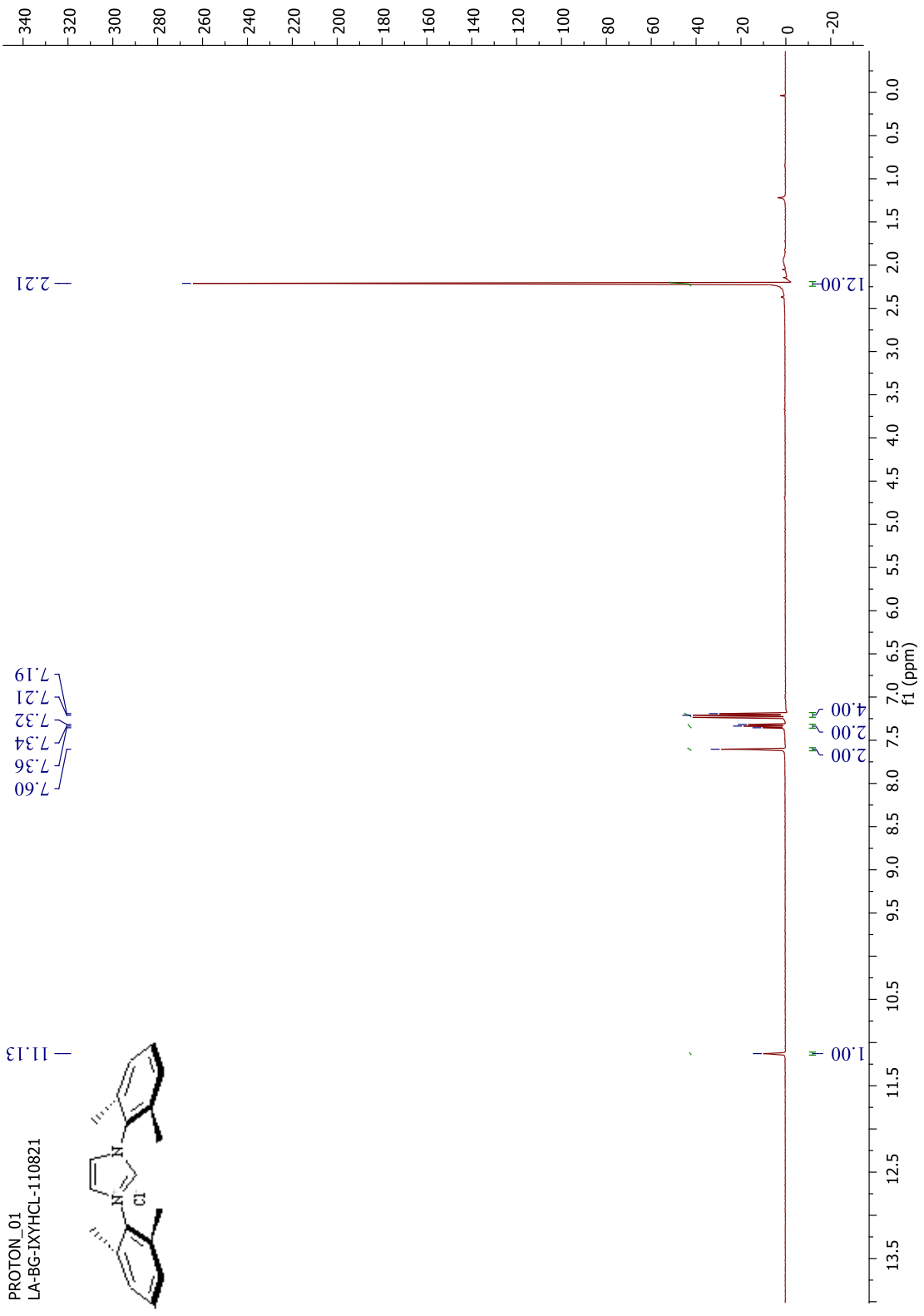
PROTON_01
LA-BG-IXYHCL-110821
11.13
2.21
7.60
7.36
7.34
7.32
7.21
7.19
1.00
2.00
2.00
4.00
12.00
f1 (ppm)

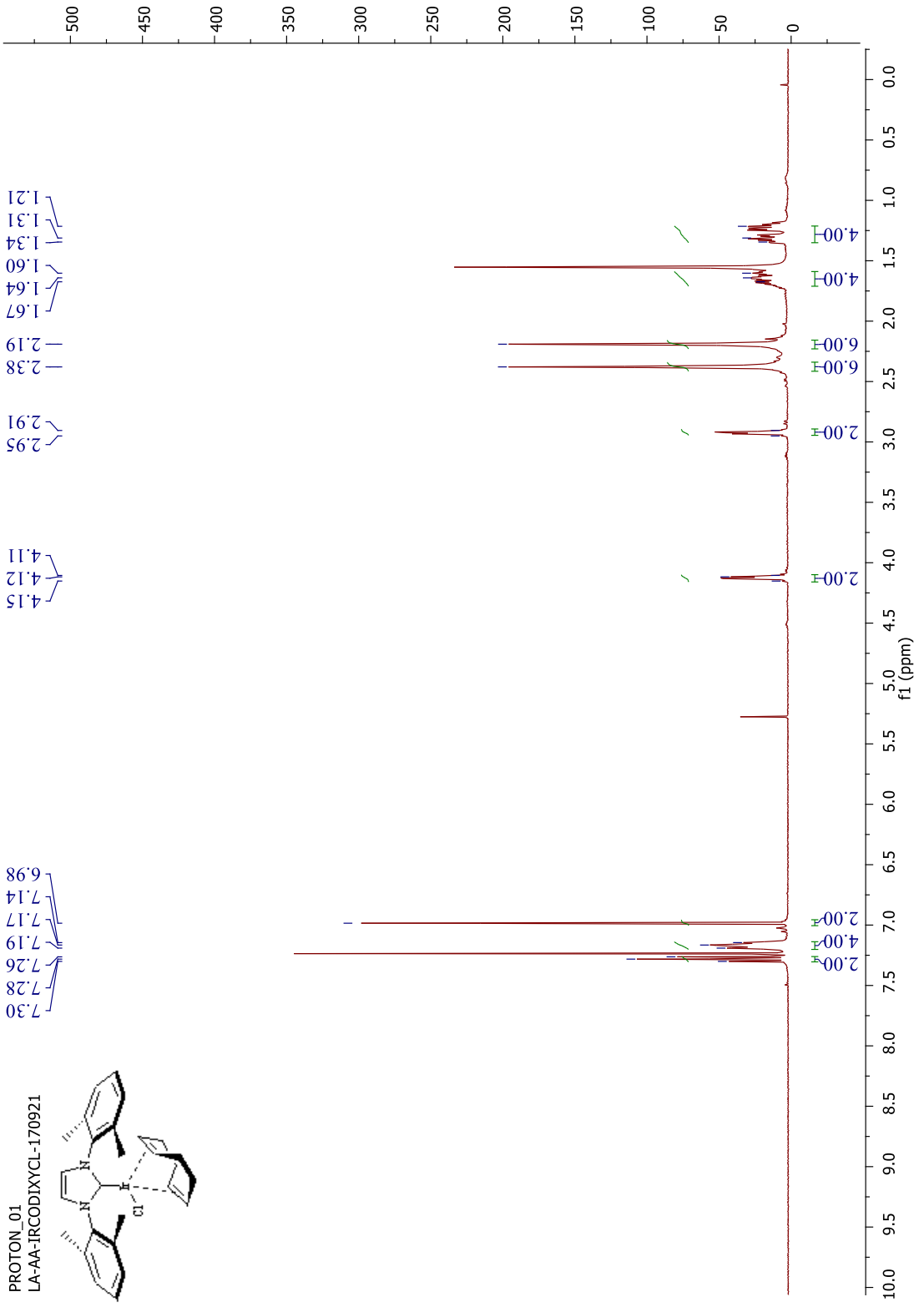
PROTON_01
LA-AA-IRCODIXYCL-170921
7.30
7.28
7.26
7.19
7.17
7.14
6.98
4.15
4.12
4.11
2.95
2.91
2.38
2.19
1.67
1.64
1.60
1.34
1.31
1.21
2.00
4.00
2.00
2.00
6.00
6.00
4.00
4.00
f1 (ppm)

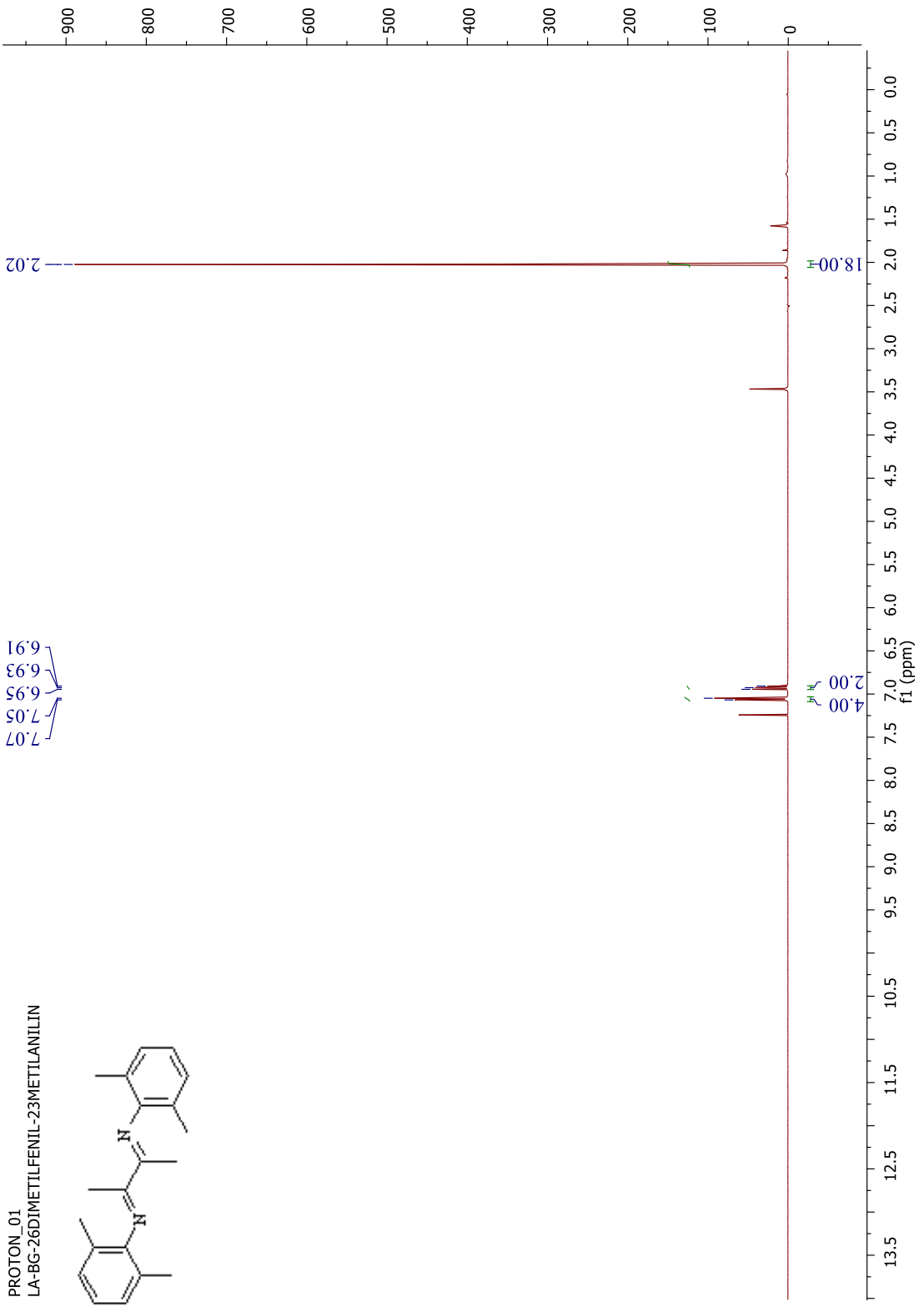
PROTON_01
LA-BG-26DIMETILFENIL-23METILANILIN
N
N
2.02
18.00
6.91
6.93
6.95
7.05
7.07
4.00
2.00
f1 (ppm)

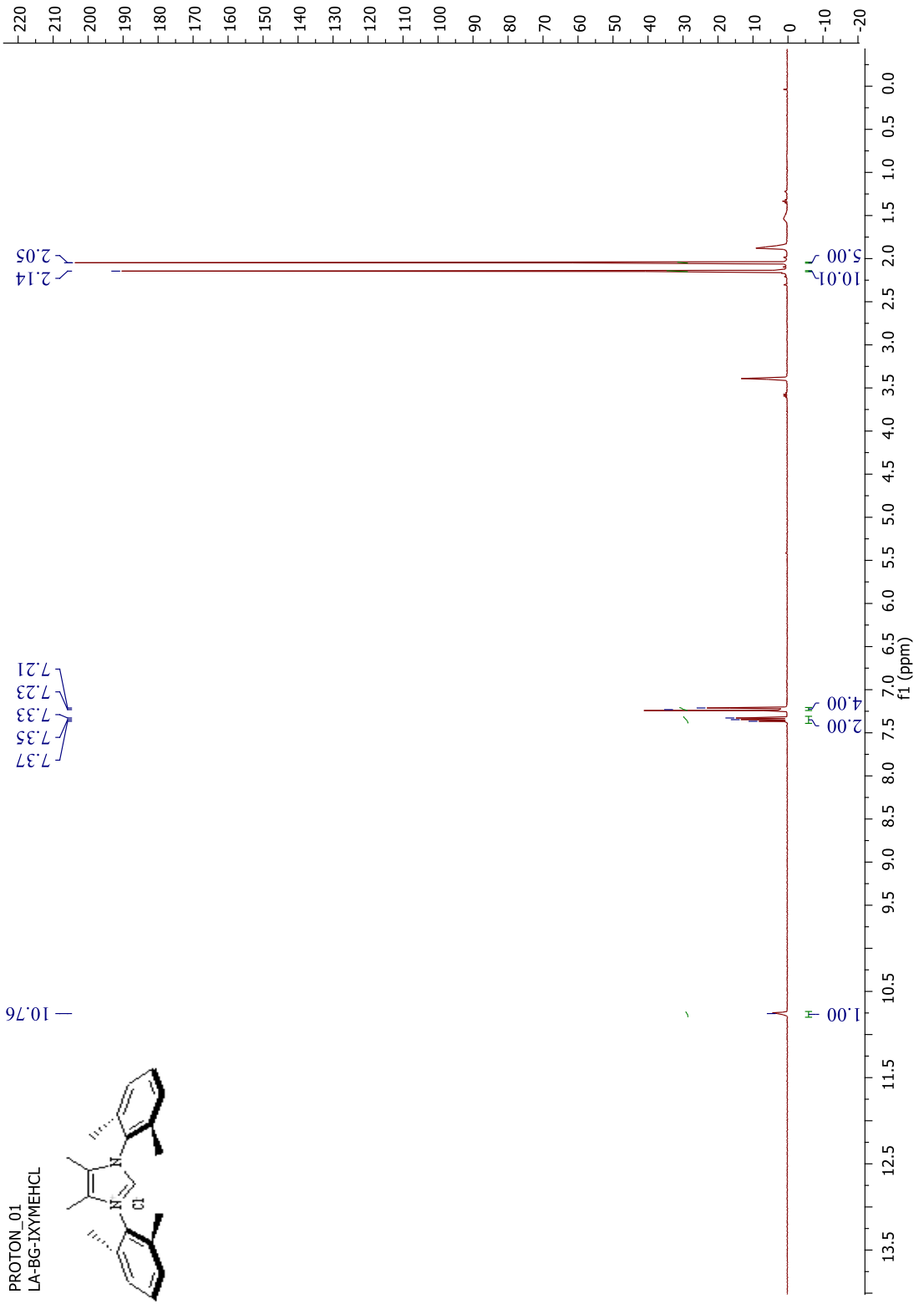
PROTON_01
LA-BG-IXYMEHCL
10.76
7.37
7.35
7.33
7.23
7.21
2.14
2.05
1.00
4.00
2.00
10.01
5.00
f1 (ppm)

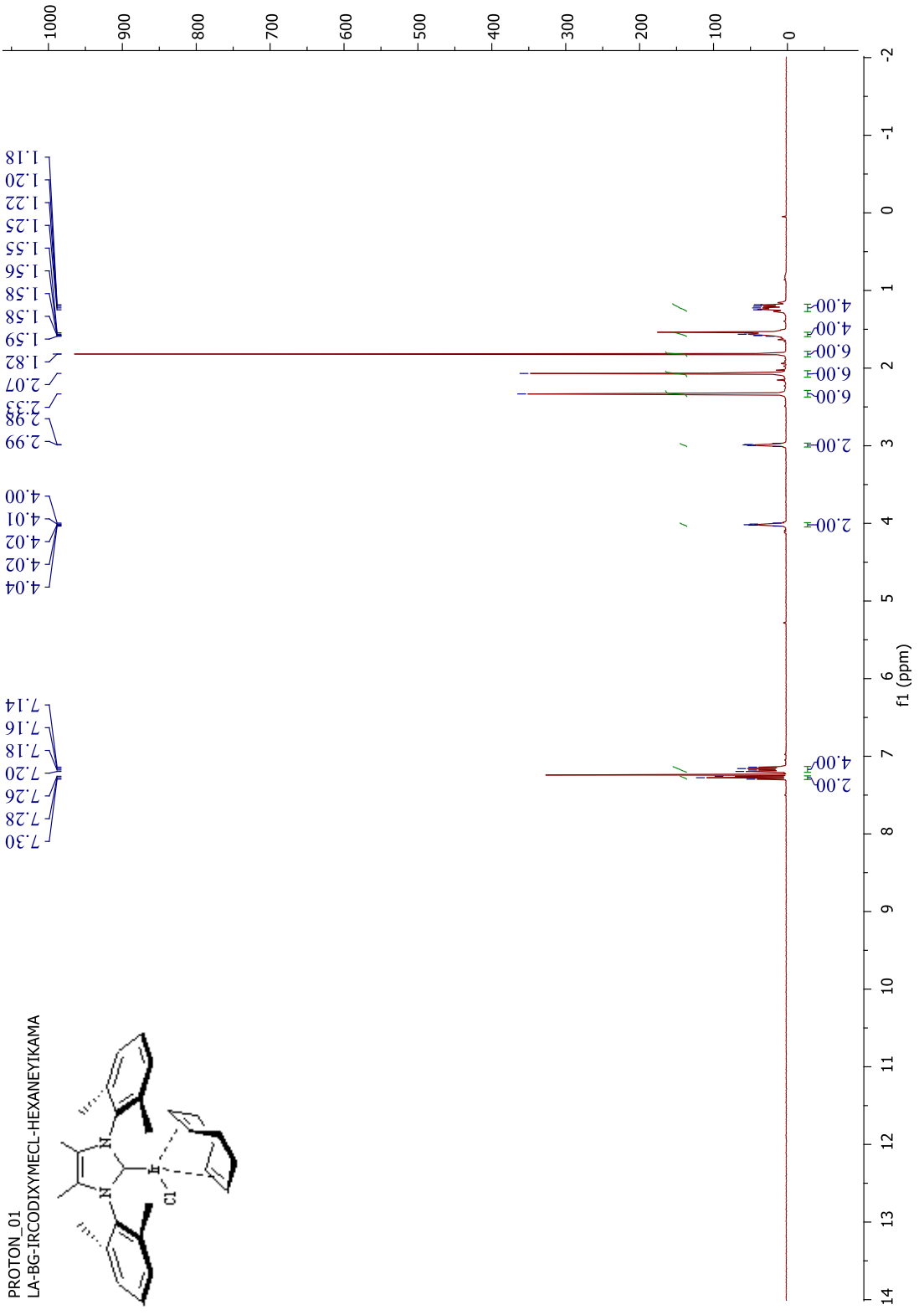
PROTON_01
LA-BG-IRCODIXYMECL-HEXANEYIKAMA
f1 (ppm)

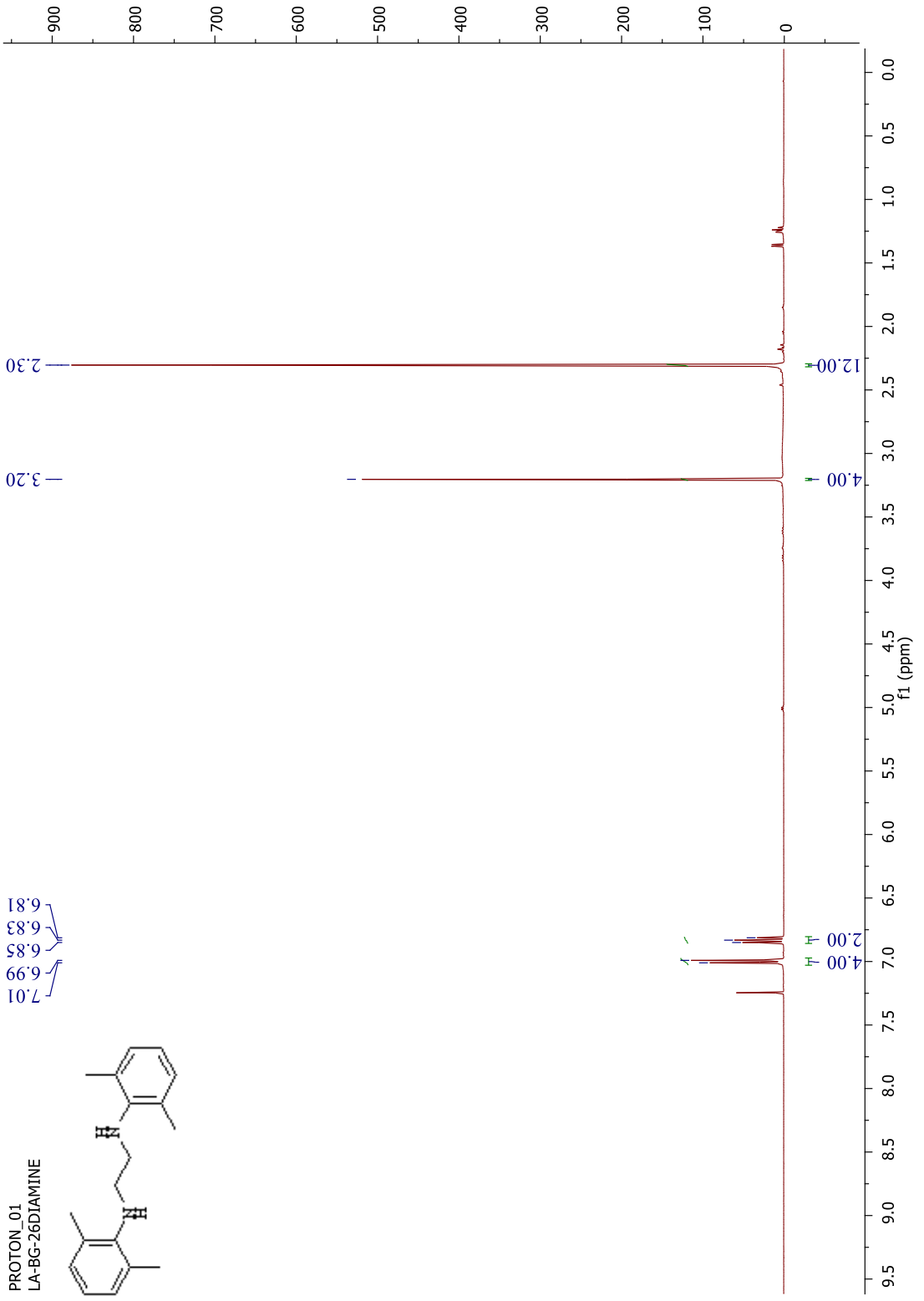
PROTON_01
LA-BG-26DIAMINE
7.01
6.99
6.85
6.83
6.81
3.20
2.30
4.00
2.00
12.00
4.00
f1 (ppm)

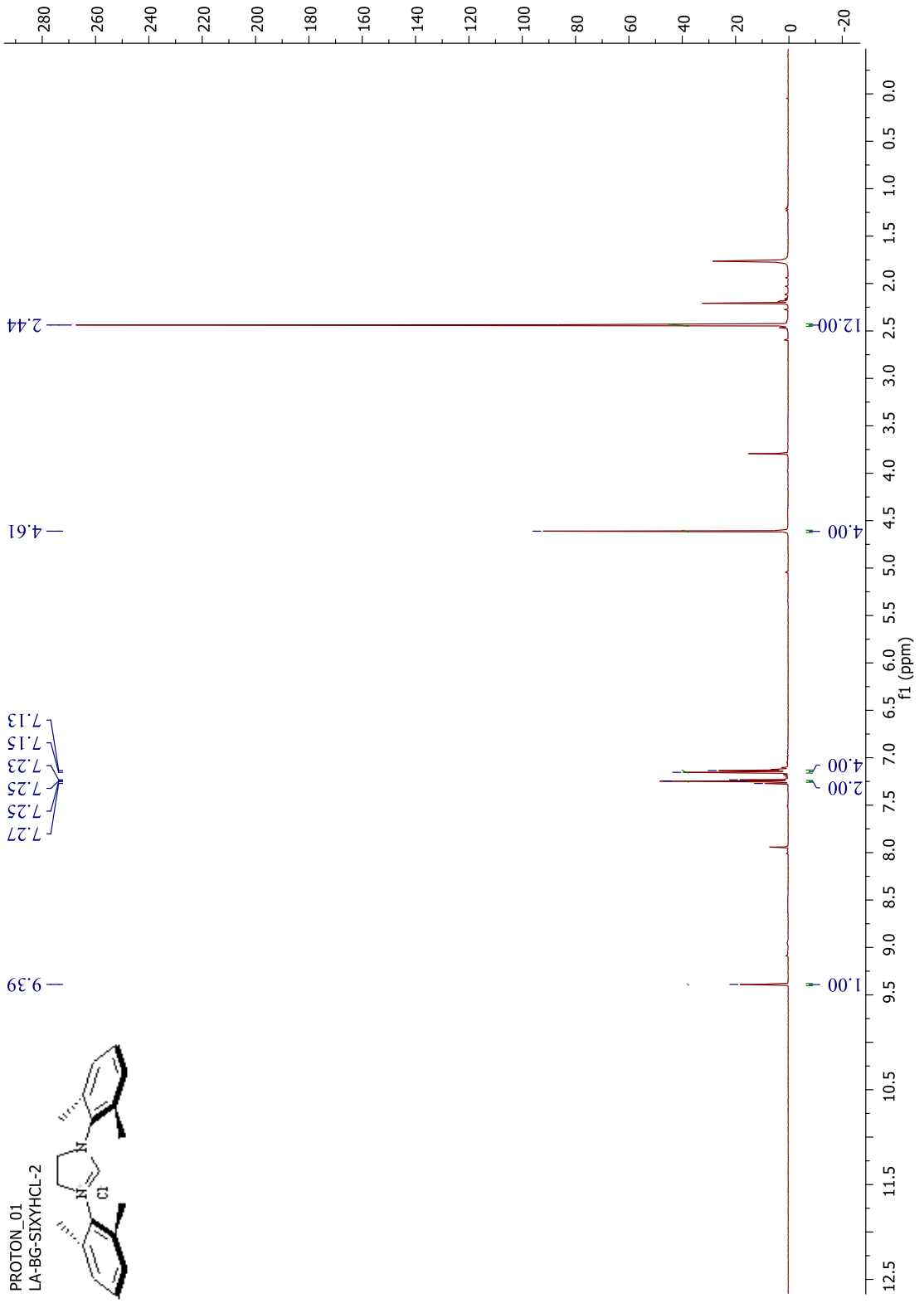
PROTON_01
LA-BG-SIXYHCL-2
9.39
7.27
7.25
7.25
7.23
7.15
7.13
4.61
2.44
1.00
4.00
2.00
4.00
12.00
f1 (ppm)

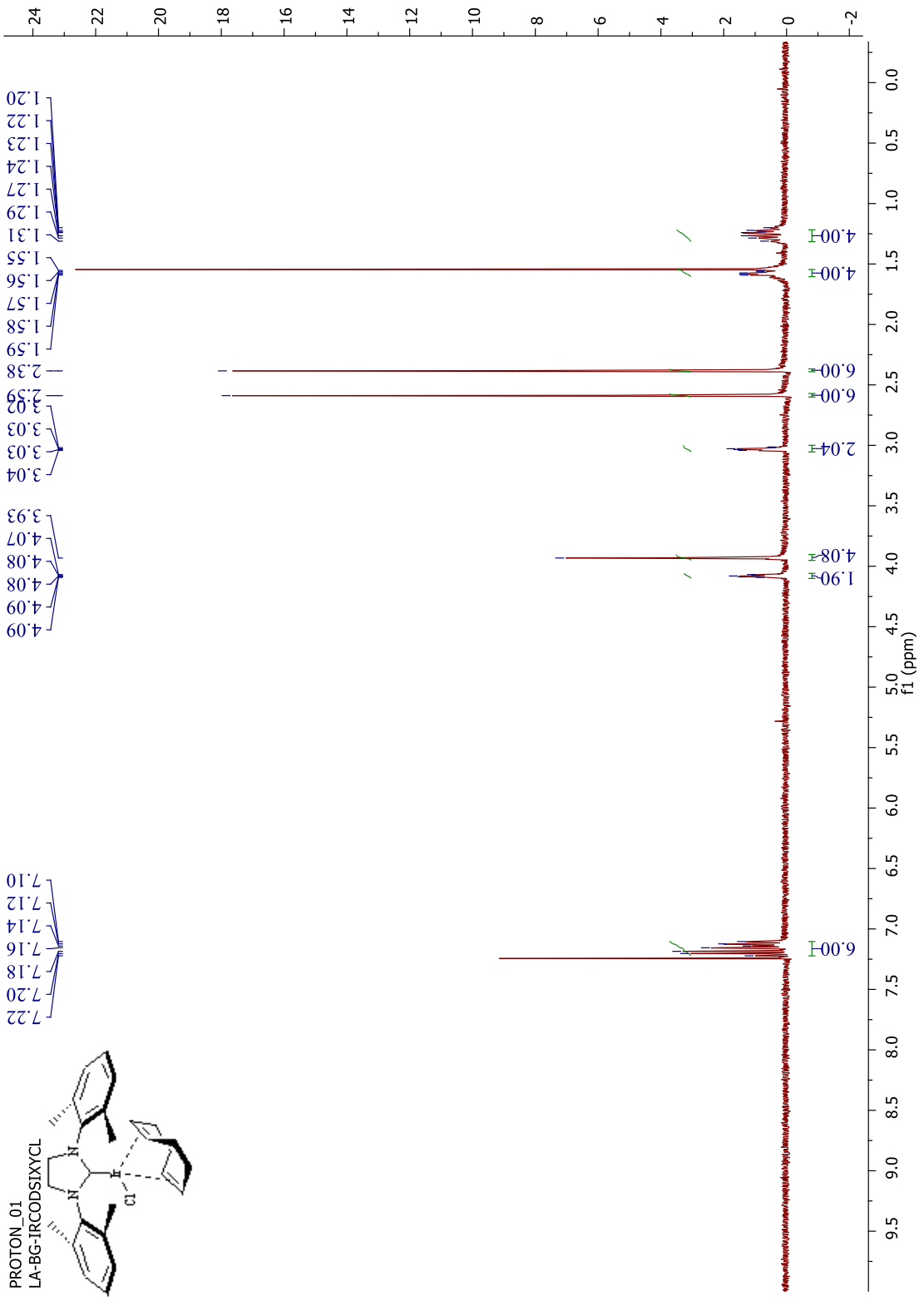
PROTON_01
LA-BG-IRCODSIXYCL
f1 (ppm)

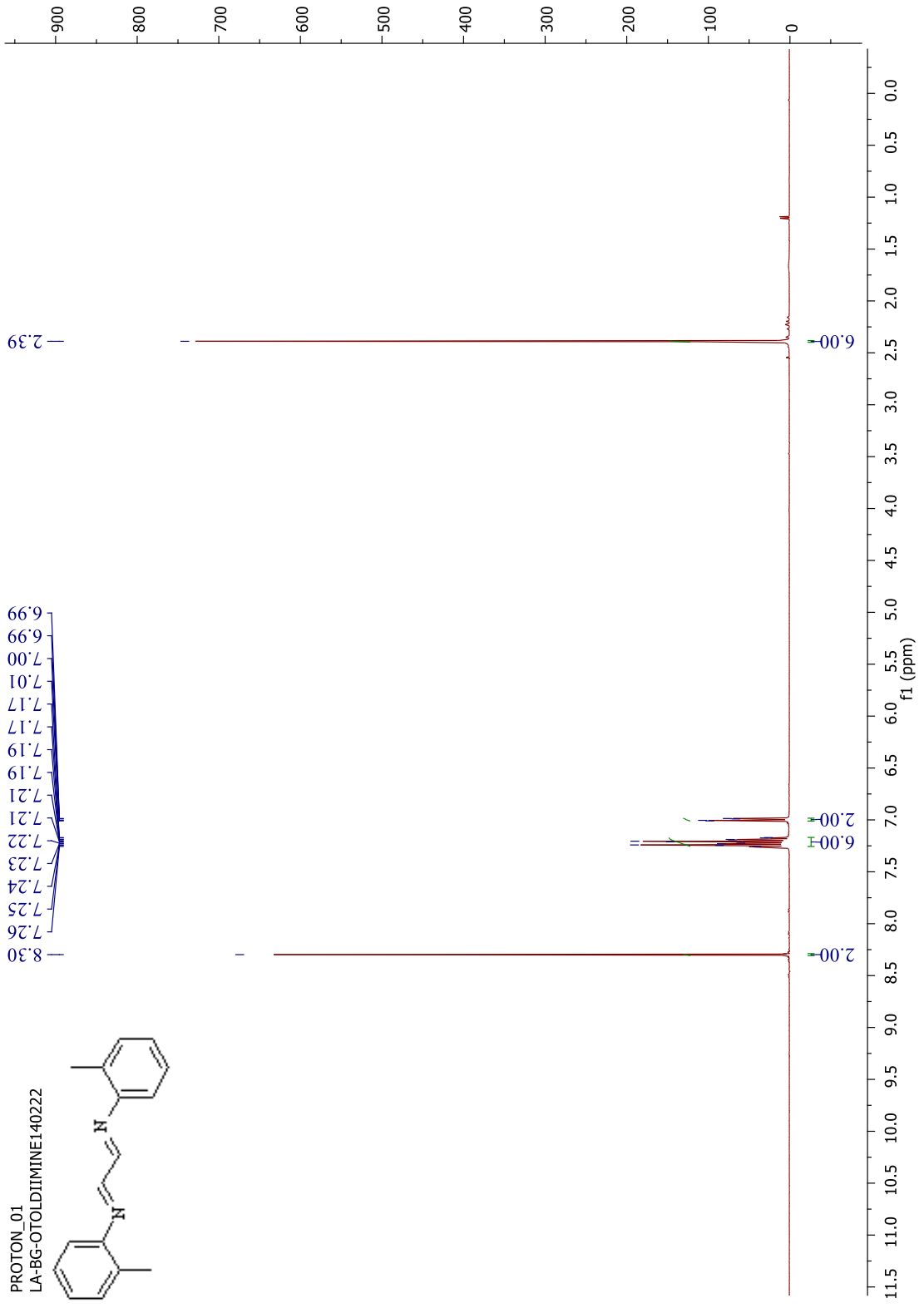
PROTON_01
LA-BG-OTOLDIIMINE140222
8.30
7.26
7.25
7.24
7.23
7.22
7.21
7.21
7.19
7.19
7.17
7.17
7.01
7.00
6.99
6.99
2.39
2.00
6.00
2.00
f1 (ppm)

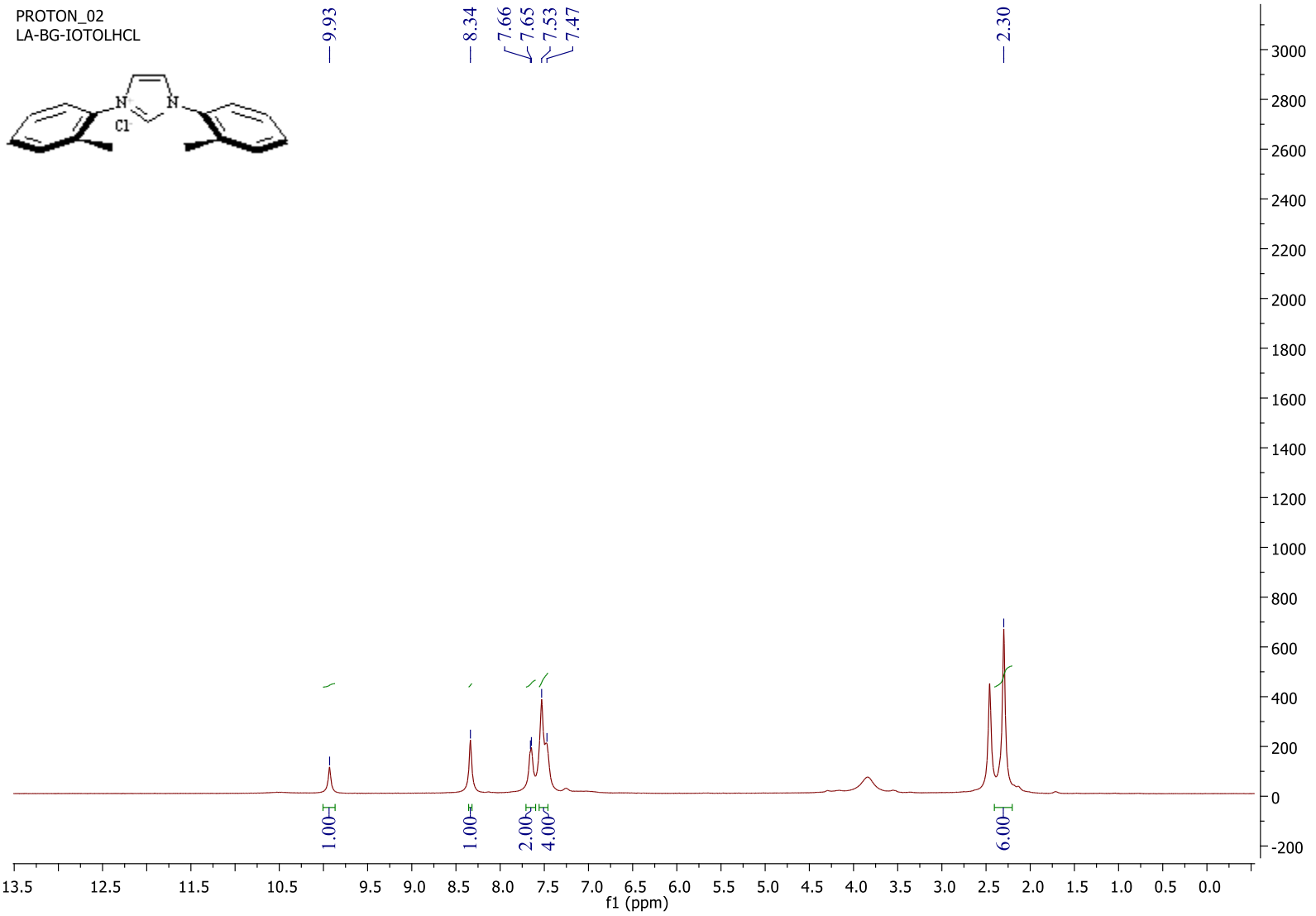
PROTON_02
LA-BG-IOTOLHCL
9.93
8.34
7.66
7.65
7.53
7.47
2.30
1.00
1.00
2.00
4.00
6.00
f1 (ppm)

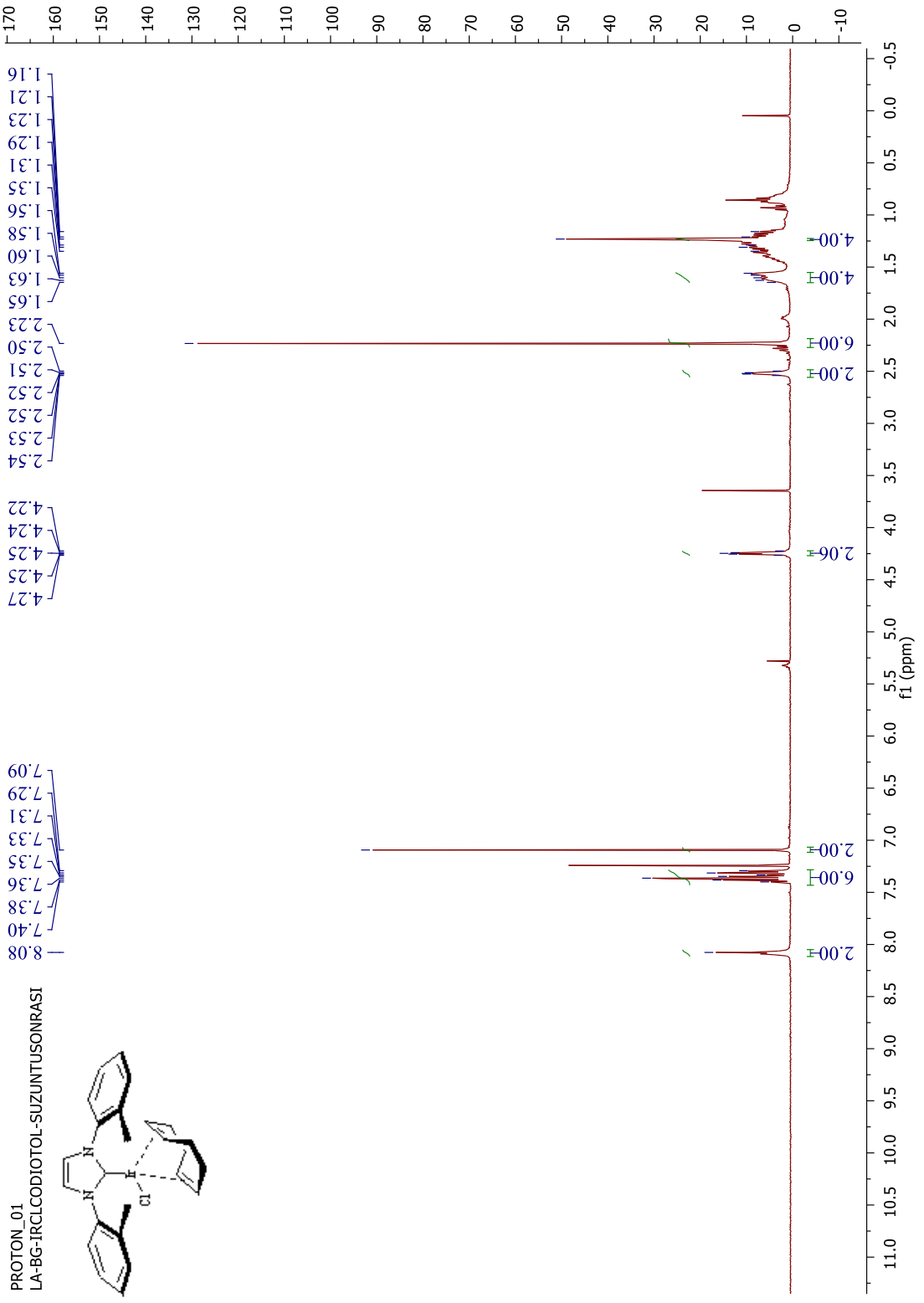
PROTON_01
LA-BG-IRCLCODIOTOL-SUZUNTUSONRASI
f1 (ppm)

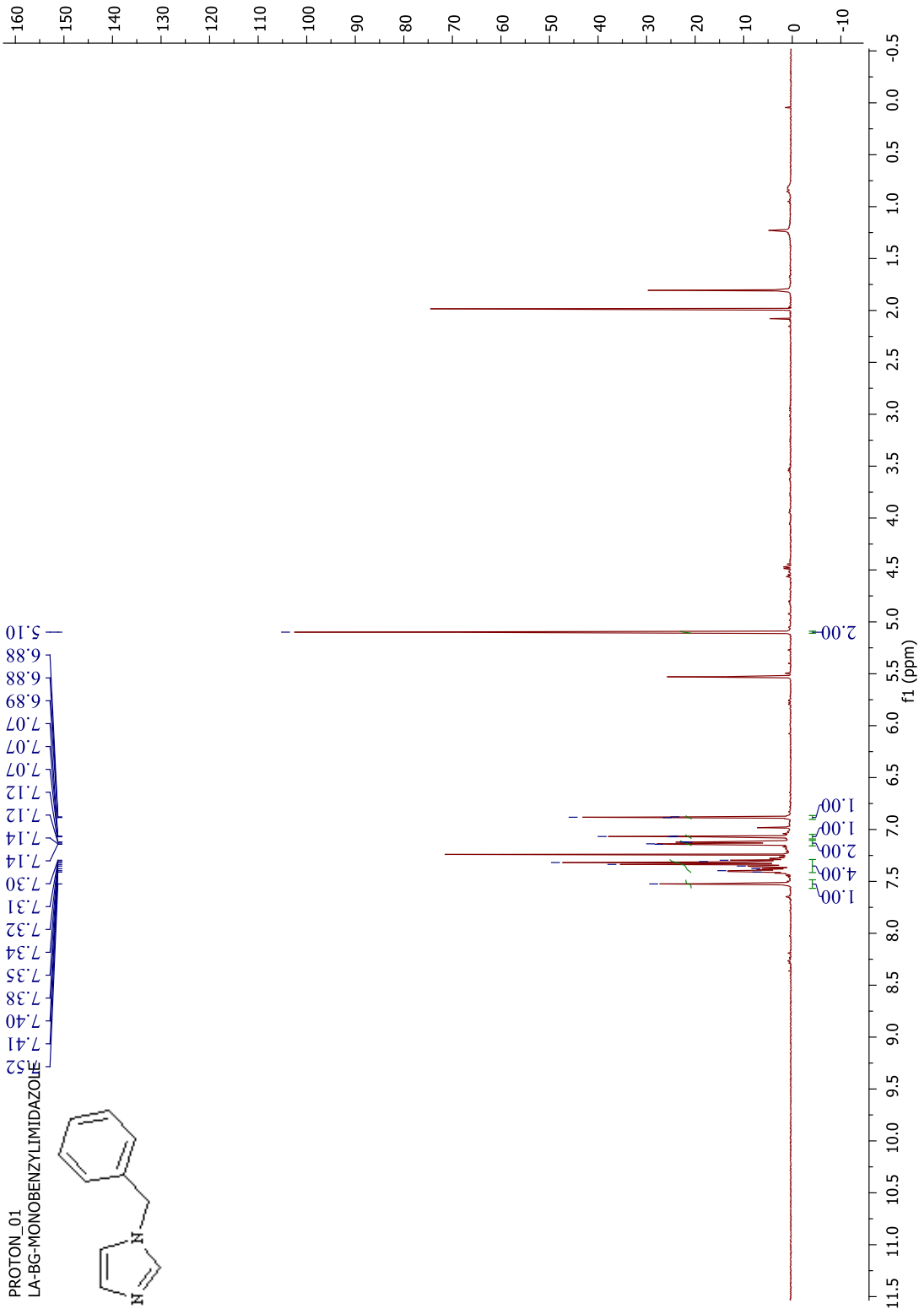
PROTON_01
LA-BG-MONOBENZYLIMIDAZOLE
7.52
7.41
7.40
7.38
7.35
7.34
7.32
7.31
7.30
7.14
7.14
7.12
7.12
7.07
7.07
7.07
6.89
6.88
6.88
5.10
2.00
1.00
1.00
2.00
4.00
1.00
f1 (ppm)

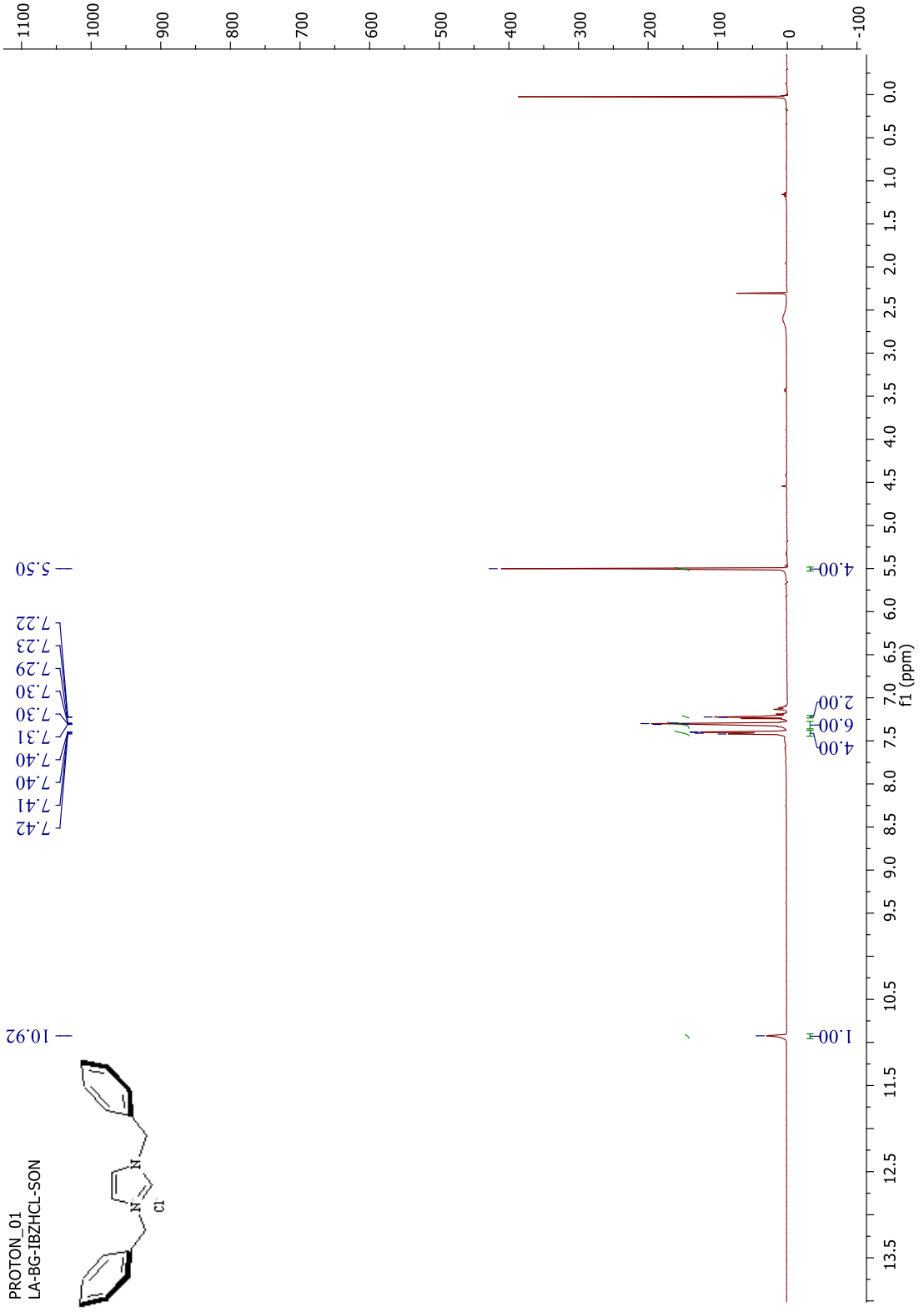
PROTON_01
LA-BG-IBZHCL-SON
10.92
7.42
7.41
7.40
7.40
7.31
7.30
7.30
7.29
7.23
7.22
5.50
1.00
4.00
2.00
6.00
4.00
f1 (ppm)

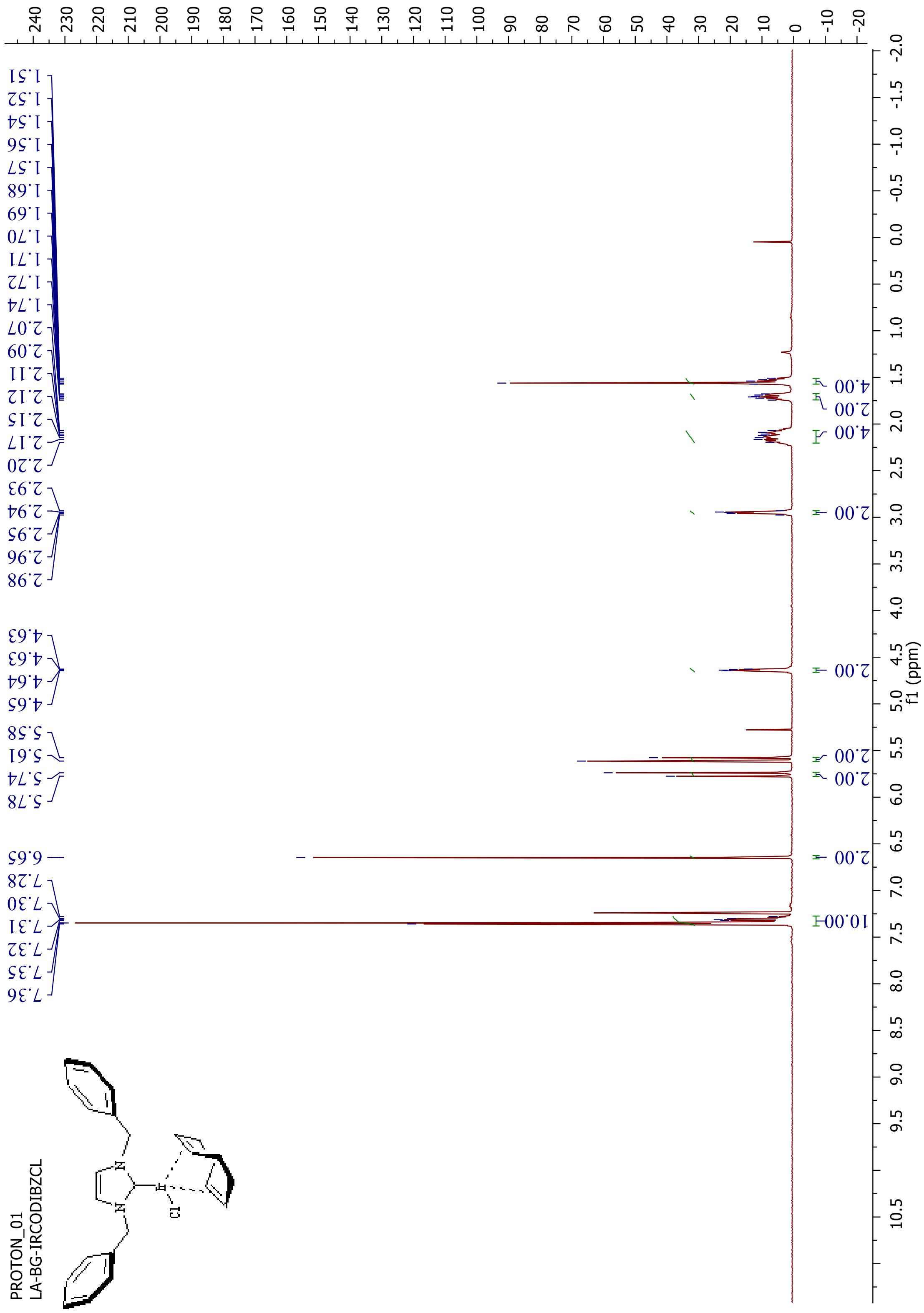
PROTON_01
LA-BG-IRCODIBZCL
1.51
1.52
1.54
1.56
1.57
1.68
1.69
1.70
1.71
1.72
1.74
2.07
2.09
2.11
2.12
2.15
2.17
2.20
2.93
2.94
2.95
2.96
2.98
4.63
4.63
4.64
4.65
5.58
5.61
5.74
5.78
6.65
7.28
7.30
7.31
7.32
7.35
7.36
4.00
2.00
4.00
2.00
2.00
2.00
2.00
2.00
10.00
f1 (ppm)
N
N
Ir
Cl

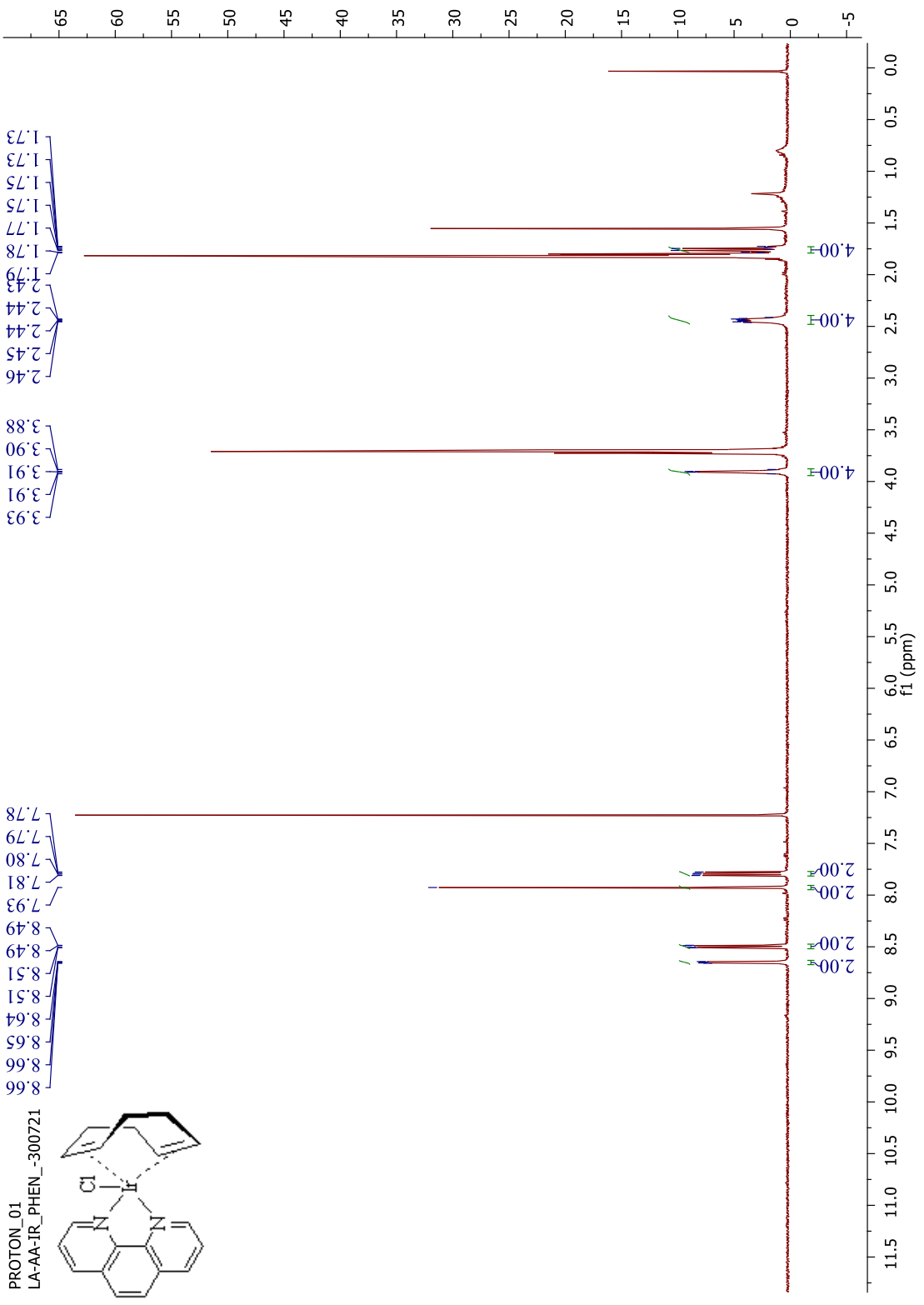
PROTON_01
LA-AA-IR_PHEN_-300721
f1 (ppm)
Cl
Ir
N
N
4.00
4.00
4.00
2.00
2.00
2.00
2.00

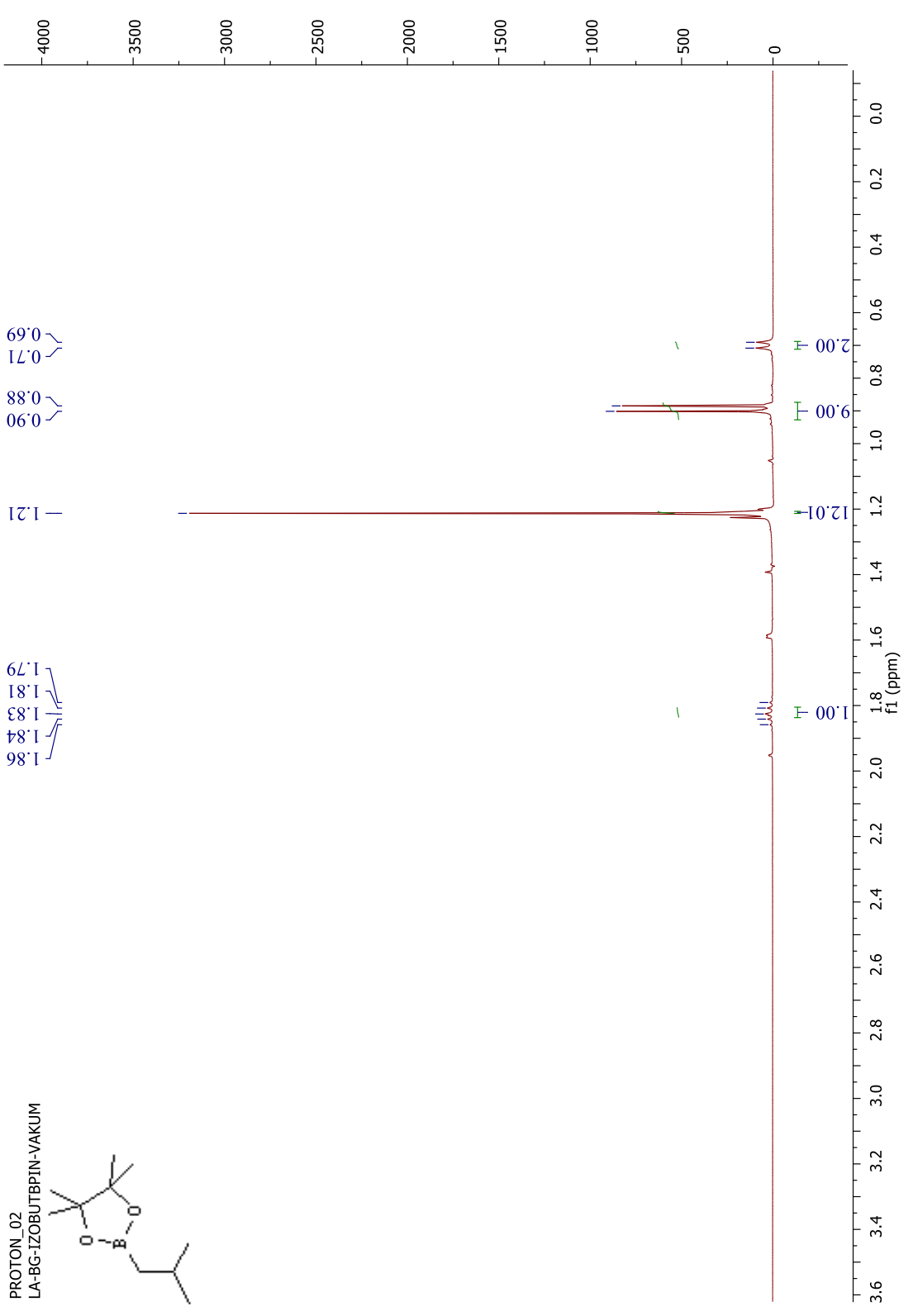
PROTON_02
LA-BG-IZOBUTBPIN-VAKUM
f1 (ppm)
0.69
0.71
0.88
0.90
1.21
1.79
1.81
1.83
1.84
1.86
2.00
9.00
12.01
1.00

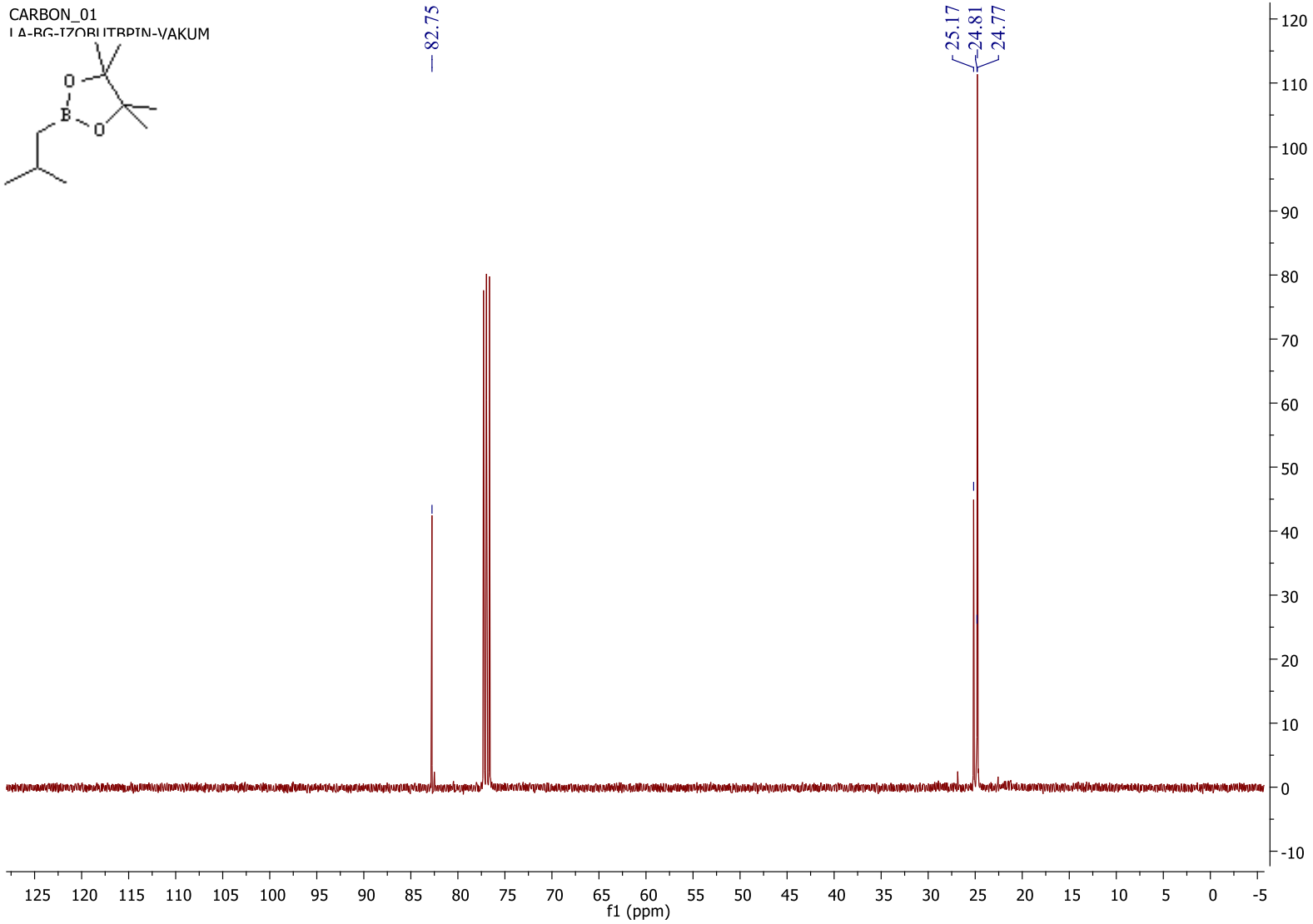
CARBON_01
82.75
25.17
24.81
24.77
f1 (ppm)

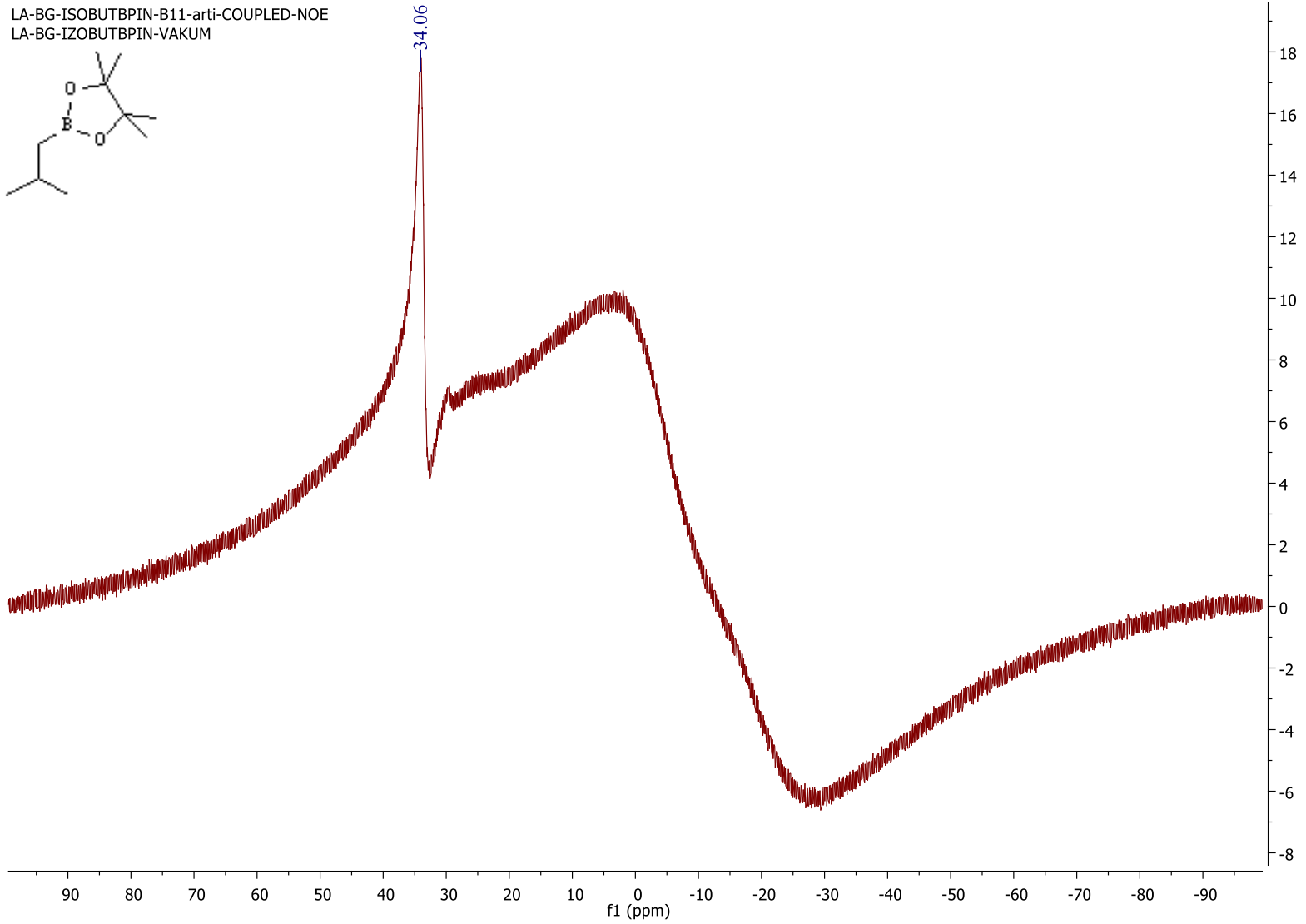
LA-BG-ISOBUTBPIN-B11-arti-COUPLED-NOE
LA-BG-IZOBUTBPIN-VAKUM
34.06
O
B
O
18
16
14
12
10
8
6
4
2
0
-2
-4
-6
-8
90
80
70
60
50
40
30
20
10
0
-10
-20
-30
-40
-50
-60
-70
-80
-90
f1 (ppm)

APPENDIX B

MASS SPECTRUMS OF COMPOUNDS

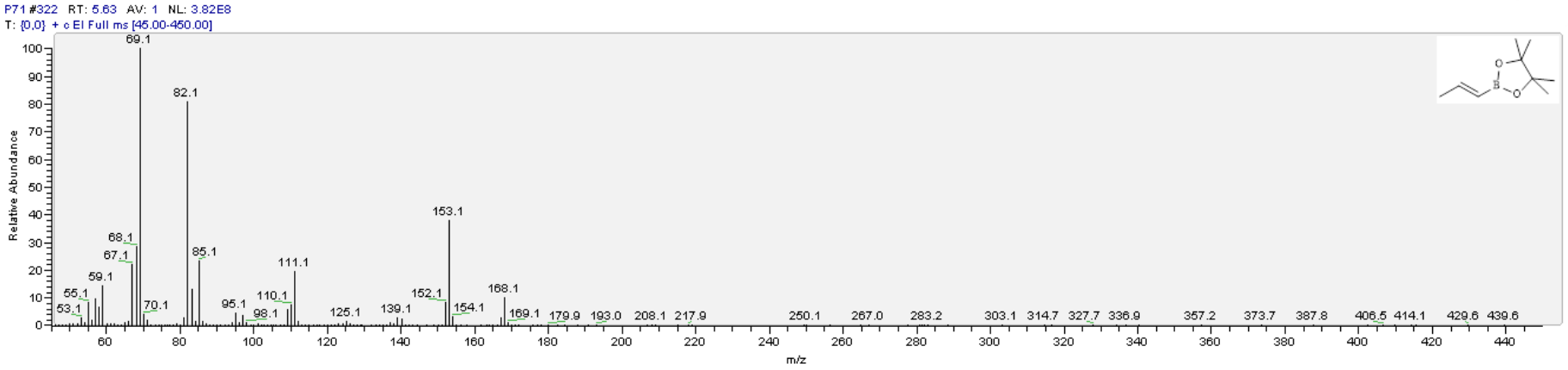
P71 #322 RT: 5.63 AV: 1 NL: 3.82E8
T: {0,0} + c EI Full ms [45.00-450.00]
Relative Abundance
m/z
69.1
82.1
153.1
68.1
67.1
85.1
111.1
59.1
55.1
53.1
70.1
95.1
110.1
98.1
125.1
139.1
152.1
154.1
168.1
169.1
179.9
193.0
208.1
217.9
250.1
267.0
283.2
303.1
314.7
327.7
336.9
357.2
373.7
387.8
406.5
414.1
429.6
439.6

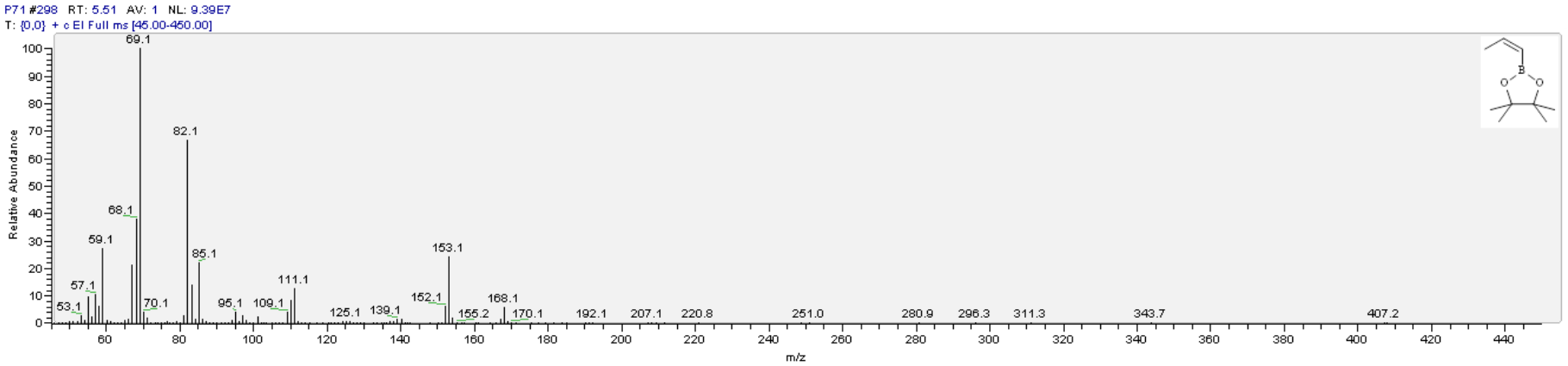
P71 #298 RT: 5.51 AV: 1 NL: 9.39E7
T: {0,0} + c EI Full ms [45.00-450.00]
Relative Abundance
m/z
69.1
82.1
68.1
59.1
85.1
153.1
111.1
57.1
53.1
70.1
95.1
109.1
125.1
139.1
152.1
155.2
168.1
170.1
192.1
207.1
220.8
251.0
280.9
296.3
311.3
343.7
407.2

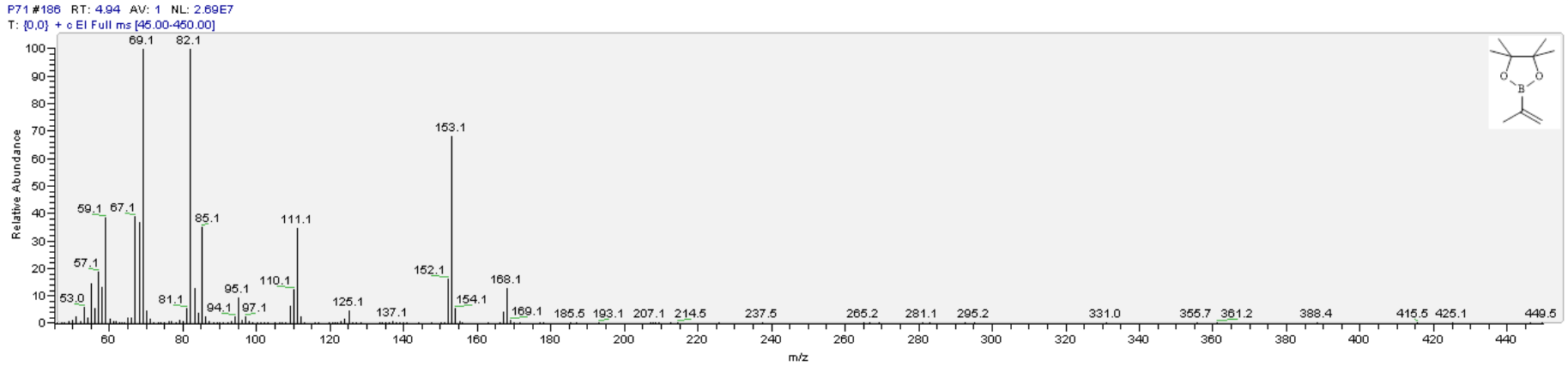
P71 #186 RT: 4.94 AV: 1 NL: 2.69E7
T: {0,0} + c EI Full ms [45.00-450.00]
Relative Abundance
m/z
69.1
82.1
153.1
59.1
67.1
85.1
111.1
57.1
152.1
168.1
110.1
95.1
53.0
81.1
94.1
97.1
125.1
137.1
154.1
169.1
185.5
193.1
207.1
214.5
237.5
265.2
281.1
295.2
331.0
355.7
361.2
388.4
415.5
425.1
449.5

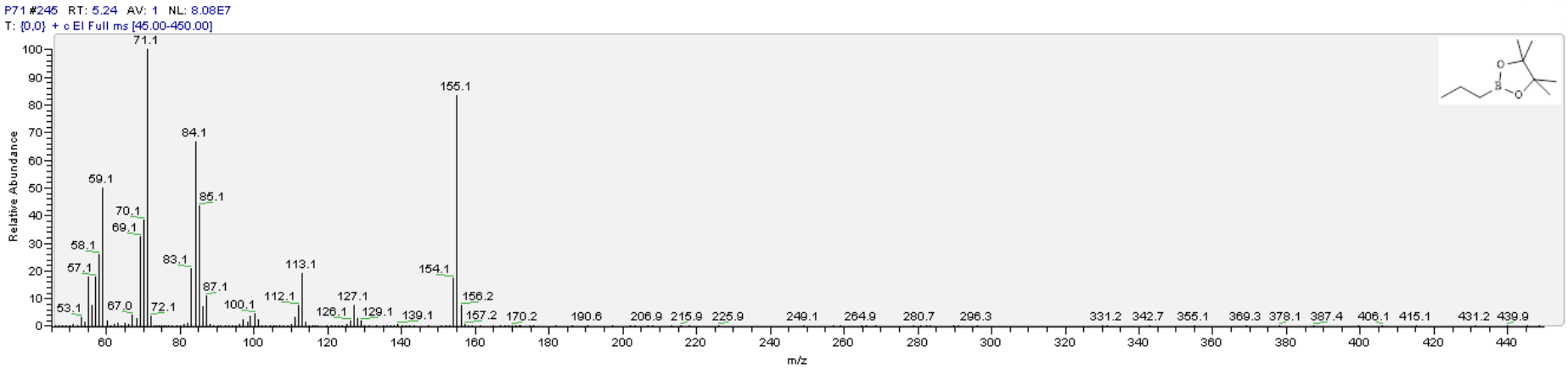
P71 #245 RT: 5.24 AV: 1 NL: 8.08E7
T: {0,0} + c EI Full ms [45.00-450.00]
Relative Abundance
m/z
71.1
155.1
84.1
59.1
85.1
70.1
69.1
58.1
83.1
57.1
113.1
154.1
87.1
156.2
112.1
127.1
53.1
67.0
72.1
100.1
126.1
129.1
139.1
157.2
170.2
190.6
206.9
215.9
225.9
249.1
264.9
280.7
296.3
331.2
342.7
355.1
369.3
378.1
387.4
406.1
415.1
431.2
439.9

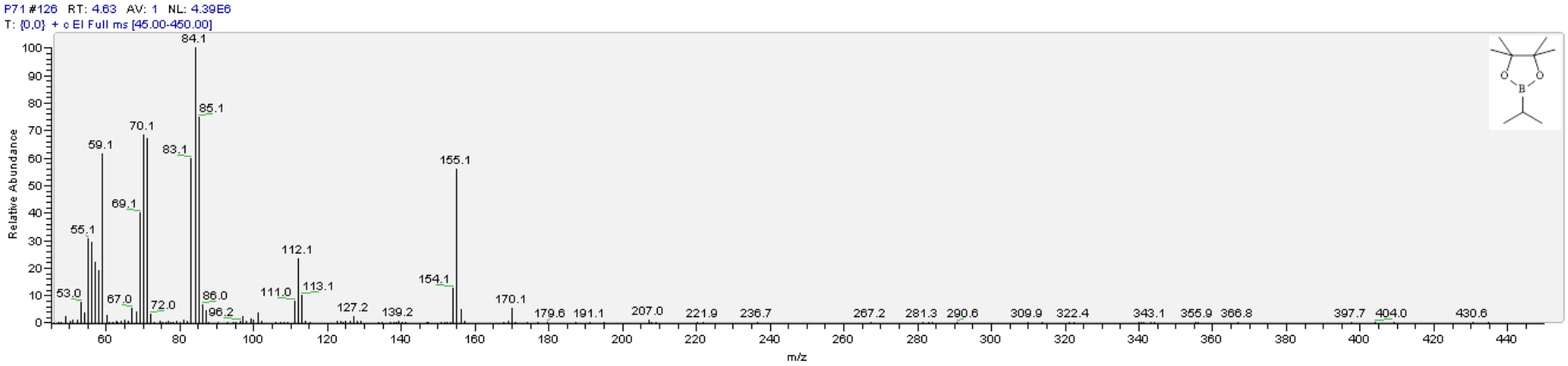
P71 #126 RT: 4.63 AV: 1 NL: 4.39E6
T: {0,0} + c EI Full ms [45.00-450.00]
Relative Abundance
m/z
84.1
85.1
70.1
59.1
83.1
155.1
69.1
55.1
112.1
154.1
53.0
67.0
72.0
86.0
96.2
111.0
113.1
127.2
139.2
170.1
179.6
191.1
207.0
221.9
236.7
267.2
281.3
290.6
309.9
322.4
343.1
355.9
366.8
397.7
404.0
430.6

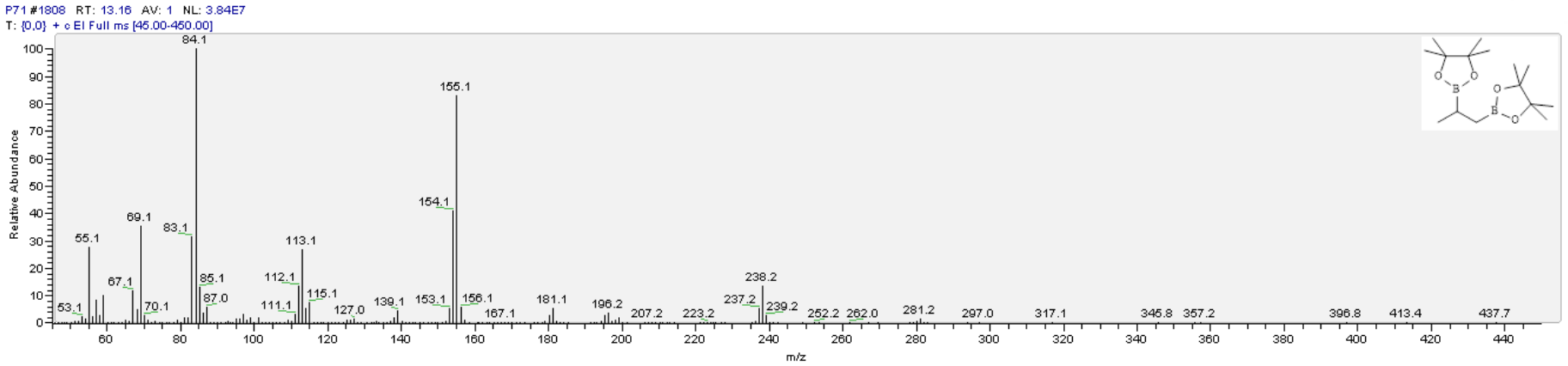
P71 #1808 RT: 13.16 AV: 1 NL: 3.84E7
T: {0,0} + c EI Full ms [45.00-450.00]
Relative Abundance
m/z
84.1
155.1
154.1
69.1
83.1
55.1
113.1
85.1
112.1
67.1
115.1
87.0
70.1
53.1
111.1
127.0
139.1
153.1
156.1
167.1
181.1
196.2
207.2
223.2
238.2
237.2
239.2
252.2
262.0
281.2
297.0
317.1
345.8
357.2
396.8
413.4
437.7

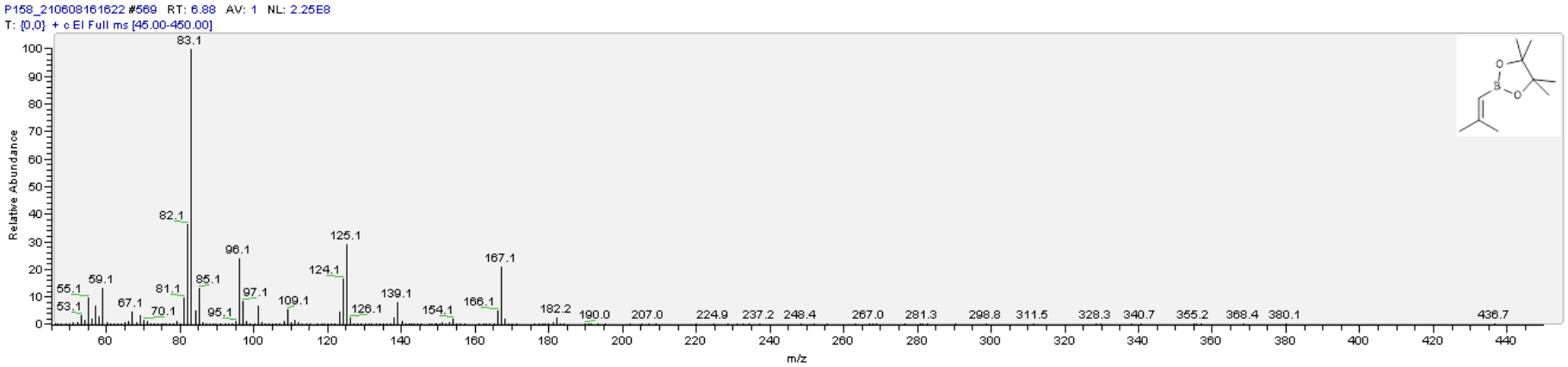
P158_210608161622 #569 RT: 6.88 AV: 1 NL: 2.25E8
T: {0,0} + c EI Full ms [45.00-450.00]
Relative Abundance
m/z
83.1
82.1
125.1
96.1
167.1
124.1
59.1
85.1
139.1
55.1
81.1
97.1
109.1
53.1
67.1
70.1
95.1
126.1
154.1
166.1
182.2
190.0
207.0
224.9
237.2
248.4
267.0
281.3
298.8
311.5
328.3
340.7
355.2
368.4
380.1
436.7

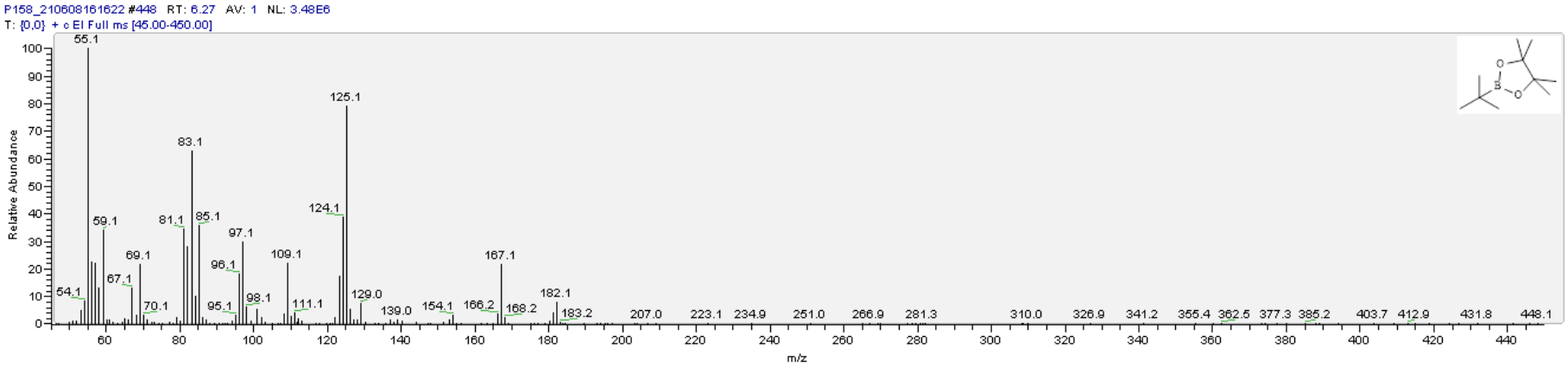
P158_210608161622 #448 RT: 6.27 AV: 1 NL: 3.48E6
T: {0,0} + c EI Full ms [45.00-450.00]
Relative Abundance
m/z
55.1
125.1
83.1
59.1
124.1
81.1
85.1
97.1
69.1
109.1
167.1
96.1
67.1
182.1
54.1
98.1
70.1
95.1
111.1
129.0
139.0
154.1
166.2
168.2
183.2
207.0
223.1
234.9
251.0
266.9
281.3
310.0
326.9
341.2
355.4
362.5
377.3
385.2
403.7
412.9
431.8
448.1

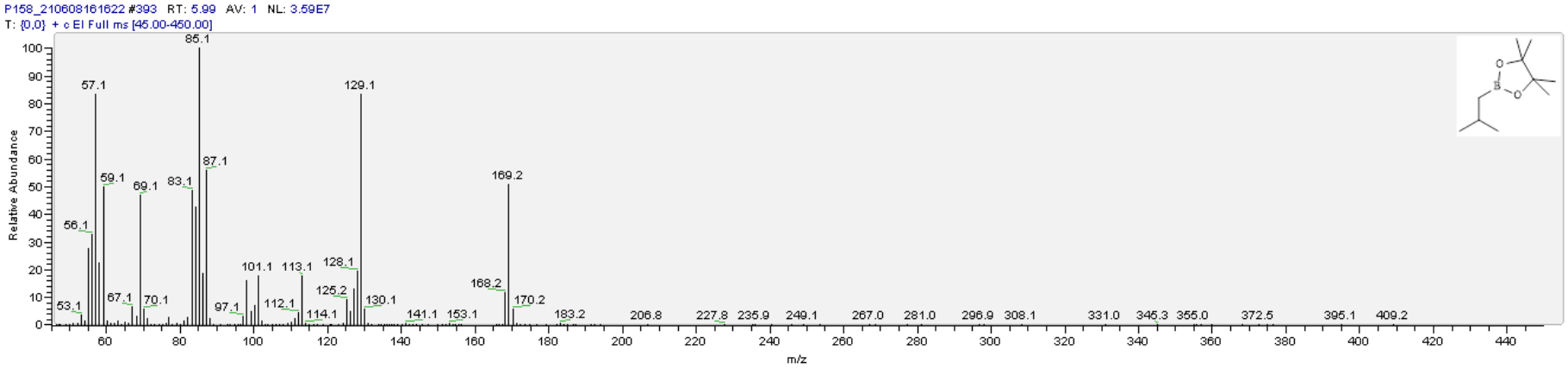
P158_210608161622 #393 RT: 5.99 AV: 1 NL: 3.59E7
T: {0,0} + c EI Full ms [45.00-450.00]
Relative Abundance
m/z
85.1
57.1
129.1
87.1
59.1
69.1
83.1
169.2
56.1
101.1
113.1
128.1
168.2
125.2
130.1
67.1
70.1
53.1
97.1
112.1
114.1
170.2
141.1
153.1
183.2
206.8
227.8
235.9
249.1
267.0
281.0
296.9
308.1
331.0
345.3
355.0
372.5
395.1
409.2

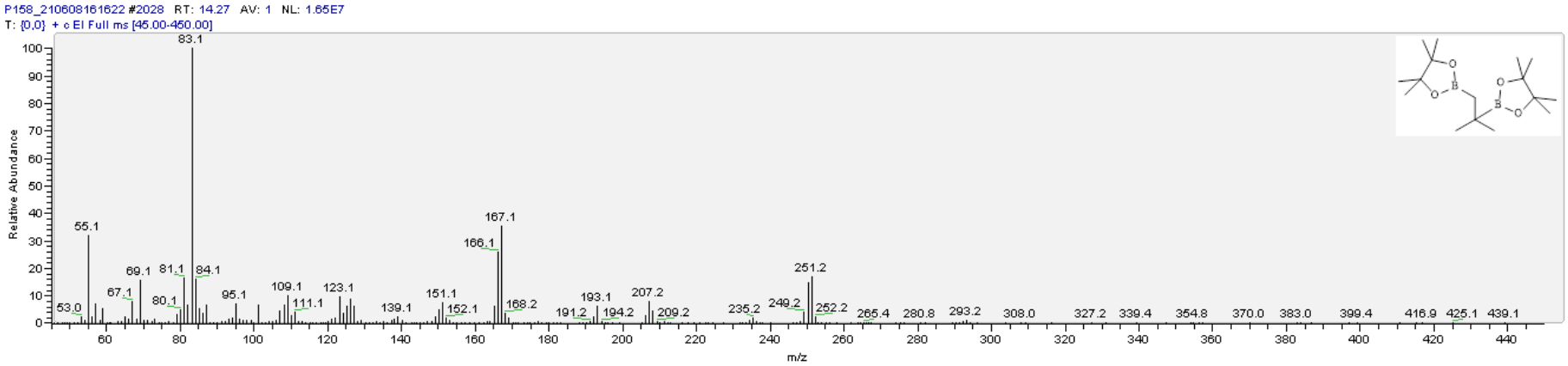
P158_210608161622 #2028 RT: 14.27 AV: 1 NL: 1.65E7
T: {0,0} + c EI Full ms [45.00-450.00]
Relative Abundance
m/z
83.1
55.1
167.1
166.1
251.2
69.1
81.1
84.1
67.1
109.1
123.1
111.1
95.1
80.1
151.1
152.1
168.2
139.1
193.1
207.2
53.0
191.2
194.2
209.2
235.2
249.2
252.2
265.4
280.8
293.2
308.0
327.2
339.4
354.8
370.0
383.0
399.4
416.9
425.1
439.1

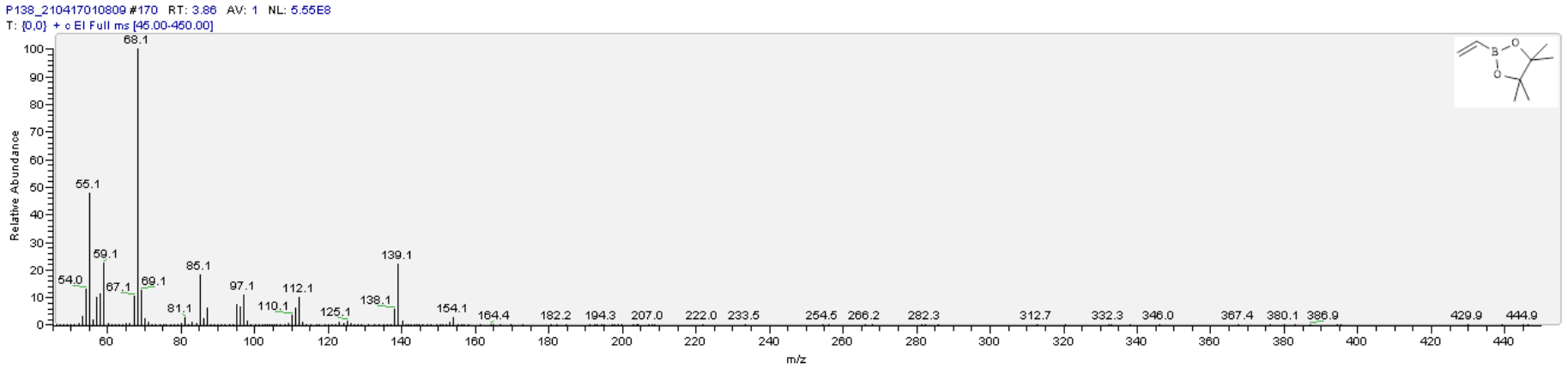
P138_210417010809 #170 RT: 3.86 AV: 1 NL: 5.55E8
T: {0,0} + c EI Full ms [45.00-450.00]
Relative Abundance
m/z
68.1
55.1
59.1
54.0
67.1
69.1
85.1
81.1
97.1
110.1
112.1
125.1
138.1
139.1
154.1
164.4
182.2
194.3
207.0
222.0
233.5
254.5
266.2
282.3
312.7
332.3
346.0
367.4
380.1
386.9
429.9
444.9

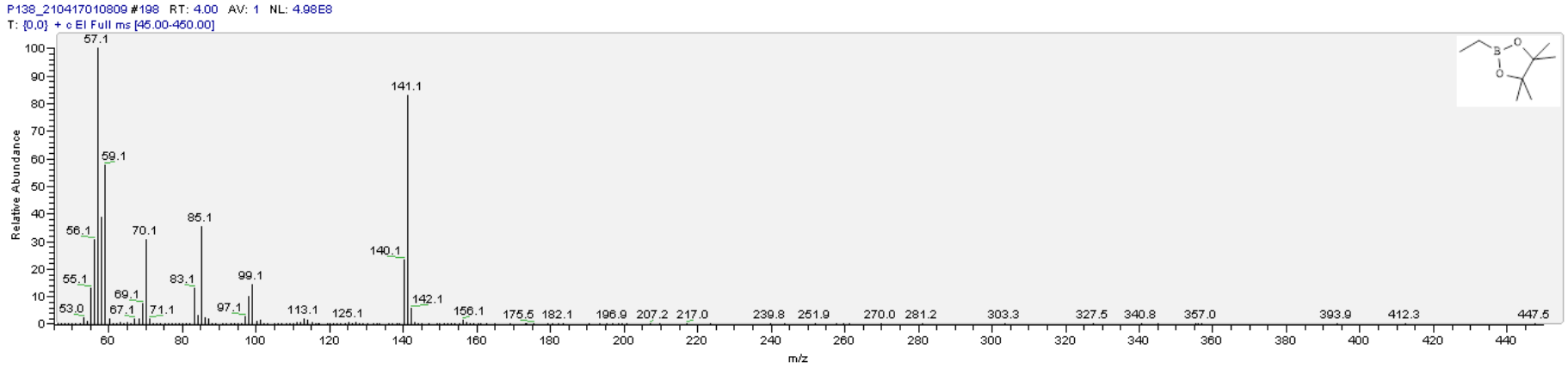
P138_210417010809 #198 RT: 4.00 AV: 1 NL: 4.98E8
T: {0,0} + c EI Full ms [45.00-450.00]
Relative Abundance
m/z
57.1
141.1
59.1
85.1
56.1
70.1
140.1
99.1
55.1
83.1
142.1
69.1
53.0
67.1
71.1
97.1
113.1
125.1
156.1
175.5
182.1
196.9
207.2
217.0
239.8
251.9
270.0
281.2
303.3
327.5
340.8
357.0
393.9
412.3
447.5

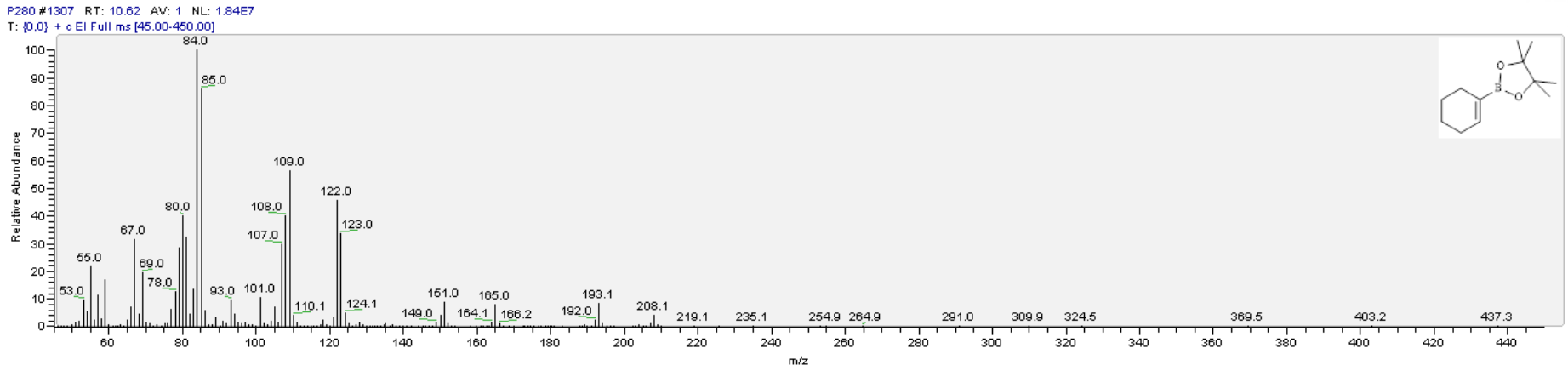
P280 #1307 RT: 10.62 AV: 1 NL: 1.84E7
T: {0,0} + c EI Full ms [45.00-450.00]
Relative Abundance
m/z
84.0
85.0
109.0
122.0
80.0
108.0
123.0
67.0
107.0
55.0
69.0
78.0
53.0
93.0
101.0
110.1
124.1
151.0
165.0
149.0
164.1
166.2
192.0
193.1
208.1
219.1
235.1
254.9
264.9
291.0
309.9
324.5
369.5
403.2
437.3

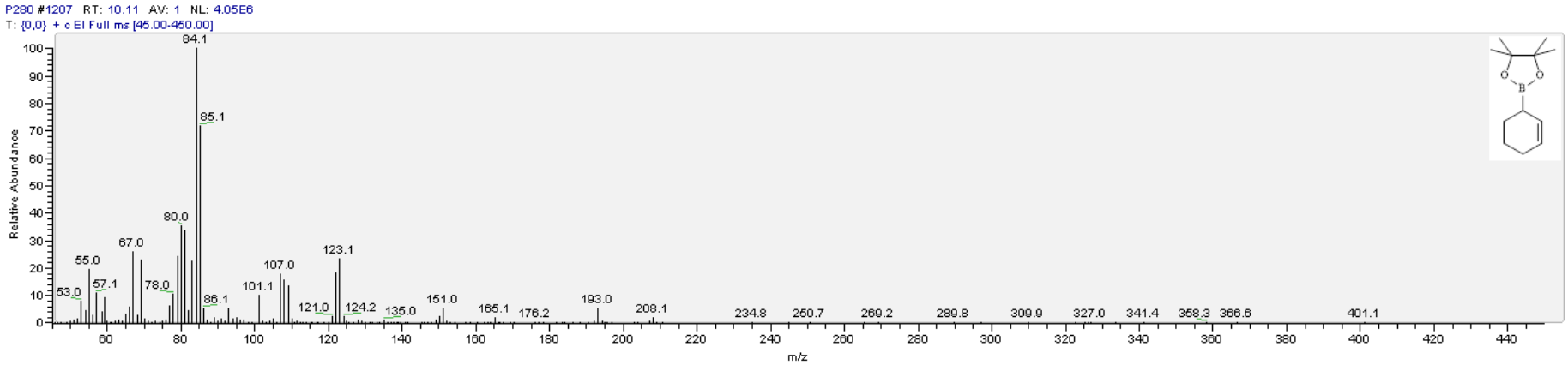
P280 #1207 RT: 10.11 AV: 1 NL: 4.05E6
T: {0,0} + c EI Full ms [45.00-450.00]
Relative Abundance
m/z
84.1
85.1
80.0
67.0
55.0
57.1
53.0
78.0
86.1
101.1
107.0
123.1
121.0
124.2
135.0
151.0
165.1
176.2
193.0
208.1
234.8
250.7
269.2
289.8
309.9
327.0
341.4
358.3
366.6
401.1

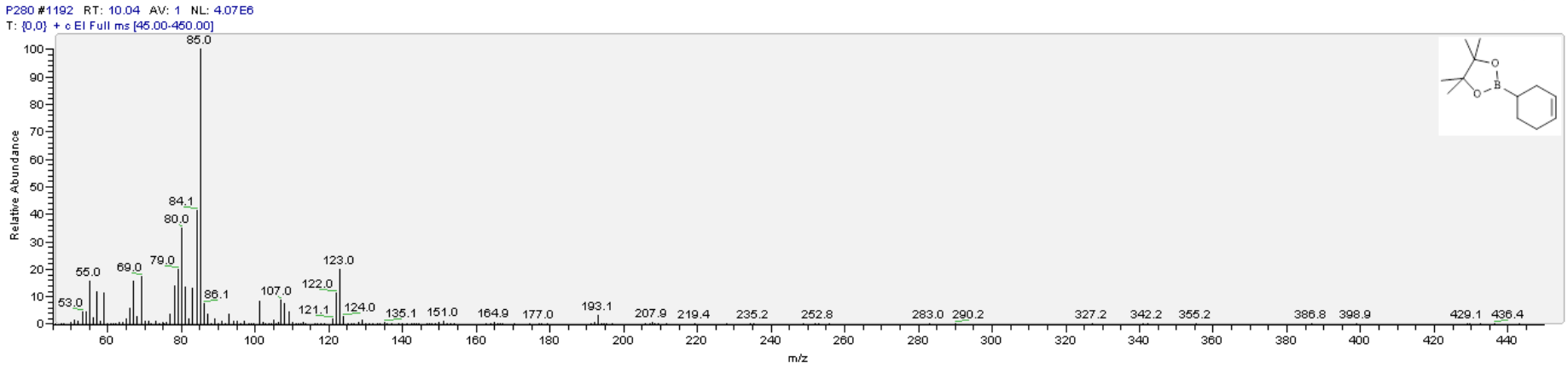
P280 #1192 RT: 10.04 AV: 1 NL: 4.07E6
T: {0,0} + c EI Full ms [45.00-450.00]
Relative Abundance
m/z
85.0
84.1
80.0
79.0
69.0
55.0
53.0
86.1
107.0
123.0
122.0
121.1
124.0
135.1
151.0
164.9
177.0
193.1
207.9
219.4
235.2
252.8
283.0
290.2
327.2
342.2
355.2
386.8
398.9
429.1
436.4

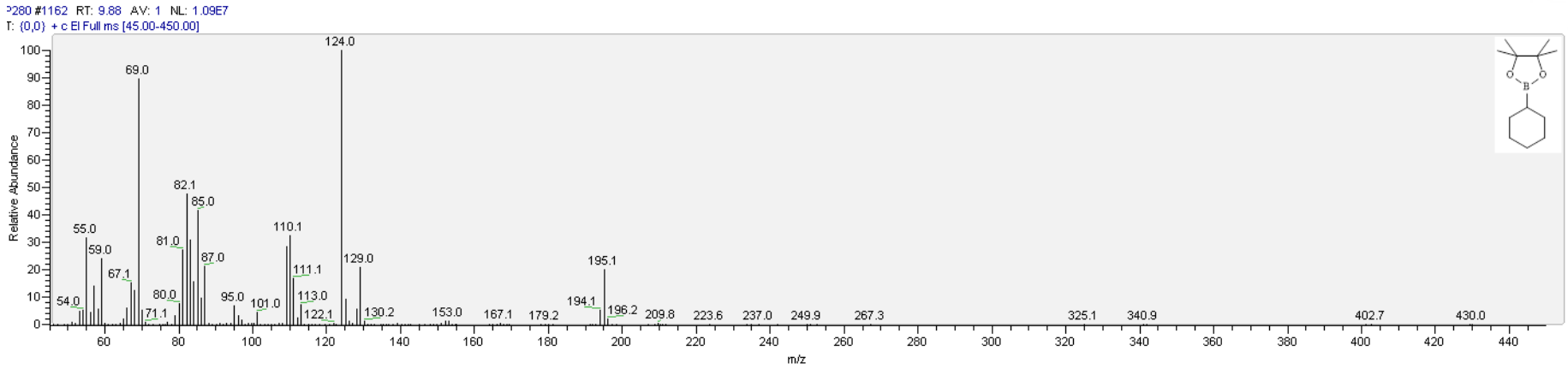
?280 #1162 RT: 9.88 AV: 1 NL: 1.09E7
T: {0,0} + c EI Full ms [45.00-450.00]
Relative Abundance
m/z
124.0
69.0
82.1
85.0
55.0
59.0
67.1
81.0
87.0
110.1
111.1
129.0
195.1
54.0
80.0
71.1
95.0
101.0
113.0
122.1
130.2
153.0
167.1
179.2
194.1
196.2
209.8
223.6
237.0
249.9
267.3
325.1
340.9
402.7
430.0

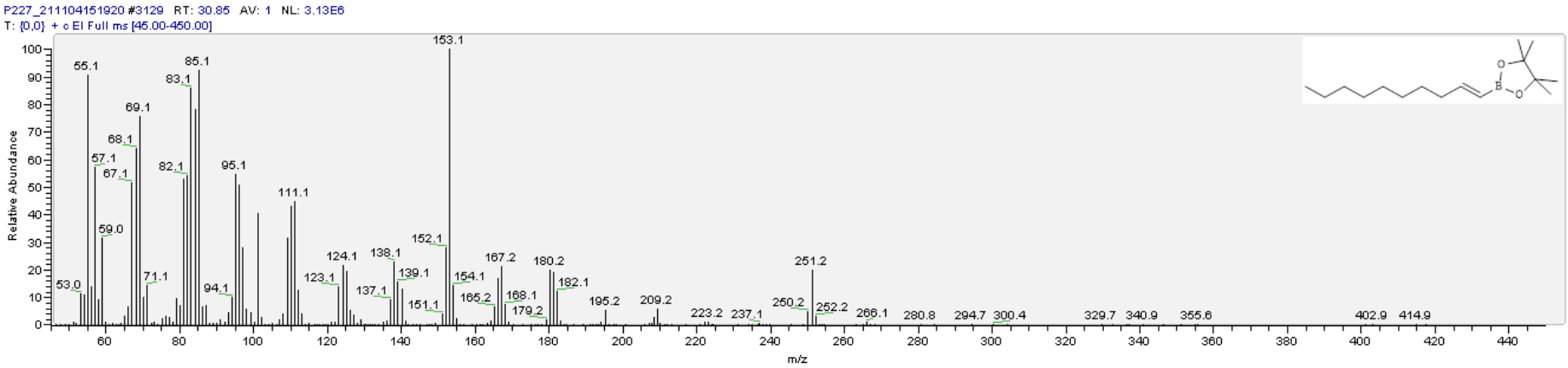
P227_211104151920 #3129 RT: 30.85 AV: 1 NL: 3.13E6
T: {0,0} + c EI Full ms [45.00-450.00]
Relative Abundance
m/z
153.1
55.1
85.1
83.1
69.1
68.1
57.1
67.1
82.1
95.1
111.1
59.0
152.1
124.1
138.1
167.2
180.2
251.2
53.0
71.1
123.1
139.1
154.1
182.1
94.1
137.1
151.1
165.2
168.1
179.2
195.2
209.2
223.2
237.1
250.2
252.2
266.1
280.8
294.7
300.4
329.7
340.9
355.6
402.9
414.9

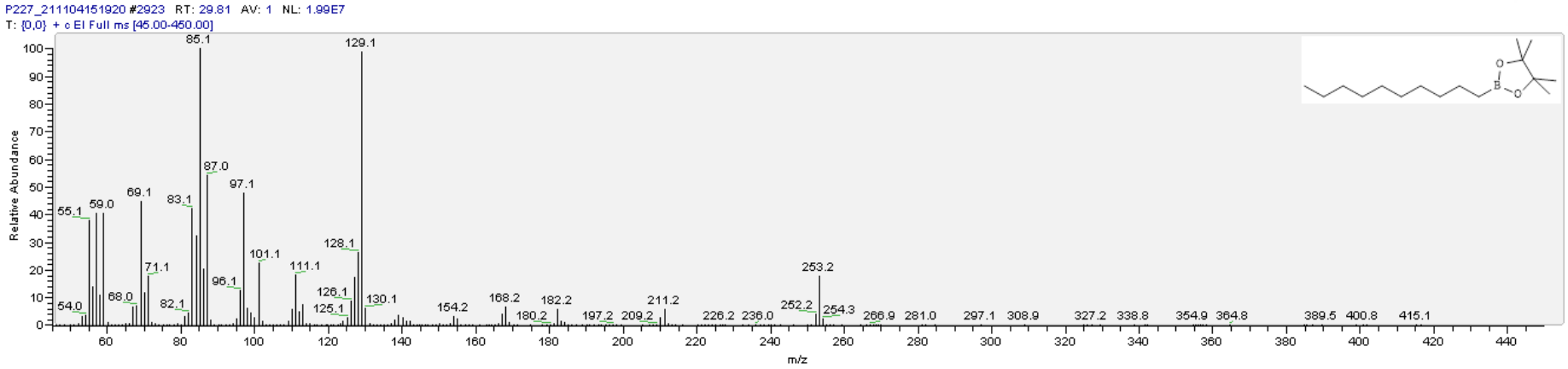
P227_211104151920 #2923 RT: 29.81 AV: 1 NL: 1.99E7
T: {0,0} + c EI Full ms [45.00-450.00]
Relative Abundance
m/z
85.1
129.1
87.0
97.1
69.1
83.1
55.1
59.0
128.1
101.1
111.1
71.1
96.1
126.1
125.1
130.1
68.0
54.0
82.1
154.2
168.2
182.2
180.2
197.2
209.2
211.2
226.2
236.0
253.2
252.2
254.3
266.9
281.0
297.1
308.9
327.2
338.8
354.9
364.8
389.5
400.8
415.1

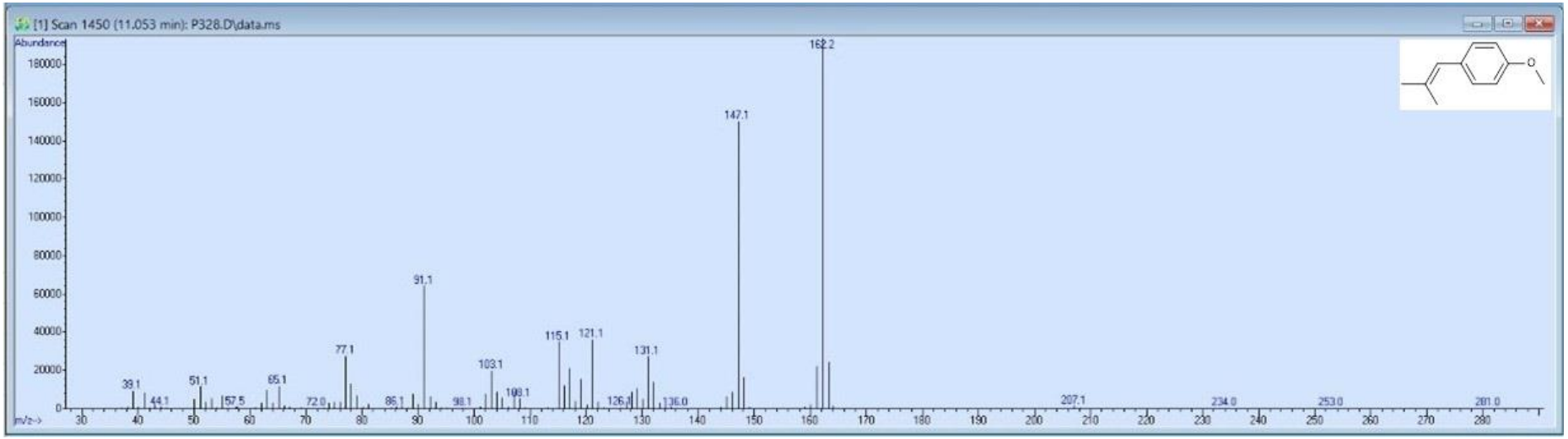
[1] Scan 1450 (11.053 min): P328.D\data.ms
Abundance
m/z-->
162.2
147.1
91.1
77.1
115.1
121.1
131.1
103.1
39.1
51.1
65.1
44.1
57.5
72.0
86.1
98.1
199.1
126.0
136.0
207.1
234.0
253.0
281.0

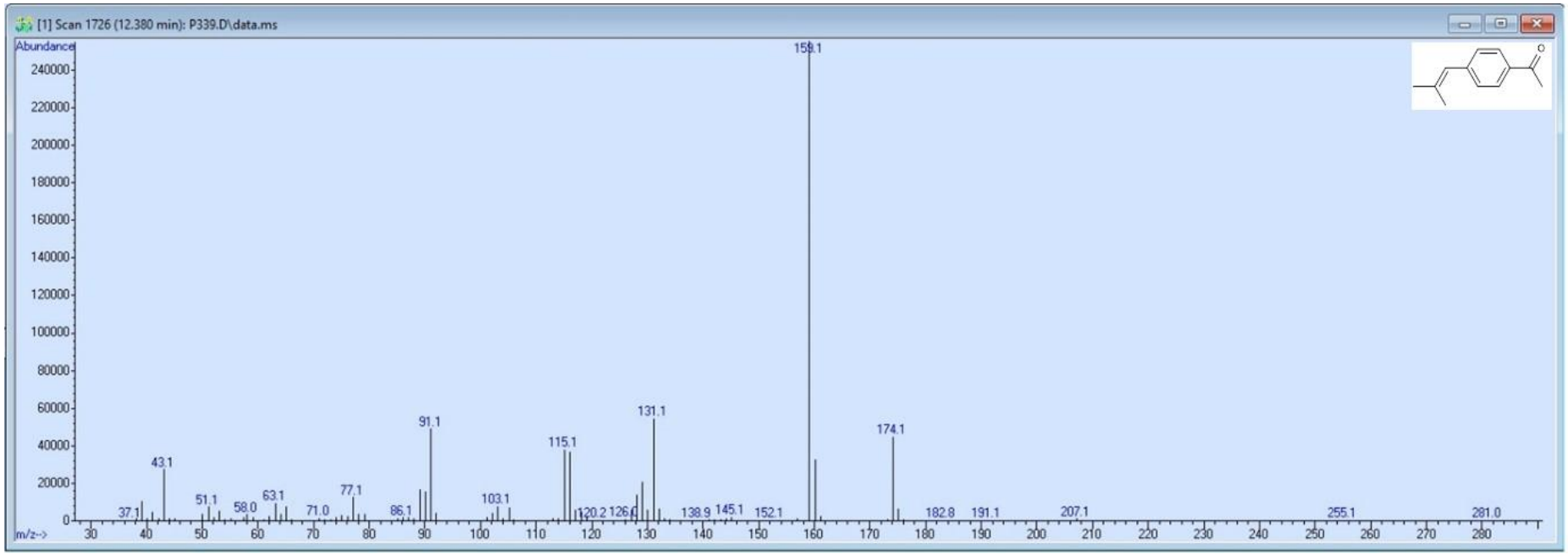
[1] Scan 1726 (12.380 min): P339.D\data.ms
Abundance
m/z-->
159.1
91.1
131.1
115.1
174.1
43.1
77.1
103.1
51.1
63.1
58.0
71.0
86.1
37.1
120.2
126.0
138.9
145.1
152.1
182.8
191.1
207.1
255.1
281.0